BORON/GRAPHITE HYBRID COMPOSITE DEVELOPMENT STUDY

FINAL REPORT
30 August 1970

by
Harold A. Evensen

Prepared for

NATIONAL AERONAUTICS AND SPACE ADMINISTRATION
George C. Marshall Space Flight Center
Huntsville, Alabama

Contract No. NAS8-24510

WHITTAKER CORPORATION
Research & Development Division
3540 Aero Court
San Diego, California 92123

BORON/GRAPHITE HYBRID COMPOSITE DEVELOPMENT STUDY

FINAL REPORT
30 August 1970

by
Harold A. Evensen

Prepared for

NATIONAL AERONAUTICS AND SPACE ADMINISTRATION
George C. Marshall Space Flight Center
Huntsville, Alabama

Contract No. NAS8-24510

WHITTAKER CORPORATION
Research & Development Division
3540 Aero Court
San Diego, California 92123

FOREWORD

This report was prepared by Whittaker Corporation Research and Development Division (WRD), San Diego, California, under Contract NAS 8-24510, entitled "Boron/Graphite Hybrid Composite Development Study." This program was administered by the National Aeronautics and Space Administration, George C. Marshall Space Flight Center, Huntsville, Alabama. Mr. Phillip H. Taylor was the Contracting Officer and Mr. H. M. Walker was the Project Officer.

Work was conducted at WRD under the general direction of Dr. Kenneth R. Berg, Manager, Structural Development Engineering, and Mr. Boris Levenetz, Manager, Advanced Composites Engineering. Harold A. Evensen served as Principal Investigator.

This report was released for publication on 15 July 1970.

ABSTRACT

A hybrid composite, consisting of boron and graphite fibers in a NMD 2387 epoxy matrix, has been investigated both analytically and experimentally, and processing and material design procedures have been established and demonstrated. It is pointed out that there are three ways to enhance the properties of a boron/epoxy composite laminate: a) Augmentation, in which the volume fraction of boron fiber is increased with no graphite fiber added, b) Interleaving, in which boron/epoxy and graphite/epoxy prepregs are interleaved prior to curing, and c) Mixing, in which boron and graphite fibers are intermixed prior to prepregging. The latter concept achieves the best improvement in transverse tensile and in-plane shear stiffness properties, but the absolute magnitudes of these improvements are not, in themselves, sufficient to warrant replacement of the Augmented composite concept. The potential improvements in longitudinal properties are rather small when considered on the basis of specific strength and modulus properties, and it is concluded that use of the mixed composite as a replacement for the boron composite is unjustified unless the fiber mixing process can be achieved at very little additional cost. For all but the most weight-critical applications, this replacement is not presently economical.

The ability of the two fiber systems to intermix suggests that the hybrid composite concept is most applicable to forming transition sections between relatively stiff boron/epoxy load-bearing elements and more workable graphite/epoxy closeout sections. Two basic transition concepts were fabricated and tested, and were shown to yield strong, aerodynamically smooth, adhesive-free transitions in a single curing process. These concepts were incorporated into a recommendation for a demonstration article, based upon the Number 5 radial beam truss of the Apollo Command Module.

NOMENCLATURE

PHYSICAL QUANTITIES

ϵ	STRAIN COMPONENT
σ, τ	STRESS COMPONENTS, ALLOWABLE STRESSES
ρ	SPECIFIC WEIGHT
γ	CALCULATED SPECIFIC GRAVITY
γ'	MEASURED SPECIFIC GRAVITY
γ_o	OVERALL SPECIFIC GRAVITY OF TRANSITION LAMINATE
α	RATIO OF GRAPHITE AND BORON FIBER WEIGHTS IN A CURED LAMINATE
w	WEIGHT FRACTION, BASED ON TOTAL WEIGHT OF LAMINATE
v	VOLUME FRACTION
$\bar{v}$	CALCULATED VOLUME FRACTION
E	YOUNG'S MODULUS
G	SHEAR MODULUS
ν	POISSON'S RATIO
η, β	CONSTANTS IN HALPIN-TSAI EQUATION

SUBSCRIPTS

11, L	PERTAINING TO LONGITUDINAL PROPERTY
22, T	PERTAINING TO TRANSVERSE PROPERTY
12, LT	PERTAINING TO IN-PLANE PROPERTY
F	PERTAINING TO FIBER PROPERTY
R	PERTAINS TO RESIN PROPERTY
B	PERTAINS TO BORON PROPERTY
G	PERTAINS TO GRAPHITE PROPERTY
a	PERTAINS TO VOIDS
w	PERTAINS TO WATER
m	PERTAINS TO INTERIM VALUE

TABLE OF CONTENTS

TABLE OF CONTENTS (Continued)

LIST OF ILLUSTRATIONS

LIST OF ILLUSTRATIONS (Continued)

LIST OF ILLUSTRATIONS (Continued)

LIST OF ILLUSTRATIONS (Continued)

LIST OF ILLUSTRATIONS (Continued)

LIST OF TABLES

SECTION I

INTRODUCTION

The demand for materials having ever higher specific strength and stiffness, yet capable of being easily manufactured, has placed a strain on advanced composite technology. In the current state-of-the-art, the commercially available boron fiber is of large diameter and lacks formability in continuous forms. The high-modulus graphite fiber has excellent formability, but is sensitive to handling procedures. Glass fiber has good formability and handling properties, but the modulus of elasticity is too low for many stiffness-critical applications. Matrix resins are available with low density and good environmental properties, but the characteristically poor shear properties severely limit the load transfer capability between adjacent fibers.

An obvious solution to this problem is the development of new fiber and matrix systems, with improved tensile and shear properties, which also operate effectively under extreme environmental conditions. Such an effort is now underway. A second approach, which builds on existing systems, is one in which the widely used "binary" composite materials are augmented by the inclusion of supplementary material. The function of this added constituent is to either enhance the shear-transfer properties of the resin matrix or to increase the volume fraction of high-modulus reinforcement in the composite. Such an augmented material can be designated a "ternary" composite. Although current application has placed the third component in a subsidiary role, the designation "ternary" should imply that the three components could be considered equal partners in the performance of a structural assignment. Moreover, the third component adds to the property-tailoring capabilities of composite materials and consequently is a feature of great potential applicability in the advanced composite technology.

The concept of ternary (and even higher-order) composite systems is nothing new in the development of material systems. The prospects for cost-effective materials with improved, tailorable properties are particularly appealing for state-of-the-art aerospace application; and many studies conducted by WRD [1] through [8] and others [9], [10] have considered rudimentary ternary composites. The majority of these studies have been concerned with matrix enhancement, rather than volume fraction improvement. In studies with filamentary composites, for example, inclusions in the form of whiskers, flakes or spheroids have been added to the matrix resin prior to incorporation of the primary fibers. Generally, the results have been tracable more to changes of the shear transfer and adhesion properties of the matrix, rather than a direct-volume fraction increase of the high-modulus reinforcement.

Under a US Government Contract (F33615-67-C-1607) WRD investigated several forms of such ternary composites.[4] In one concept, a thin "β"- glass fiber was wrapped continuously around the boron fiber. This system provided an excellent means of maintaining fiber spacing and secondary reinforcement for the resin matrix. The presence of the glass restricted the resin flow (critical in the curing of large-diameter fiber composites), and restrained the boron/fiber movement during the curing process. The glass also provided a supplemental load-transfer mechanism between adjacent fibers and adjacent plies. Under the same contract WRD also determined the potential of glass scrim cloth, which was placed between the boron/epoxy plies. This additional constituent improved the transverse strength, provided protection of boron fibers, and helped to maintain ply spacing and fiber orientation.

In more recent years, actual supplementation of the fiber volume fraction has been performed. In an earlier study by WRD [1], short boron fibers and continuous glass fibers were laminated and tested and the properties of this ternary composite were compared with those of boron-resin and glass-resin binary composites. Not only did the boron fiber inclusions improve the shear-related properties of the composite, but a definite volume fraction benefit was noticed in the longitudinal modulus of elasticity. It was demonstrated that, by variations of the volume fraction of boron and glass fibers, the modulus could be adjusted over a range between 10×10^6 and 40×10^6 psi. The results also indicated that a well-designed ternary composite material could not only be cost effective but could also be more efficient than the "parent" binary composite.

Graphite fibers have come under increased consideration recently because of the high modulus attainable with this small-diameter fiber. The handling of graphite fiber is similar in many respects to the handling of glass fiber, but the inclusion of graphite fibers into boron composites would have a more significant volume-fraction effect on stiffness than would an equal weight of glass. The potential of graphite for achieving a more efficient composite material has attracted recent interest, and is the basis for this study.

The objective of the research program presented in this report is to develop, evaluate and demonstrate feasibility of the high-modulus, mixed-fiber plastic composite concept. It is particularly desired to determine whether the mixed-fiber concept, when incorporated into a single structure, will yield a more efficient structure than one consisting of a single-fiber composite. The emphasis of this study has been placed on the mixed composite, with the various fibers thoroughly intermingled, rather than the laminated composite, with alternating layers of different prepregs. In this connection, a prepreg containing both boron and graphite fibers in an epoxy matrix has been developed and evaluated. Two joining concepts have also been proposed for transferring loads from boron/graphite/epoxy laminates into metallic closeouts. In order to provide a program directed toward aerospace structures, WRD teamed with the Space Division of North American Rockwell Corporation (NAR) to develop a representative demonstration hardware concept. A structural component was selected and recommendations made concerning future evaluation.

This study was performed under Contract NAS8-24510, "Boron/Graphite Hybrid Composite Development Study", awarded 30 June 1969 by the George C. Marshall Space Flight Center, National Aeronautics and Space Administration, and is in response to RFP No. DCN 1-9-30-35384, issued under the same title 1 April 1969.

SECTION II

ANALYSIS OF THE HYBRID CONCEPT

INITIAL CONSIDERATIONS

Fiber-resin composite materials possess several useful volumetric proportions, each of which results in the most desirable material response for a particular structural requirement. Much of composite material development is devoted to determining these optima. Commercially available forms of these materials must necessarily represent compromises between all the optimum proportions, since they do not necessarily coincide. A third component could be used, not only to improve the optimum composite properties, but to bring the corresponding optimum mixtures closer together. In such an application, it is necessary that the inclusion effects on the microstructure be clearly understood.

Consider the binary composite depicted in Figure 1a. The theoretical maximum fiber volume fraction, assuming round fibers, is 91%. Even if this fraction could be attained in practice, the high matrix stress concentrations occurring in this close-packed configuration would considerably degrade the strength properties of the composite. Increasing the fiber volume fraction of this composite would have several effects:

- The increased fiber volume fraction would lead to a rule-of-mixtures increase in tensile and compressive stiffnesses.
- The decreased fiber spacing would result in increased resistance to shearing displacement relative to planes AA' and BB'.
- The decreased fiber spacing would lead to increased matrix stress concentrations.
- Good matrix-to-fiber adhesion would be more difficult to attain, and good adhesion-dependent properties would be more difficult to achieve and maintain.

Evidently, the improvements to be gained by the volume-fraction increase are achieved at the expense of other important properties.

Figure 1b represents an attempt to recover some of the degraded properties using a third component. In this Figure, the system depicted in Figure 1a is repeated, but the resin is partially replaced by small diameter fibers. The theoretical maximum fiber volume content is 99.2% of the total cross section but resin wetting requirements dictate that the fiber volume must be much lower. In either event, inclusion of the smaller diameter fibers has an obvious volume fraction effect on this composite, but the effects on

shear and adhesion-related properties are no longer evident. No known analysis treates these important aspects of ternary composite behavior.

If, in Figure 1b, the large diameter fibers are assumed to be boron and the small diameter fibers are assumed to be graphite, several problems of considerable magnitude can arise in the production of the composite. At typical cure temperatures of 350°F, the boron fibers expand both radially and longitudinally (α = 2.8 x 10^{-6} in/in °F) [11] while the graphite fibers have a negligible coefficient of expansion in the longitudinal direction ($\alpha_L \doteq$ -0.55 x 10^{-6} in/in °F, α_T = 9.32 x 10^{-6} in/in °F) [12]. Upon cooling the cured composite this particular ternary system develops internal stresses due to the differential contractions of the three constituents. Not only is the matrix (α = 32 x 10^{-6} in/in °F) [11] under tension as a result of the different fiber radial contractions, but it is also stressed in shear as a result of the differences in longitudinal fiber contractions. Unless the matrix has sufficient toughness to withstand the resultant strains, a large number of cracks could be expected to develop between the fibers.

An important additional requirement is that of strain compatibility under load. Let us assume that a unidirectional composite has been laminated which consists of all the fiber materials shown in Figure 2. When the laminate strains uniformly under tension, the boron fiber will fail at a strain of about 0.70%. The diagram shows, however, that before this strain level is achieved, the high modulus graphite fibers (Modmor I, Thornel 50 and HMG 50) will have already exceeded their strain capability and have failed. Since failure of any fiber within the composite creates local resin failures which could, in turn, spread progressively through the material, it follows that glass, asbestos and high-strength graphite fibers are the best currently available candidates for reinforcing boron composites.

Of the three candidate fibers, the high strength graphite fiber appears to be the most feasible reinforcement material. Its high strength rivals that of glass, and its relatively high modulus exceeds that of both S-glass and asbestos. More important to the reinforcement concept, the graphite fiber is significantly lighter (γ = 1.75) than either S-glass (γ = 2.63) or asbestos (γ = 2.4 to 3.3). The high specific properties are important since reinforcement of the boron/epoxy composite will always result in a heavier composite; the higher modulus or strength of the reinforced composite is achieved at the expense of increased weight. The low modulus of glass fibers precludes their effective use in volume-fraction improvements since the laminate could be more effectively augmented (with the same weight increase) by increasing the boron volume fraction. Asbestos has potentially high strength and a fairly high modulus range, but it is very sensitive to processing and handling parameters. Special cures, related more to those of asbestos/epoxy composites than boron/epoxy composites, would be necessary. The small diameter of the asbestos fiber lends itself well to matrix-improvement, and its effects on interlaminar shear properties would be expected to be similar to that achieved by "Whiskerizing" graphite fibers. On the other hand, volume-fraction effects could be achieved more easily with the stiffer, stronger, lighter graphite fiber.

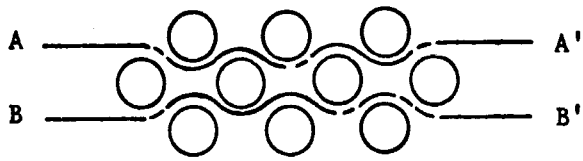

FIGURE 1a. BINARY COMPOSITE

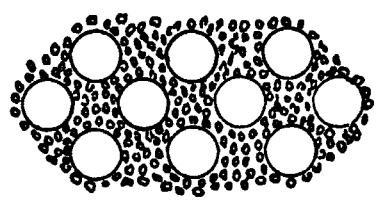

FIGURE 1b. TERNARY COMPOSITE

Figure 1. Filamentary Composite Cross Sections.

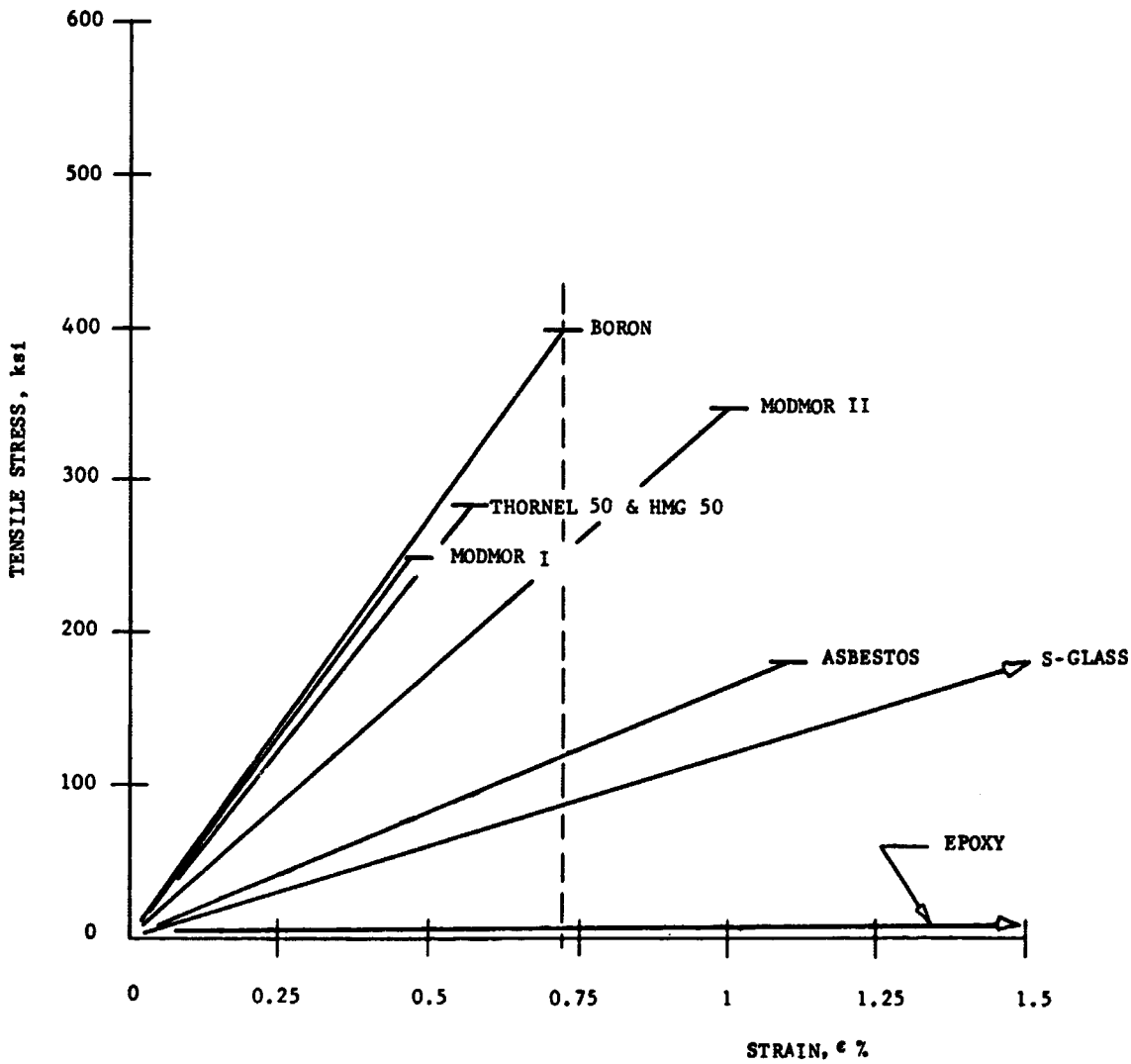

Figure 2. Stress-Strain Characteristics of Six Filamentary Materials.

In this preliminary study, the high-strength graphite fiber will be considered because of its superior handling and cure characteristics, as well as its high specific properties.

THE TERNARY DIAGRAM

The ternary diagram is a valuable tool of presentation in the fields of metallurgy and chemistry, and is particularly well-suited for describing the properties of the mixed composite. By means of this diagram, the properties can be presented in one display as a function of all possible component volume fractions. Its use will be briefly discussed in this section.

Consider the equilateral triangle shown in Figure 3 with vertices A, B and C and bisectors AE, BF and CD. If a point is chosen at random within the triangle, and the line segments GX, HX and IX are drawn perpendicular to the sides of the triangle, it can be proven that the sum of the lengths GX, HX and IX is a fixed value equal to the length CD (or AE or BF). It is this property that provides the basis for the use of the ternary diagram. If the length of CD is set at 100 units, for example, then the lengths GX, HX and IX will always total 100 units. In this case the lengths of these segments could each be determined directly in terms of percentages. With this in mind, consider Figure 4, which is a repetition of Figure 3 except that the lines AE, BF and CD (each 100 units long) are replaced by the lines v_B, v_G and v_R (each 100 percentage points long). Since these lines are each 100 units long, then the lengths GX, HX and IX are the volume fractions v_G, v_R and v_B, respectively, of the mixture designated "X". Correspondingly, the mixture X has volume fractions v_G = 18%, v_R = 52% and v_B = 30%, while the mixture Y has volume fractions v_G = 25%, v_R = 12% and v_B = 63%. If we designate v_B, v_G and v_R the volume fraction of boron, graphite and resin, respectively, then the positions X and Y represent particular ternary composites of these three components.

Properties which are functions of the volume fractions (i.e., modulus, strength or density) can be plotted on the ternary diagram in map form, in much the same way that isotherms are plotted on a heated body. Consider the longitudinal modulus E_{11} of a unidirectional ternary composite consisting of boron, Modmor II and 2387 epoxy. This modulus is determined by the rule of mixtures

$$E_{11} = v_B E_B + v_G E_{GL} + v_R E_R \qquad (1)$$

where E_B, E_{GL} and E_R are the longitudinal moduli of boron, Modmor II and 2387 epoxy, respectively. Using the moduli shown in Table I, the traces

for E_{11} = 10, 20, 30, 40 and 50 x 10^6 psi are shown in Figure 5. Once this "map" is plotted, the moduli of mixtures X and Y can be determined by locating their positions on the ternary diagram and interpolating. Thus, for mixture X the modulus E_{11} is slightly over 25 x 10^6 psi, while for mixture Y it is 4.75 x 10^6 psi.

The ternary diagram can also be used to estimate the errors in the modulus. Suppose, for example, the mixture Z shown in Figure 5 can be controlled within ±2% on each volume fraction. The modulus E_{11} of this mixture then varies over the range indicated by the hexagon, i.e., $E_{11} \doteq 35 \pm 2 \times 10^6$ psi. If this modulus must be more precisely controlled, the ternary diagram can be used to determine the necessary improvements in volume-fraction control.

Any function of the three constituent volume fractions can be mapped on the ternary diagram. Since it provides the overall picture in a single graph, it becomes a valuable aid to interpretation and design of ternary composites. Some properties of the Boron/Modmor II/2387 Epoxy ternary composite will be developed in the next section.

DETERMINATION OF VOLUME FRACTIONS FOR THE BORON/MODMOR II/2387 EPOXY COMPOSITE

The properties of the hybrid composite can be determined by means of the rule of mixtures and the Halpin-Tsai [13] equation, once the constituent volume fractions have been determined. Ideally, only three volume fractions v_B, v_G and v_R need to be determined, but it is always necessary to include the void volume fraction v_a in the calculations. These four "unknowns" can only be determined by means of four independent relationships, either analytical or experimental in nature. In this program, the volume fractions were computed from the experimentally determined specific gravity (γ'), resin weight fraction (w_R) and the fiber weight ratio (α). The fourth relationship is simply an anlytical requirement that the sum of the volume fractions equal unity, i.e.;

$$v_B + v_G + v_R + v_a = 1 \tag{2}$$

The methods for determining these values will be outlined in the following paragraphs.

a) The measured specific gravity γ' is obtained from the weight of test samples in water and in air, by the equation

$$\gamma' = \frac{W_a}{W_a - W_w} \tag{3}$$

where W_a = weight of laminate in air
W_w = weight of laminate in water

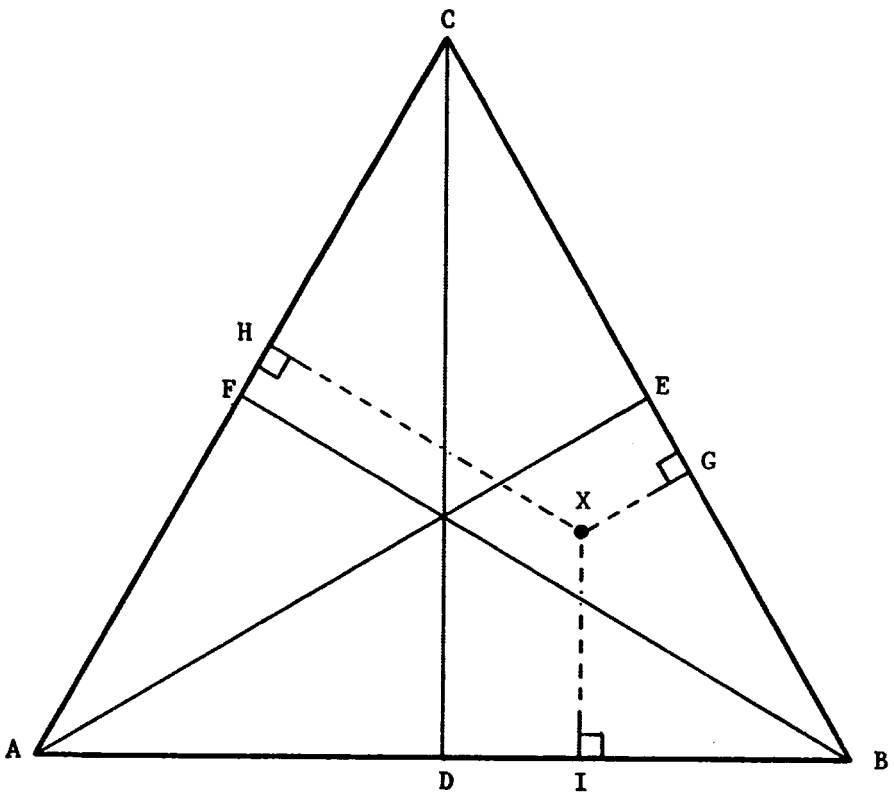

Figure 3. Basic Ternary Diagram.

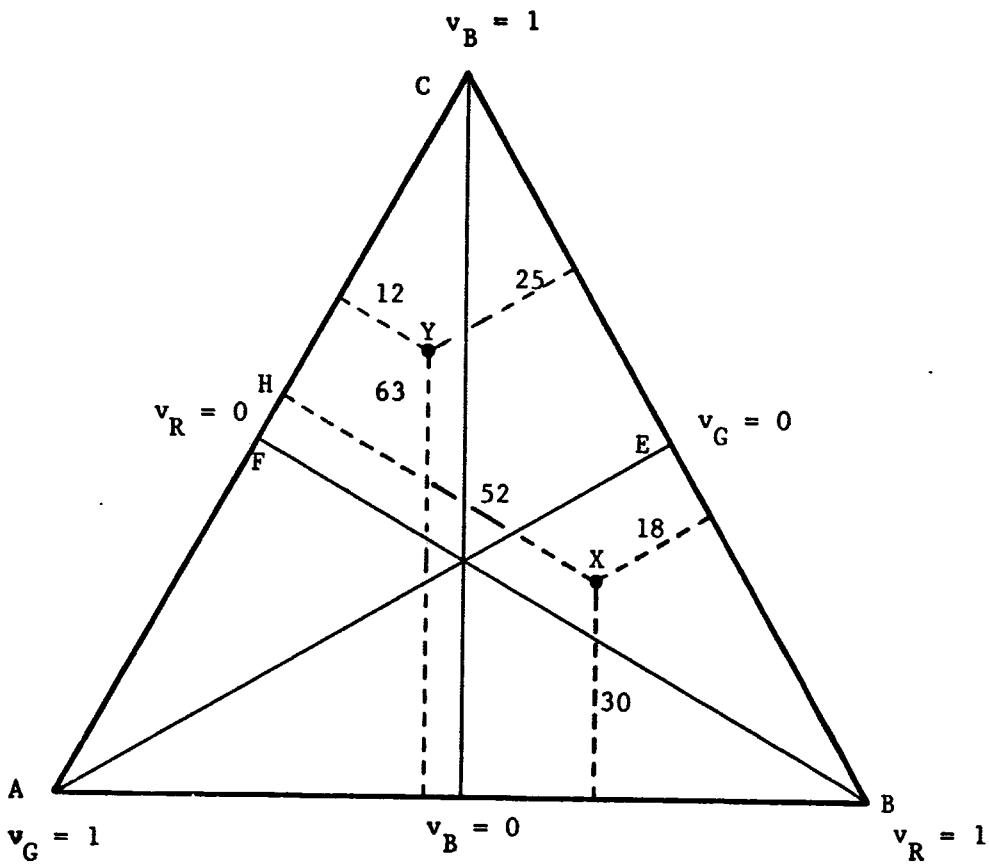

Figure 4. Ternary Diagram with Volume Fraction Coördinates.

TABLE I. TYPICAL PROPERTIES OF CONSTITUENTS

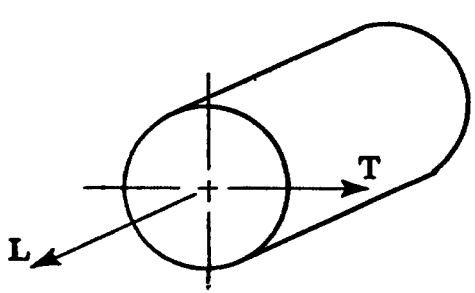

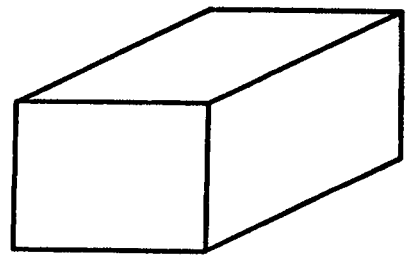

	FIBER			MATRIX	
	BORON	MODMOR I	MODMOR II	EPOXY	POLYIMIDE
E_{fL}, psi	60×10^6 [11]	64.9×10^6 [18]	38.6×10^6 [18]	0.5×10^6 [11]	0.4×10^6 [11]
E_{fT}, psi [1]	60×10^6	1.5×10^6	1.5×10^6	0.5×10^6	0.4×10^6
ν_{LT} [1]	0.2	0.2	0.2	0.35	0.33
G_{LT}, psi [1]	25×10^6	4×10^6	4×10^6	0.19×10^6	0.17×10^6
γ, gm/cc	2.63 [11]	2.00 [18]	1.74	1.23	1.3
$(\sigma)_{ult}$, psi	400,000 [11]	247,000	403,000	----	----

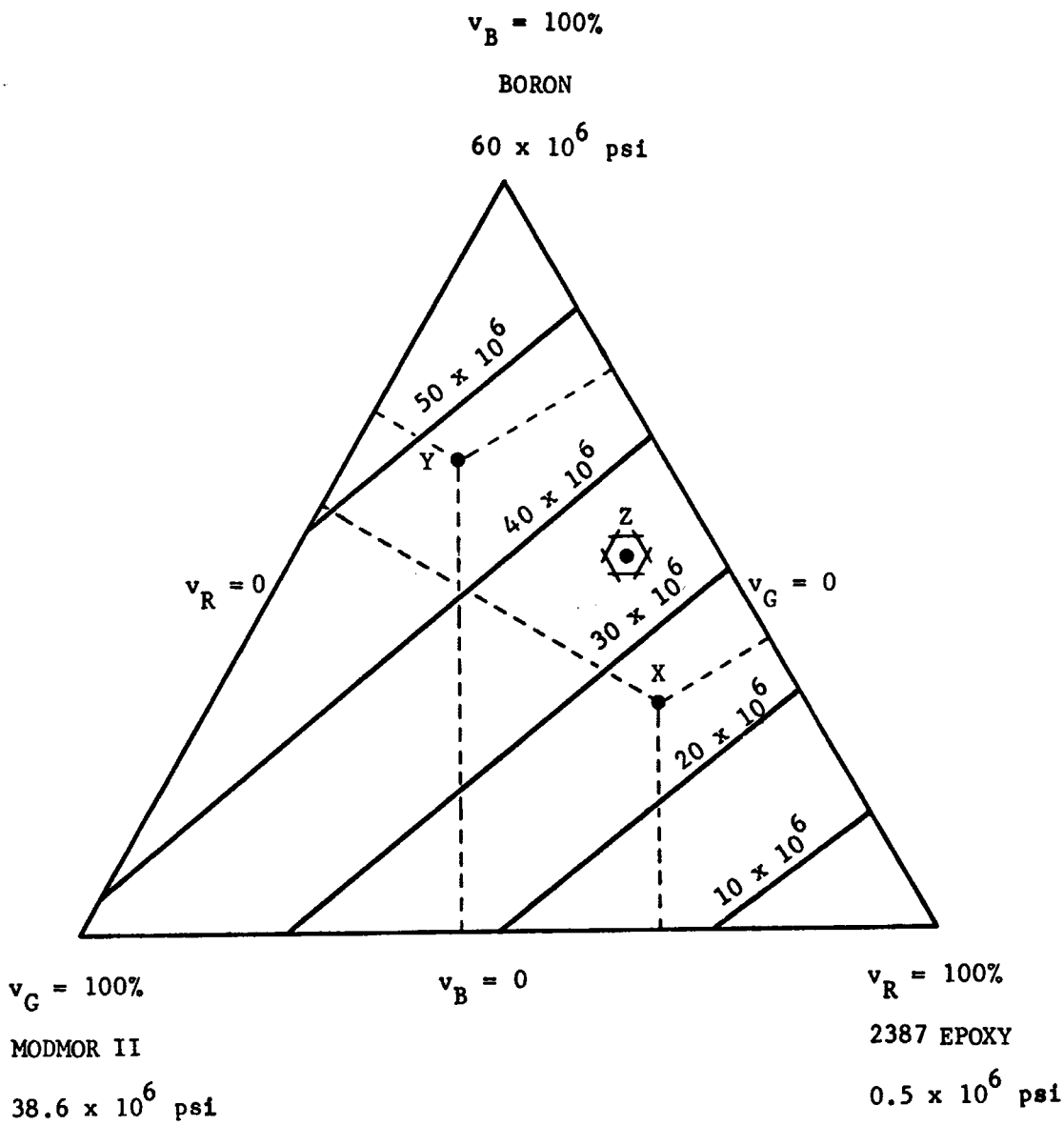

Figure 5. Longitudinal Modulus E_{11} for Boron/Modmor II/2387 Epoxy Composite, Plotted on the Ternary Diagram.

b) The resin weight fraction w_R is obtained after an acid digestion of the laminate, by means of the equation

$$w_R = \frac{W_a - W_F}{W_a} \tag{4}$$

where W_a = weight of laminate in air

W_F = weight of fiber residue after acid digestion

The acid digestion procedure is detailed in Appendix B.

c) The fiber weight ratio α is obtained from weight records made during the layup:

$$\alpha = \frac{W_G}{W_B} \tag{5}$$

where W_G is the weight of Modmor II fiber, referred to a reference area of the prepreg

W_B is the weight of boron fiber, referred to the same reference area of the prepreg

The volume fractions can be determined from the relations (2-5) after first determining the weight fractions w_B and w_G of the boron and graphite fibers.

d) The boron weight fraction w_B is obtained from the fiber weight fraction and resin weight fraction:

$$w_B = \frac{1 - w_R}{1 + \alpha} \tag{6}$$

where w_R is the resin weight fraction from (4)

α is the fiber weight ratio from (5)

e) The Modmor II weight fraction w_G is obtained from the boron weight fraction and resin weight fraction:

$$w_G = \alpha\, w_B \tag{7}$$

where w_B is the boron weight fraction from (6)

α is the fiber weight ratio from (5)

The fiber and resin volume fractions v_B, v_R and v_G can then be determined directly from the weight fractions and the measured specific gravity γ'.

f) The resin volume fraction v_R is determined from the resin weight fraction by the relation:

$$v_R = \frac{\gamma'}{\gamma_R} w_R \tag{8}$$

where γ' is the measured specific gravity of the laminate, from (3)

γ_R = 1.23, specific gravity of 2387 resin

w_R is the resin weight fraction from (4)

g) The boron volume fraction v_B is determined in a manner analogous to that for v_R:

$$v_B = \frac{\gamma'}{\gamma_B} w_B \tag{9}$$

where γ' is the measured specific gravity of the laminate, from (3)

γ_B = 2.63, specific gravity of the boron fiber

w_B is the weight fraction of the boron fiber, from (6)

h) The Modmor II volume fraction v_G is determined in a manner analogous to that for v_R:

$$v_G = \frac{\gamma'}{\gamma_G} w_G \tag{10}$$

where γ' is the measured specific gravity of the laminate from (3)

γ_G = 1.74, specific gravity of Modmor II fiber

w_G is the weight fraction of the Modmor II fiber from (7)

The void volume fraction v_a must be determined by comparing the actual specific gravity γ' and the ideal (void free laminate) specific gravity γ.

i) The ideal specific gravity γ, is determined from the measured resin weight fraction and the measured fiber weight fraction, assuming no voids:

$$\gamma = \frac{1}{\frac{1-w_R}{1+\alpha}\left(\frac{1}{\gamma_B} + \frac{\alpha}{\gamma_G}\right) + \frac{w_R}{\gamma_R}} \qquad (11)$$

where w_R is the resin weight fraction from (4)

γ_R = 1.23, specific gravity of 2387 resin

γ_G = 1.74, specific gravity of Modmor II fiber

γ_B = 2.63, specific gravity of boron fiber

α is the fiber weight ratio from (5)

j) The void volume fraction v_a is obtained from the ideal actual specific gravities by the relationship

$$v_a = \left(1 - \frac{\gamma'}{\gamma}\right) \qquad (12)$$

where γ = calculated specific gravity of the laminate, from (11)

γ' = measured specific gravity of the laminate, from (3)

The relationship (12) is inherently a more accurate one than (2) for obtaining the void volume fraction. This arises because, in the latter, the result is subject to relatively large round-off error in the subtraction of nearly equal calculated quantities, while the former relies directly on measured and known quantities.

The equations (2) through (12) are cumbersome for use in determining volume fractions and void content, and it is of practical value to have a graphical method for transforming from the measured values (γ', w_R and α) to these quantities. The ternary diagrams provide this method.

The ideal specific gravity γ of a void-free hybrid laminate is plotted in Figure 6. The lines shown in this diagram represent loci of mixtures having equal specific gravity Γ. Thus, the mixture A, with $v_B = 0.55$, $v_G = 0$, $v_R = 0.45$, has the same specific gravity ($\gamma = 2.0$) as the mixture B, with $v_B = 0.475$, $v_G = 0.20$, $v_R = 0.325$. The most effective means of reducing the specific gravity of laminate B would be to alter component volume fractions along the line BC, rather than along BD, for example. Similarly, Figure 7 represents lines of equal resin weight fraction w_R for the void-free laminate. In this case, paths BC and BD lead to essentially the same weight fraction, and the choice between them becomes determined by other factors, such as economics. Figure 8 is a chart simultaneously showing the ideal specific gravity γ, the resin weight fraction w_R and the fiber weight ratio α. When the laminate is void-free, the intersection of the lines w_R = constant and α = constant will not only determine the ideal laminate volume fractions $\bar{v}_B$, $\bar{v}_G$ and $\bar{v}_R$, but will also determine the specific gravity Γ. Thus for a fiber weight ratio $\alpha = 0.20$ and a resin weight fraction $w_R = 0.25$, the laminate A is found to have a specific gravity $\gamma = 1.95$, with ideal volume fractions $\bar{v}_B = 0.465$, $\bar{v}_G = 0.140$ and $\bar{v}_R = 0.395$. When the panel is void-free, the ideal and actual specific gravities will coincide. When the panel contains voids, the actual specific gravity (γ') will be lower than the ideal value (Γ). Thus, if the specific gravity for panel A is actually $\gamma' = 1.93$, by measurement, the panel void content can be determined using (12):

$$v_a = 1 - \frac{\gamma'}{\gamma} = 1 - \frac{1.93}{1.95} = 0.01.$$

The actual volume fractions of the laminate A are then found by proportion:

$$v_B = 0.99\ (0.465) \doteq 0.460$$

$$v_G = 0.99\ (0.140) \doteq 0.140$$

$$v_R = 0.99\ (0.395) \doteq 0.390$$

$$v_a = 0.01$$

The void fraction v_a can also be determined directly from the graph in Figure 9, given the specific gravities γ' and γ:

Figure 8 and 9 serve as the basic diagrams from which the four volume fractions can be determined. Their use in this report is summarized as follows:

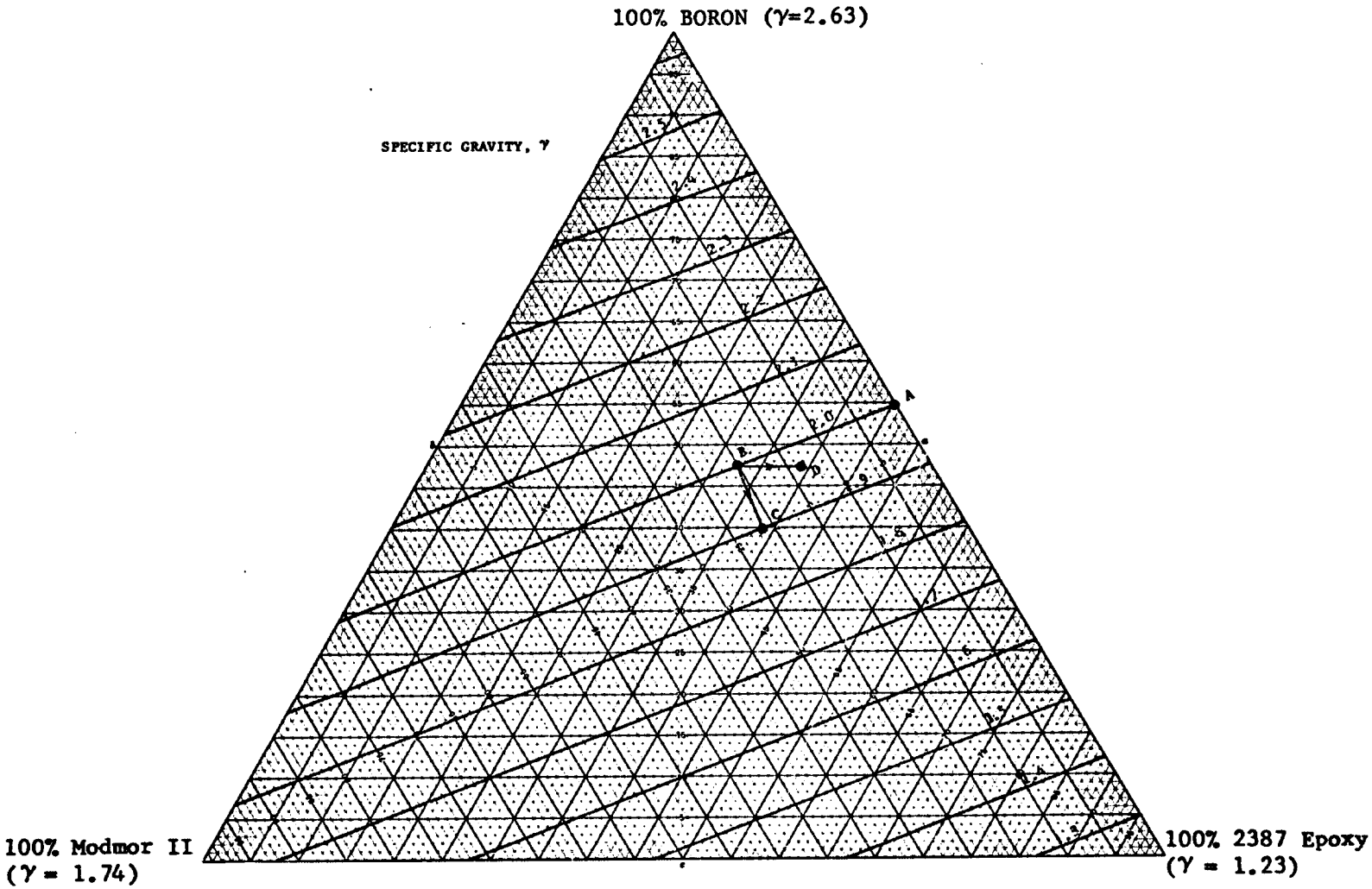

Figure 6. Specific Gravity γ of a Void-Free Boron/Modmor II/2387 Epoxy Laminate.

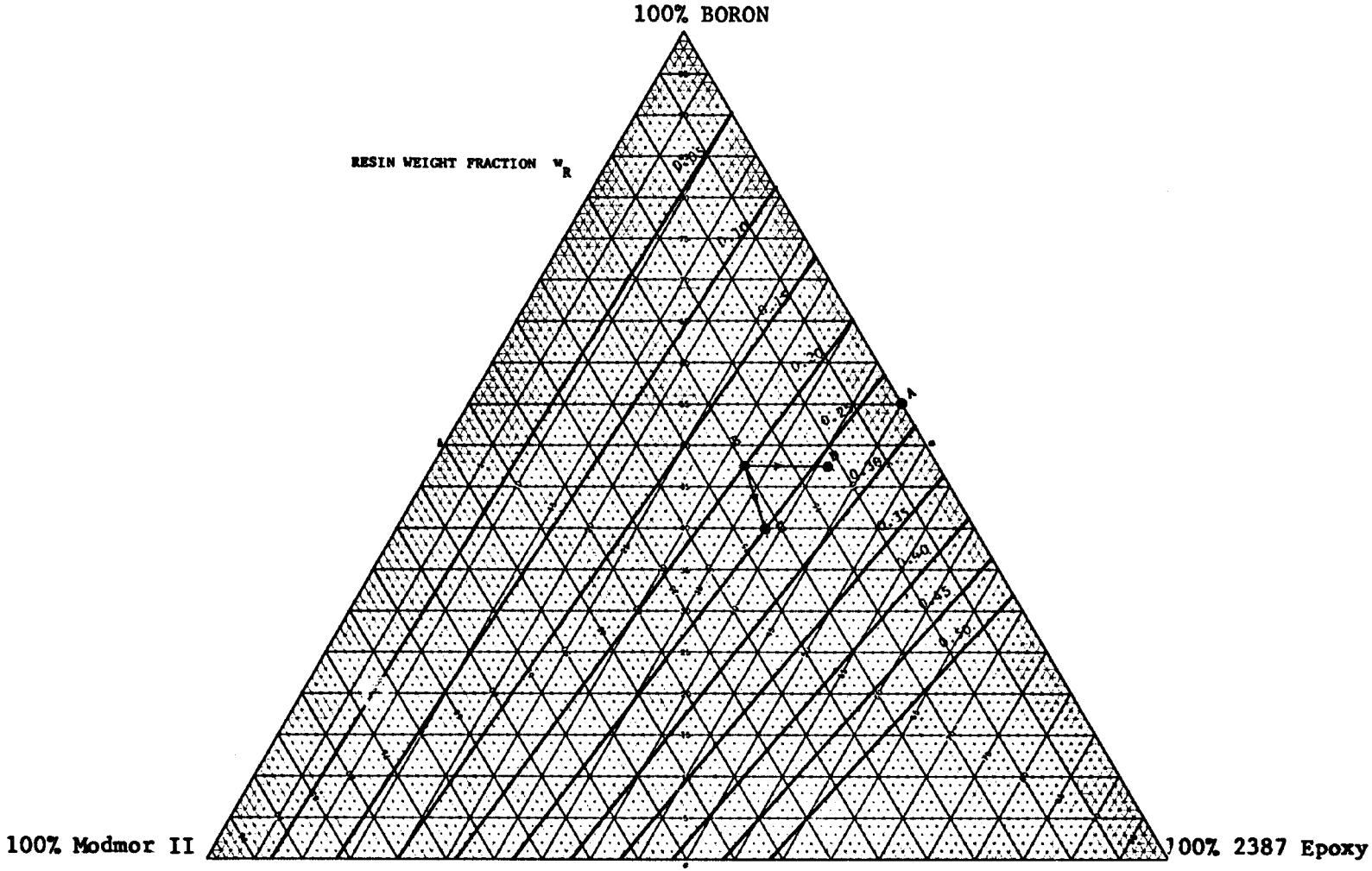

Figure 7. Resin Weight Fraction w_R for a Void-Free Boron/Modmor II/2387 Epoxy Laminate.

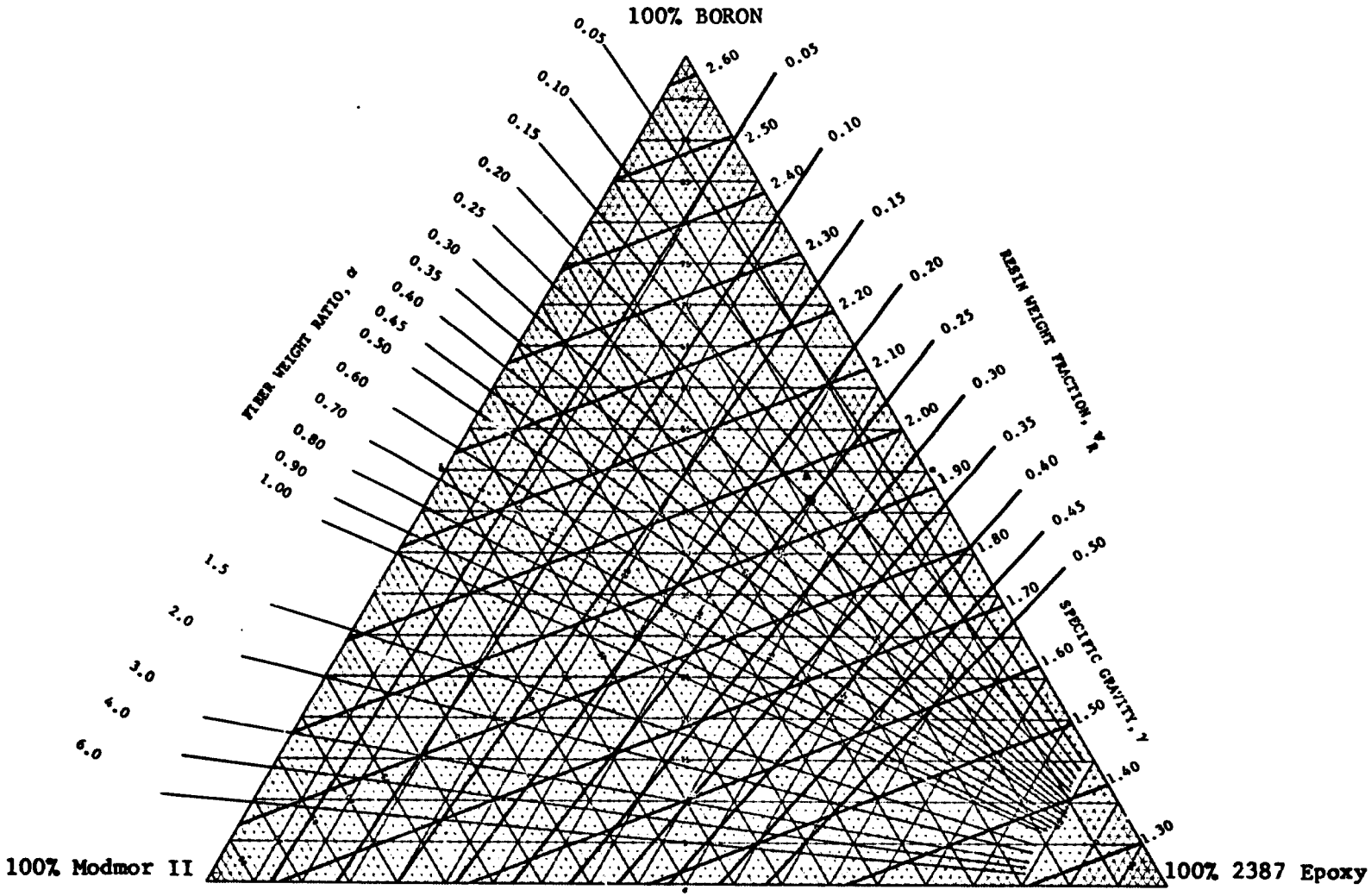

Figure 8. Specific Gravity γ, Fiber Weight Ratio α and Resin Weight Fraction w_R for a Void-Free Boron/Modmor II/2387 Epoxy Laminate.

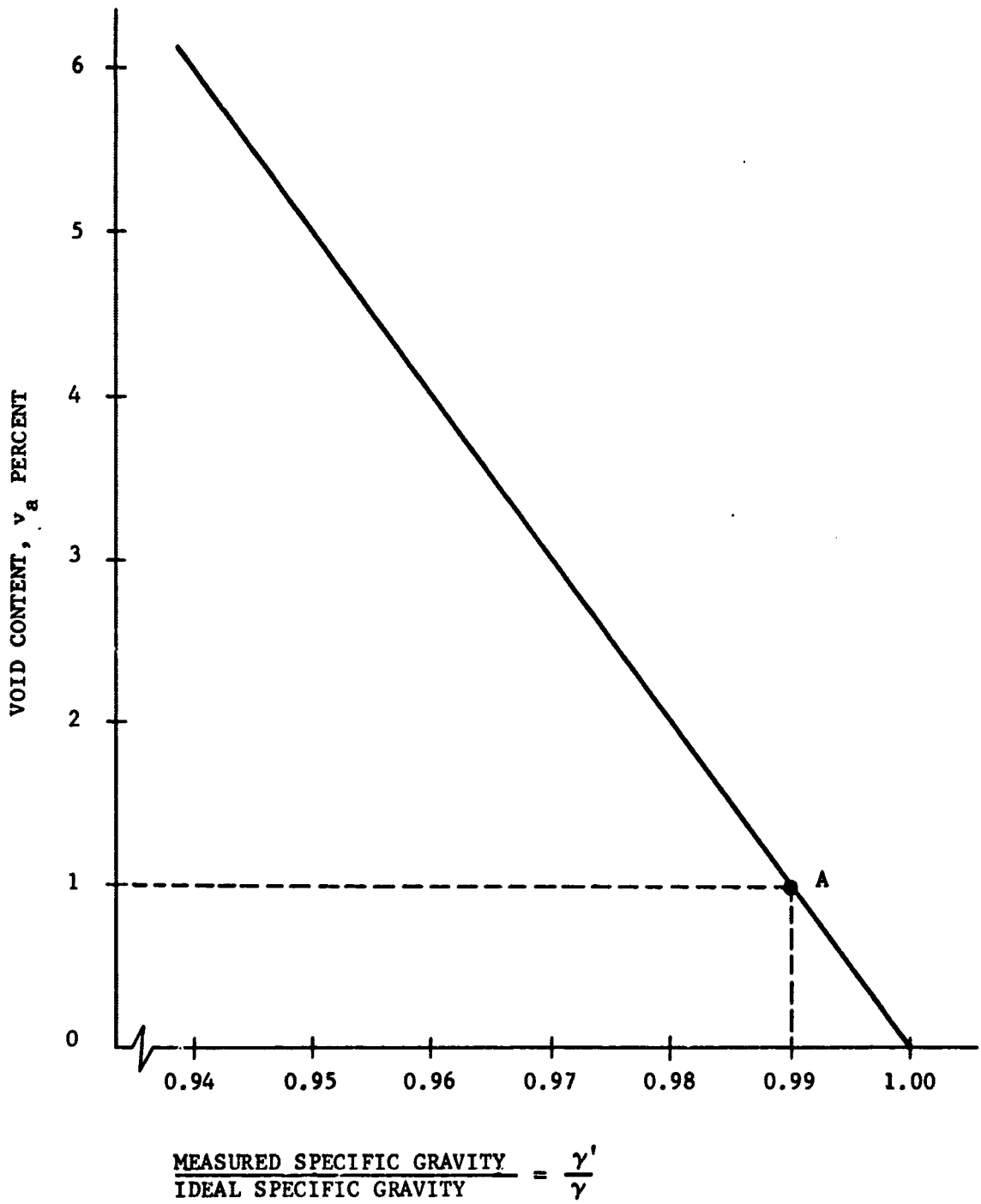

Figure 9. Relationship Between Measured and Ideal Specific Gravities and the Void Content v_a.

- Determine a) the fiber weight ratio α from lay up control, b) the resin weight fraction w_R from acid digestion of the cured laminate, and c) the specific gravity γ' by weighing the cured laminate in air and water.

- From the intersection of the corresponding α = constant and w_R = constant lines in Figure 8, determine the ideal specific gravity γ and the ideal fractions $\bar{v}_B, \bar{v}_G, \bar{v}_R$.

- Determine the ratio γ'/γ and, from Figure 9, the corresponding void volume fraction v_a.

- Compute actual volume fractions v_B, v_G, v_R of the laminate from the relationships $v_G = (1-v_a)\bar{v}_G$, $v_B = (1-v_a)\bar{v}_B$ and $v_R = (1-v_a)\bar{v}_R$

STIFFNESS PROPERTIES OF THE BORON/MODMOR II/2387 EPOXY COMPOSITE

The moduli of the unidirectional hybrid laminate can be determined using the known volume fractions and constituent properties. The longitudinal modulus E_{11} and the Poisson's ratio ν_{12} are determined with suitable accuracy using the rule of mixtures, while the transverse modulus E_{22} and in-plane shear modulus G_{12} can be determined (for small graphite volume fractions) by means of the Halpin-Tsai [11, 13] equations. The procedure will be reviewed in the following paragraphs.

a) The Longitudinal Modulus E_{11} is determined from the rule of mixtures:

$$E_{11} = v_B E_B + v_G E_{GL} + v_R E_R \tag{13}$$

where $E_B = 60 \times 10^6$ psi, modulus of boron fiber

$E_{GL} = 38.6 \times 10^6$ psi, longitudinal modulus of Modmor II fiber

$E_R = 0.5 \times 10^6$ psi, modulus of 2387 Epoxy Resin

b) The Poisson's Ratio ν_{12} is also determined from the rule of mixtures:

$$\nu_{12} = v_B \nu_B + v_C \nu_{12G} + v_R \nu_R \tag{14}$$

where ν_B = 0.2, Poisson's ratio of boron fiber

ν_{12G} = 0.2, Poisson's ratio of Modmor II fiber

ν_R = 0.35, Poisson's ratio of 2387 epoxy resin

c) The Transverse Modulus E_{22} is estimated by means of the Halpin-Tsai equations [11]

$$E_{22} = \frac{1 + 2\eta v_B}{1 - \eta v_B} \cdot E_m \tag{15}$$

where

$$\eta = \left(\frac{E_B}{E_m} - 1\right) \Big/ \left(\frac{E_B}{E_m} + 2\right) \tag{16}$$

$$E_m = \frac{1 + 2\beta v_{G/(1-v_B)}}{1 - \beta v_{G/(1-v_B)}} \cdot E_R$$

$$\beta = \left(\frac{E_{GT}}{E_R} - 1\right) \Big/ \left(\frac{E_{GT}}{E_R} + 2\right) \tag{18}$$

E_B = 6.0 x 10^6 psi, modulus of boron fiber

E_{GT} = 1.5 x 10^6 psi, transverse modulus of Modmor II fiber

E_R = 0.5 x 10^6 psi, modulus of 2387 epoxy resin

E_m = Intermediate modulus of graphite/epoxy matrix

This relationship is good only for small graphite volume fractions v_G. When the graphite volume fraction approaches that of boron (v_B), the graphite fibers can no longer be considered "matrix reinforcement", and more complex finite-element analyses are needed to perform the estimation.

d) The In-plane Shear Modulus G_{12} is estimated in a similar manner from the Halpin-Tsai relations [11]

$$G_{12} = \frac{1 + \eta v_B}{1 - \eta v_B} \cdot G_m \tag{19}$$

where

$$\eta = \left(\frac{G_B}{G_m} - 1\right) \Big/ \left(\frac{G_B}{G_m} + 1\right) \tag{20}$$

and

$$G_m = \frac{1 + \beta v_G/(1 - v_B)}{1 - \beta v_G/(1 - v_B)} \cdot G_R \tag{21}$$

where

$$\beta = \left(\frac{G_{GLT}}{G_R} - 1\right) \Big/ \left(\frac{G_{GLT}}{G_R} + 1\right) \tag{22}$$

$G_B = 25 \times 10^6$ psi, shear modulus of boron fiber

$G_{GLT} = 4 \times 10^6$ psi, shear modulus of Modmor II fiber

$G_R = 0.185 \times 10^6$ psi, shear modulus of 2387 epoxy resin

G_m = intermediate shear modulus of graphite/epoxy "matrix"

The same assumptions for E_{22} also apply to G_{12}.

The Halpin-Tsai equations can not be construed as being exact, but they are believed to provide good indications of the effects of fiber reinforcement.

The longitudinal modulus E_{11} is plotted in Figure 10, as a function of graphite volume fraction, for five values of resin volume fraction. Note for mixture A that the replacement of boron by graphite (v_R = constant) results in a reduction of composite modulus (mixture B), while the replacement of resin by graphite (v_a = constant) results in a substantially increased modulus (mixture C). This is better illustrated in Figure 11, where the results of (13) are plotted on a ternary diagram. Here, it can be seen that the paths AB and AC are not optimum for increasing the longitudinal modulus. In fact, the optimum path is actually AD, which is perpendicular to the line $E_{11} = 40 \times 10^6$ psi. Path AD is also shown in Figure 10, but its optimum nature is not so obvious here.

The specific modulus E_{11}/ρ is a nonlinear function since it is the quotient of two linear functions modulus E_{11} and specific weight ρ. Figure 12 shows this property as a function of v_G for five values of v_R. The paths AB and AC are plotted as before, and the effects of the various changes are similar to those discussed earlier. The same property is shown in the

ternary diagram of Figure 13. Note here that the optimum path AE is slightly different from path AD. Path AE is also shown in Figure 12, where its special character is not readily apparent.

The Poisson's ratio ν_{12} is shown in Figure 14. Note that the ν_{12} = constant lines are parallel to the v_R = constant lines. This is due to the fact that the boron and Modmor II fibers have the same Poisson's ratio, and the laminate value is essentially a function of the resin volume fraction alone.

The transverse modulus E_{22} is plotted in the ternary diagram of Figure 15. Only a limited range of volume fractions is shown in this Figure, in accord with the limitations of the Halpin-Tsai equations. Note that the function is nonlinear. The paths AB and AC lead to the expected reductions and increases of transverse modulus, while the path AF (replacement of resin by boron, or direct augmentation) is nearly optimum. The in-plane shear modulus G_{12} is shown in Figure 16. Note similar behavior for paths AB and AC, with the optimum path AG. Path AG would correspond to a removal of resin from the laminate mixture A. In other words, a "drier" (but void-free) prepreg would yield a higher shear modulus G_{12} than that of mixture A.

In determing both E_{22} and G_{12}, the effects of the Modmor II fiber anisotropy have been taken into account; thus, the longitudinal modulus $E_{GL} \doteq 1.5 \times 10^6$ psi is used for the graphite fiber, while the modulus $E_L = E_T = E_B = 60 \times 10^6$ psi has been used for the nearly isotropic boron fiber. It should be emphasized that significant errors and misjudgements can result if the graphite fiber is assumed isotropic. Consider, for example, a boron/Modmor II/2387 epoxy laminate with a fixed graphite volume fraction $v_G = 0.15$. Figure 17 shows the effects of the assumed transverse modulus E_{GT} on the predicted laminate transverse modulus E_{22}, for three different boron fractions. Note that if the fiber were assumed isotropic, a very optimistic prediction would be obtained for the improvement of transverse modulus. In the neighborhood of more typical values of fiber modulus ($E_{GT} \sim 1.5 \times 10^6$ psi), somewhat smaller improvements could be expected, and the estimated modulus E_{22} would be quite sensitive to variations in E_{GT}. Figure 18 shows a similar plot for the laminate in-plane shear modulus G_{12}. This "isotropic-fiber" shear modulus $G_{Lt} \doteq 16.5 \times 10^6$ psi leads to higher estimates of panel shear modulus G_{12} than the more typical value $G_{Lt} \doteq 4 \times 10^6$ psi. In this case, however, the errors incurred by the higher assumed value are not large. Obviously, it would be most desirable to use an isotropic fiber with the specific properties and handling characteristics of graphite, in which case the

improved transverse and in-plane shear moduli of the hybrid composite would become significant design factors. Because of the anisotropy of the graphite fiber, however, the laminate moduli E_{22} and G_{12} are apparently not increased sufficiently to change current design practices.

The significance of fiber anisotropy in graphite composites is discussed in more detail in Reference [14].

STRENGTH PROPERTIES OF THE BORON/MODMOR II/2387 EPOXY COMPOSITE

The longitudinal strength σ_{11} of the mixed composite cannot be determined directly from the rule of mixtures, because the maximum strains are not the same for the two classes of fibers. Although boron features high strength and modulus, its maximum strain (~0.7%) is less than that of Modmor II (~1.0%). Thus, when the laminate is strained uniformly, the boron fibers will fail first at an overall laminate strain of 0.7%. The remaining graphite fibers may possess enough residual strength to assume the boron fiber loads, in which case the laminate will be capable of sustaining even higher loads before the final catastrophic failure at 1% strain. After the initial boron failures, however, the laminate will exhibit reduced modulus due to partial loss of the boron reinforcements, and will exhibit and ultimate strength less than that of a boron-free graphite/epoxy laminate.

When small quantities of graphite are used, failure of the boron fibers will still occur at 0.7% strain, but the remaining graphite fibers will be insufficient to further sustain the load. In this case, the initial failure at 0.7% is the beginning of a catastrophic laminate failure.

The dead-load stress-strain curves for these two cases are shown in Figure 19. The behavior of two hybrid mixtures are depicted: Mixture I with relatively high graphite volume fraction ($v_G = 0.63$, $v_B = 0.07$, $v_R = 0.30$) and mixture II with intermediate volume fraction ($v_G = 0.35$, $v_B = 0.35$, $v_R = 0.30$). Note the step in the response of Mixture I. This "yield" load effect is achieved at the price of lower final modulus; the initially-failed laminate would, upon unloading, exhibit the reduced modulus of a Modmor II panel with low volume fraction. On the other hand, the initial failure would not be catastrophic. Mixture II would behave as a reinforced boron laminate, with improved modulus and strength (over a $v_B = 0.35$, $v_R = 0.65$ "basic" laminate), and exhibiting a linear stress-strain curve to ultimate failure. The curves shown in Figure 19 are strictly correct only if the boron fibers fail simultaneously and completely at 0.7% strain. Since failed fibers with reduced length can still sustain a fraction of their original loads, and since they do not fail simultaneously, the actual dead-load curves would possess continuous slope changes rather than the straight-line segments shown.

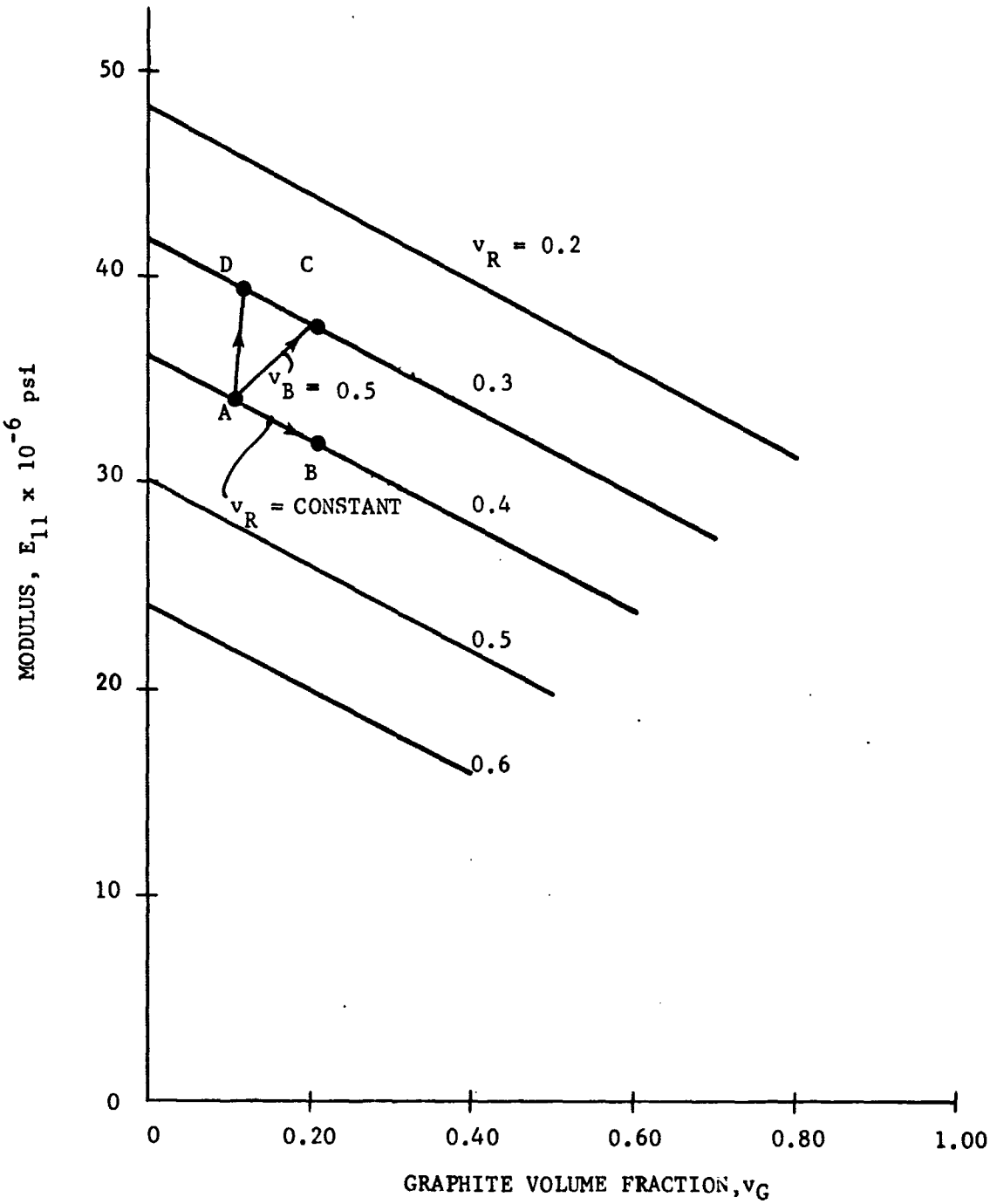

Figure 10. Longitudinal Modulus E_{11} of Boron/Modmor II/2387 Epoxy Composite.

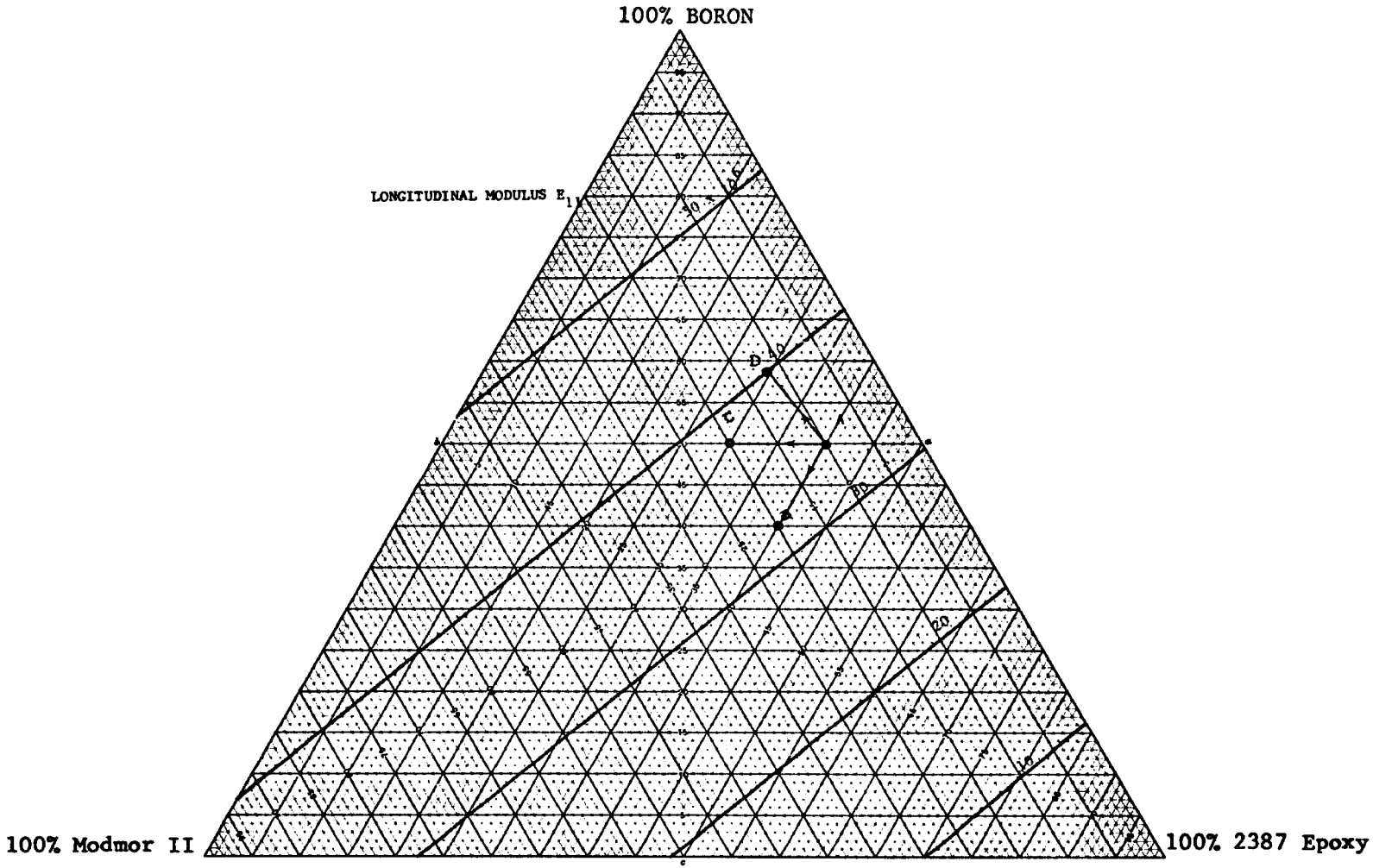

Figure 11. Longitudinal Modulus E_{11} of Boron/Modmor II/2387 Composite; Ternary Diagram.

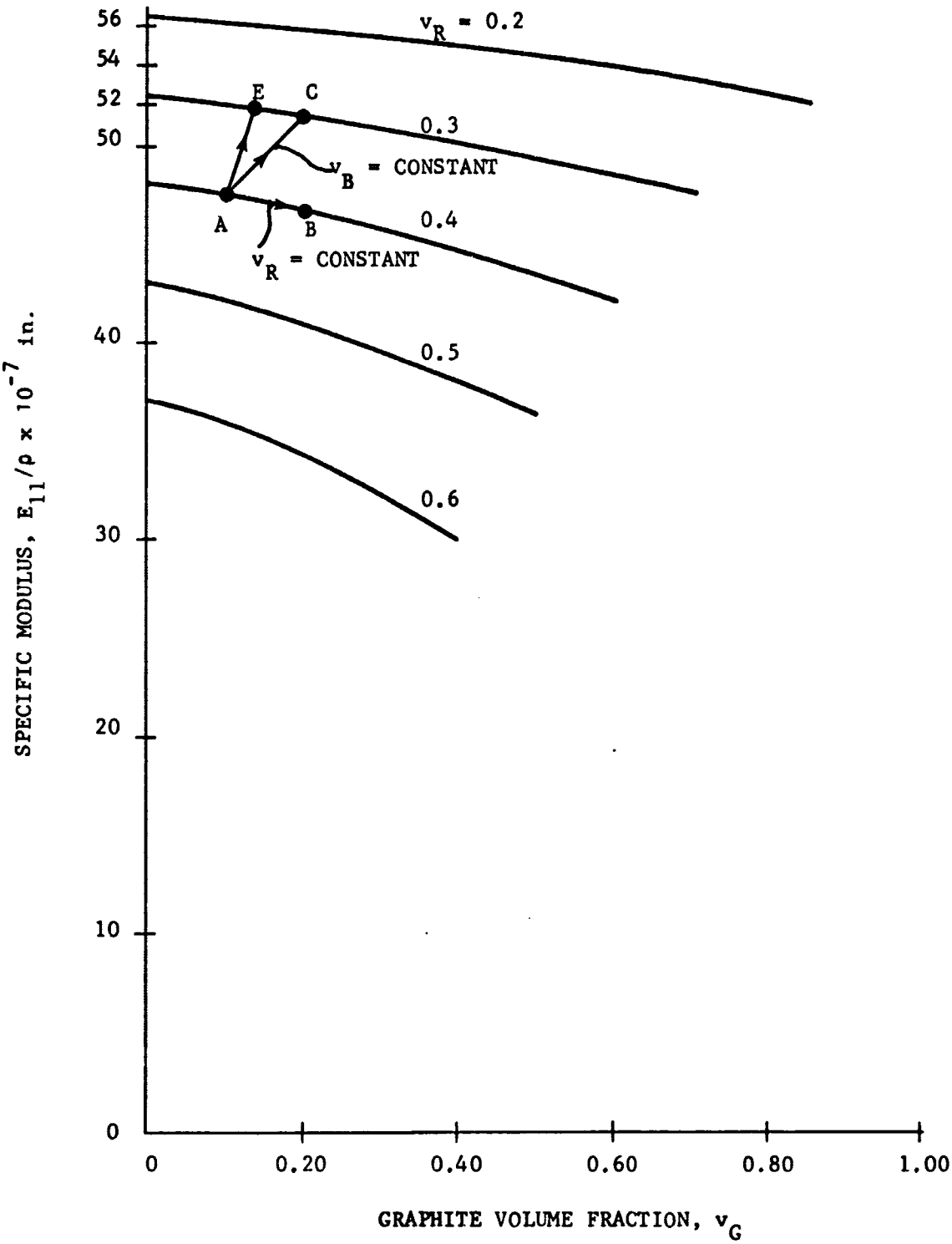

Figure 12. Specific Modulus E_{11}/ρ of Boron/Modmor II/2387 Epoxy Composite.

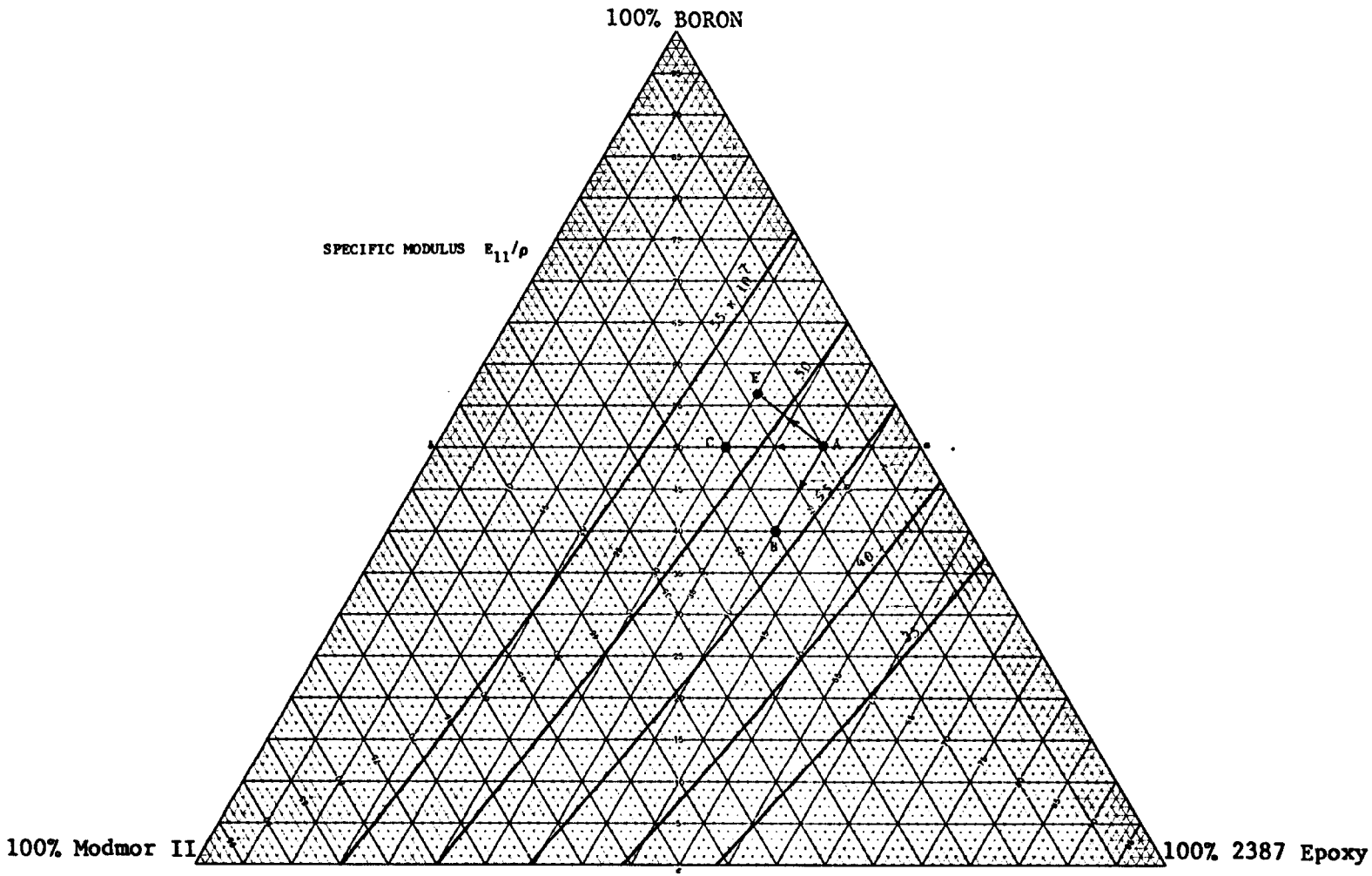

Figure 13. Specific Modulus E_{11}/ρ of Boron/Modmor II/2387 Epoxy Composite; Ternary Diagram.

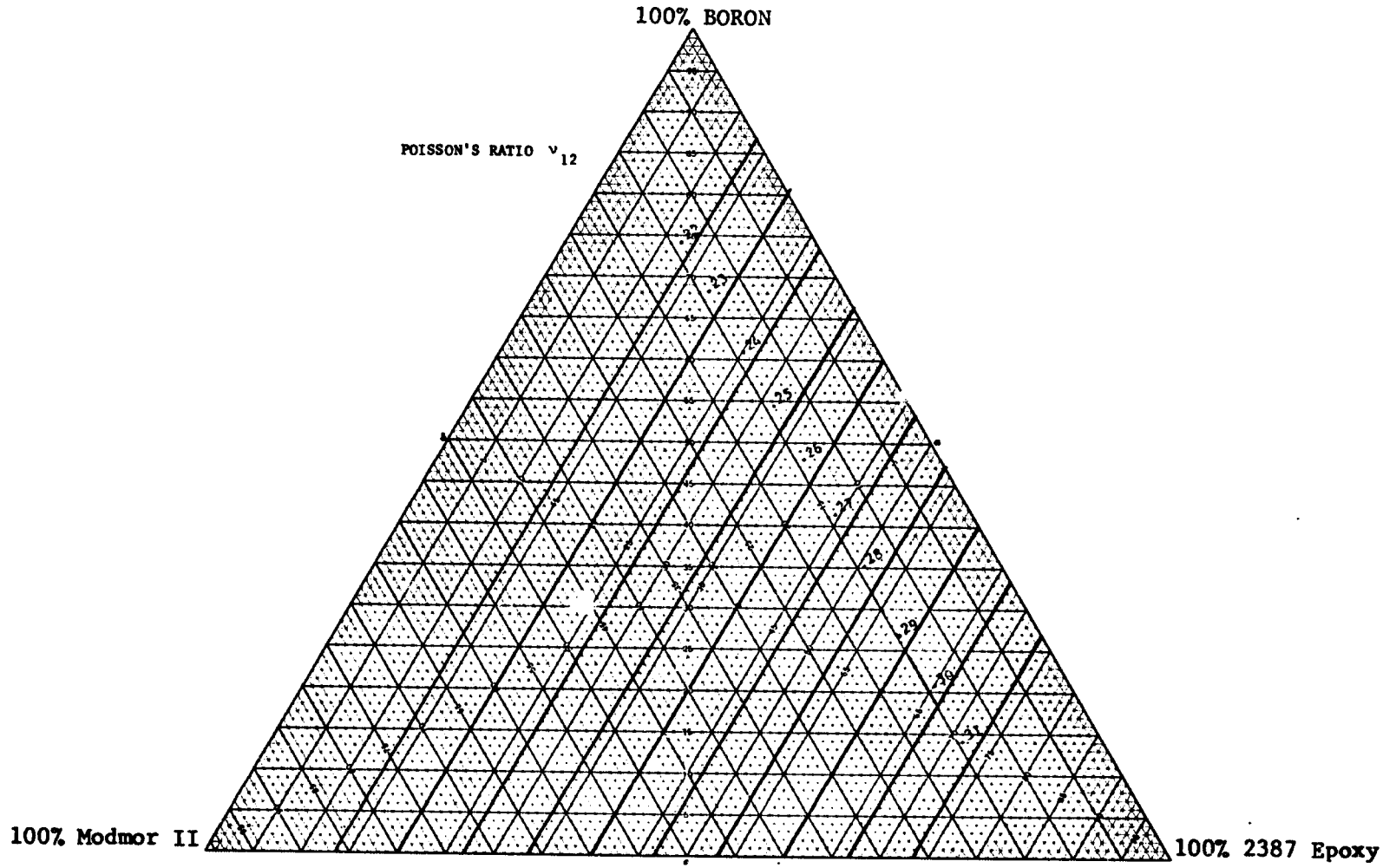

Figure 14. Poisson's Ratio ν_{12} of Boron/Modmor II/2387 Epoxy Composite.

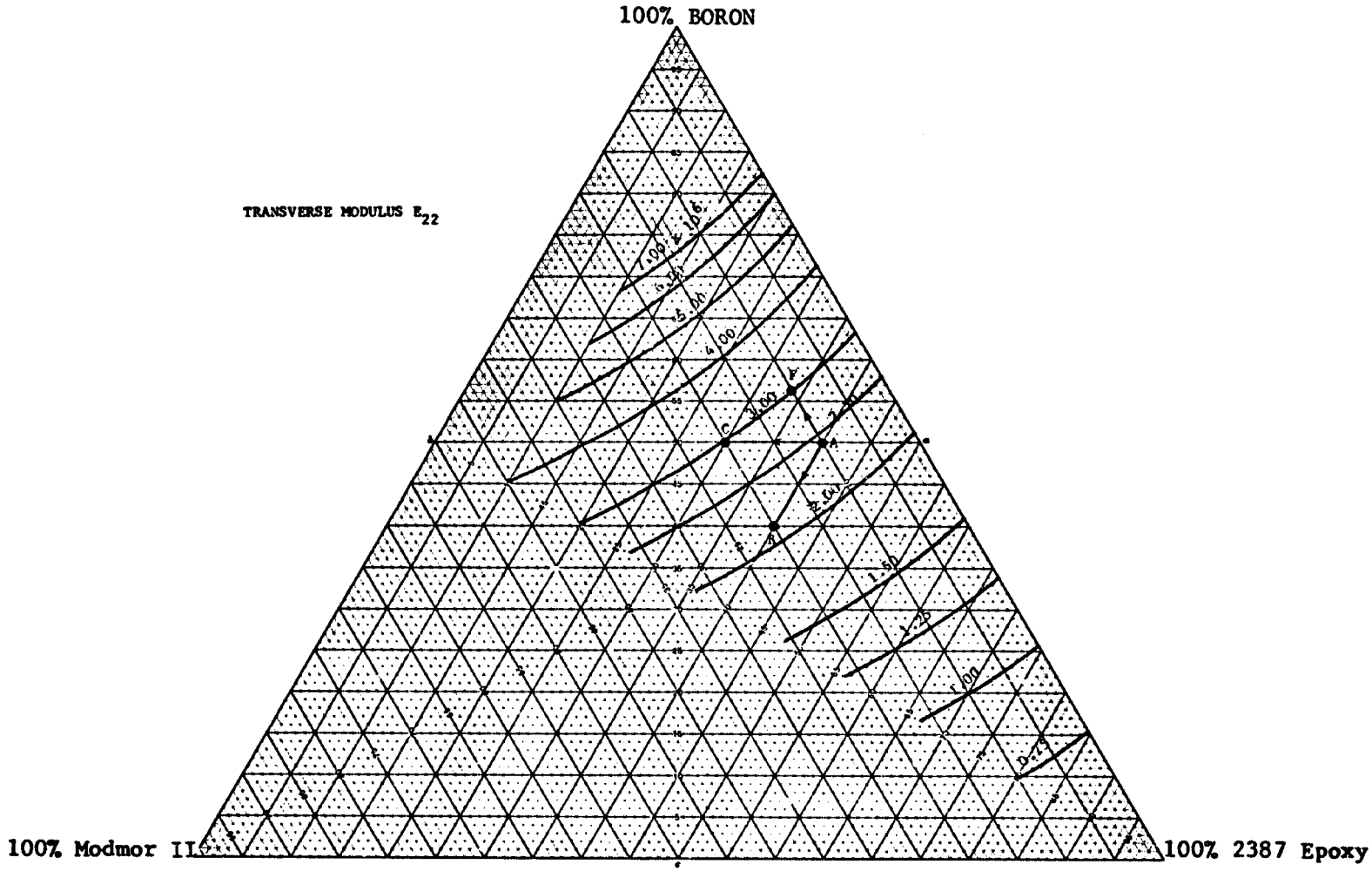

Figure 15. Transverse Modulus E_{22} of Boron/Modmor II/2387 Epoxy Composite.

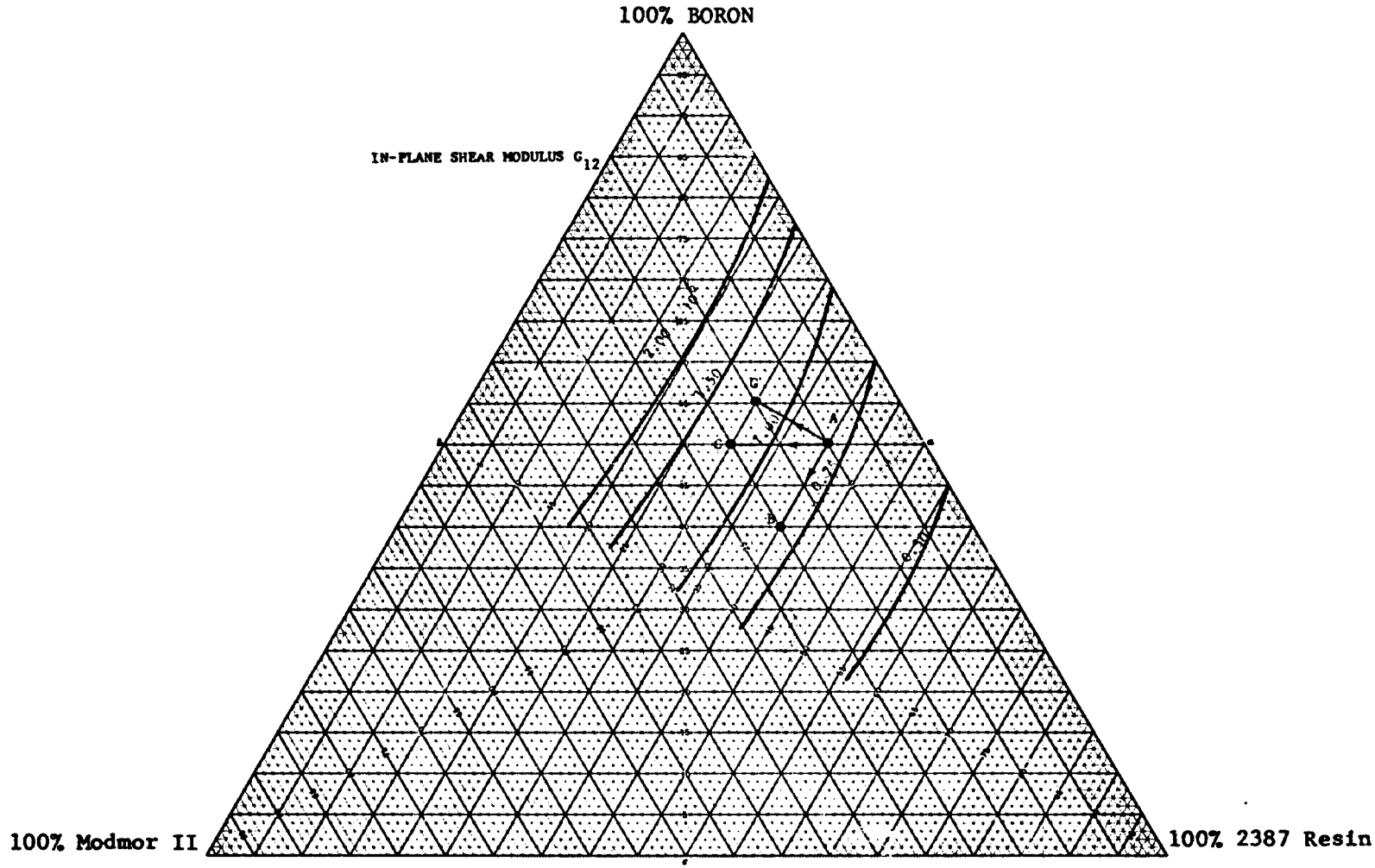

Figure 16. In-Plane Shear Modulus G_{12} of Boron/Modmor II/2387 Epoxy Composite.

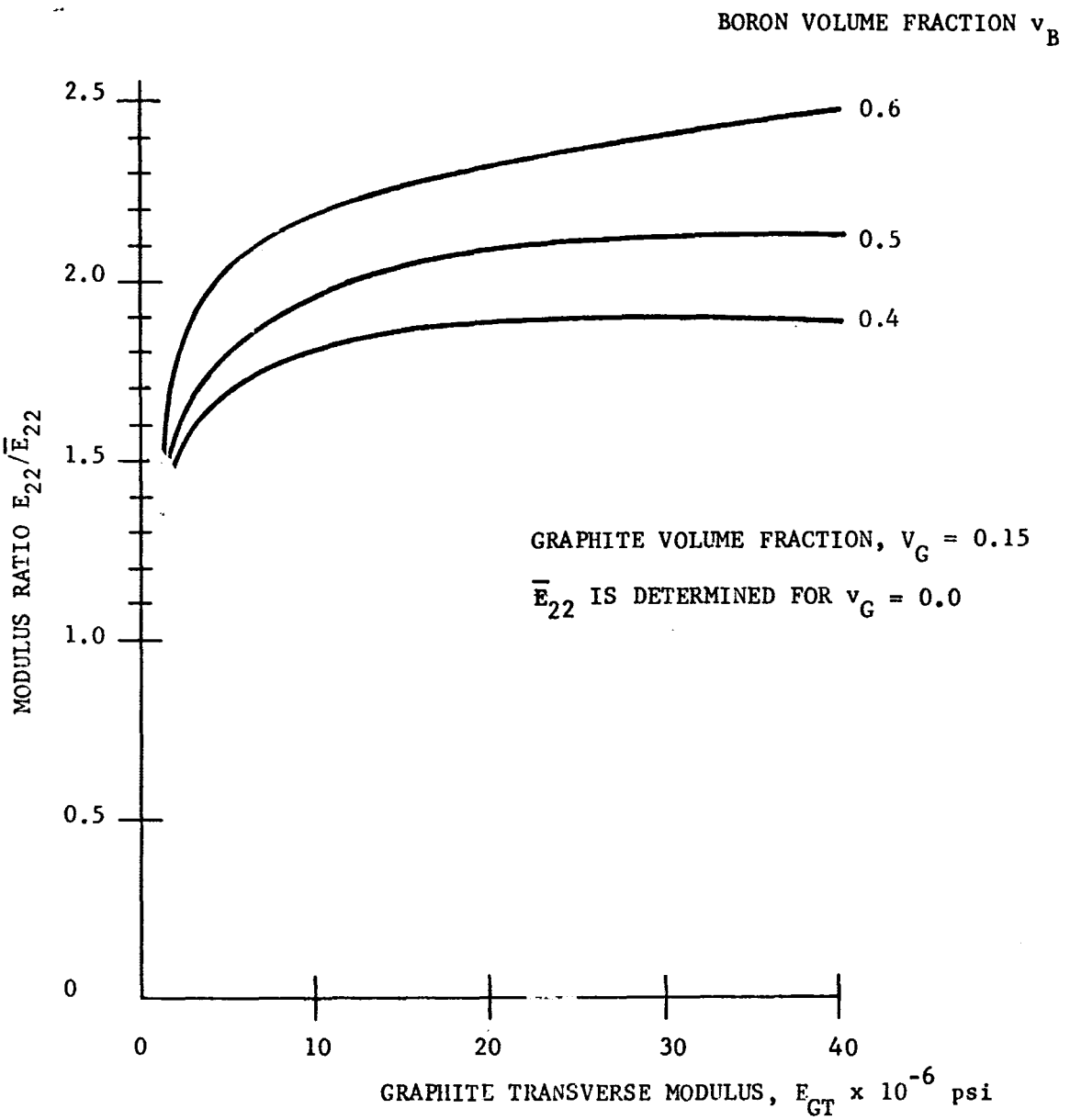

Figure 17. Effect of Graphite Fiber Anisotropy on the Transverse Modulus E_{22} of the Hybrid Composite.

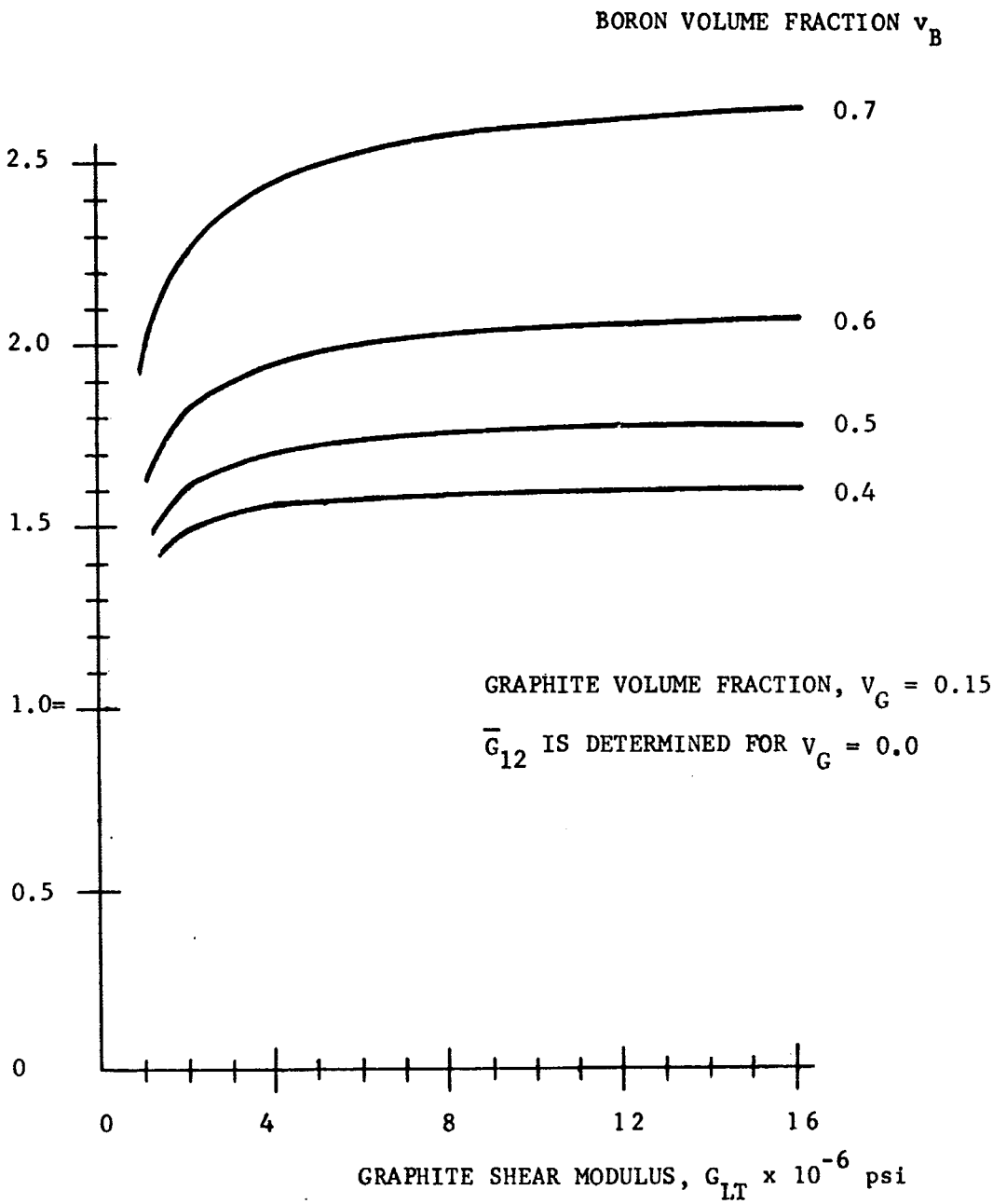

Figure 18. Effect of Graphite Fiber Anisotropy on the Shear Modulus G_{12} of the Hybrid Composite.

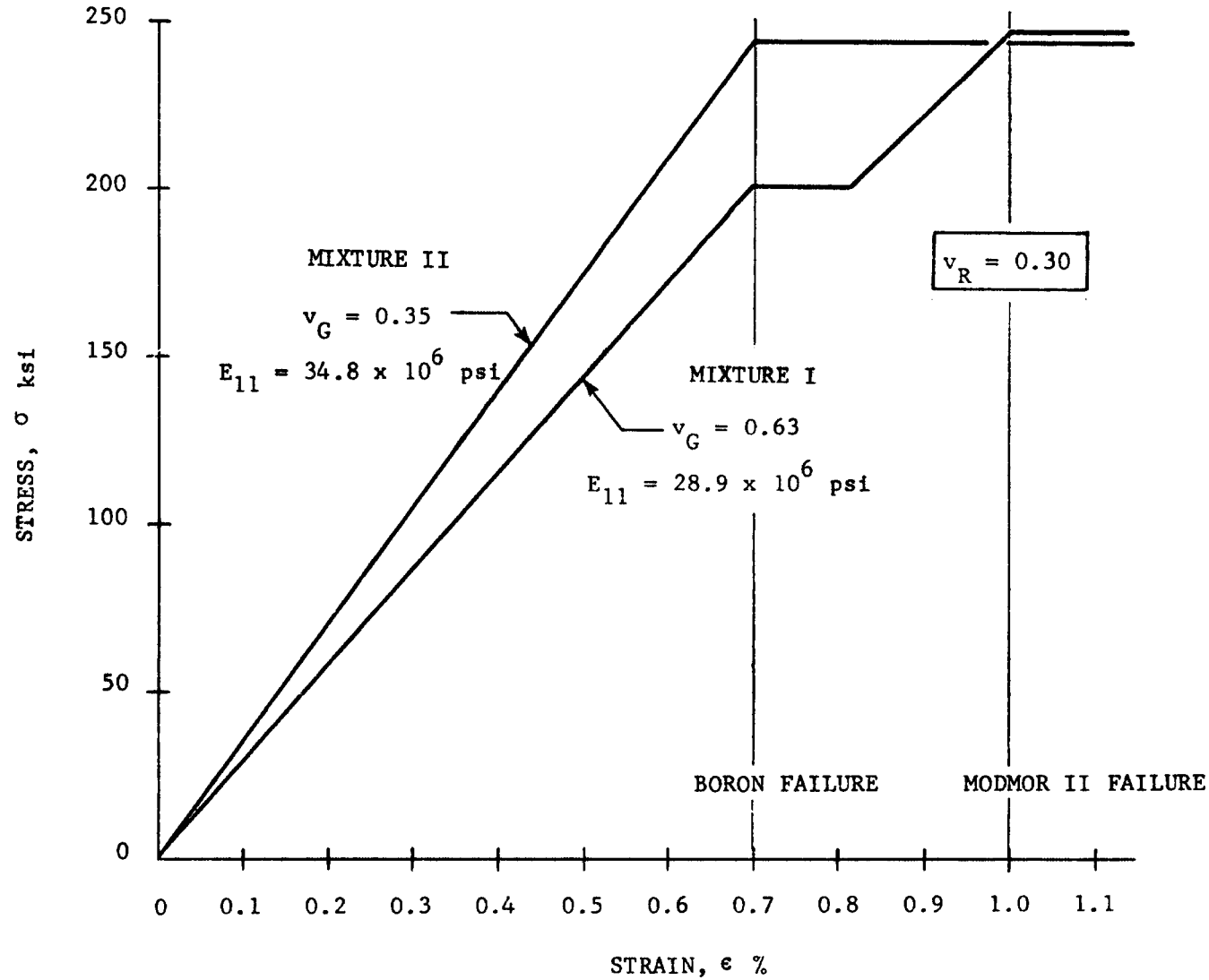

Figure 19. Dead-Weight Stress-Strain Curve for Boron/Modmor II/2387 Epoxy Composite.

The ultimate strength σ_{11} of the hybrid composite is plotted as a function of graphite volume fraction for five resin fractions, in Figure 20. Since these strengths are based on rule-of-mixtures assumptions, they are generally upper limits of values expected in practice. As should be expected, the replacement of boron by graphite (path PQ, for example) usually results in a reduced strength, while the replacement of resin by graphite (path PR) usually results in an improvement. When the mix proportion places it on line MN, both types of replacement lead to strength increases. These effects are better illustrated when replotted in the ternary diagram of Figure 21. The paths PQ and PR are shown for comparison. Note that neither path is optimum; in fact, the path PS, representing replacement of resin by boron, is more nearly optimum.

The specific strength $\sigma_{11/\rho}$ is not a linear function of graphite volume fraction, but the curves in Figure 22 reveal that it is nearly so. The paths PQ and PR are shown on this Figure for reference. The ternary diagram of Figure 23 presents the same results in map form. Note here that the optimum path PT is not the graphite-for-boron replacement curve, but more closely describes the process of resin removal. In other words, if laminate P were laid up and cured so as to remove more resin, the result would be a nearly optimum increase in specific strength.

GRAPHITE REINFORCEMENT OF NMD 5505 BORON/EPOXY COMPOSITE

The properties of a boron/epoxy laminate can be enhanced in one of three ways:

A. Augmentation. The volume fraction of the boron fiber is increased. No graphite is added.

B. Interleaving. Boron/Epoxy prepreg is interleaved with graphite/epoxy prepreg prior to cure. Unidirectional laminates of this material have a distinctly laminated microstructure, similar to that illustrated in Figure 24a.

C. Mixing. Boron and graphite fibers are intermixed prior to prepregging. Unidirectional laminates made from this prepreg display the uniform fiber distribution illustrated in Figure 24b.

The augmented boron/epoxy composite A has obvious potential for improvement of modulus properties, but the overall strength properties are unfavorably affected when the volume fraction v_B exceeds 55%.

Particularly affected are the transverse tensile and in-plane shear strengths, due to the increased stress concentration factors associated with the closer fiber packing. These factors have been evaluated in References [15], [16], and [17], to which the reader is referred for further

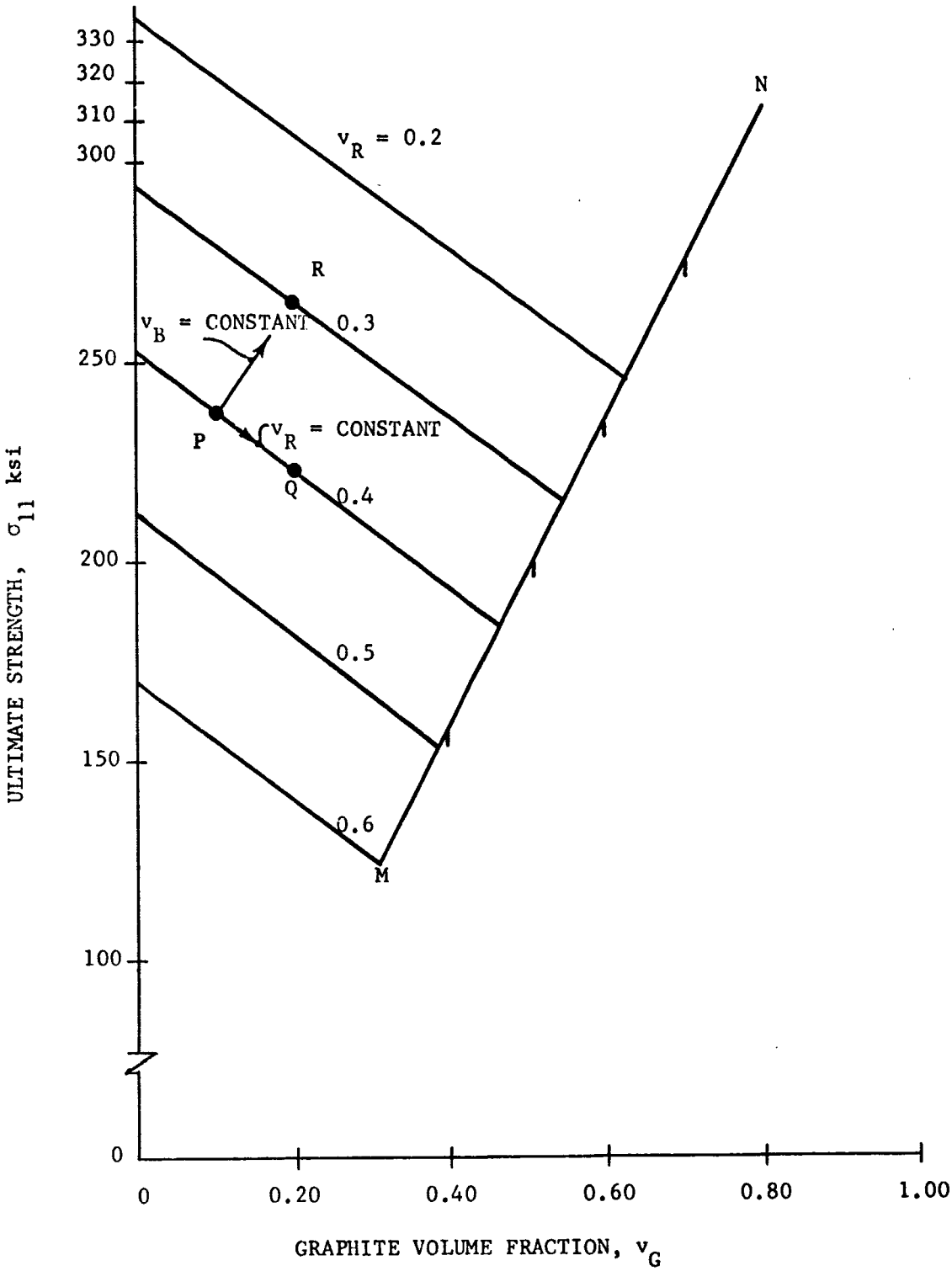

Figure 20. Ultimate Strength σ_{11} of Boron/Modmor II/2387 Epoxy Composite.

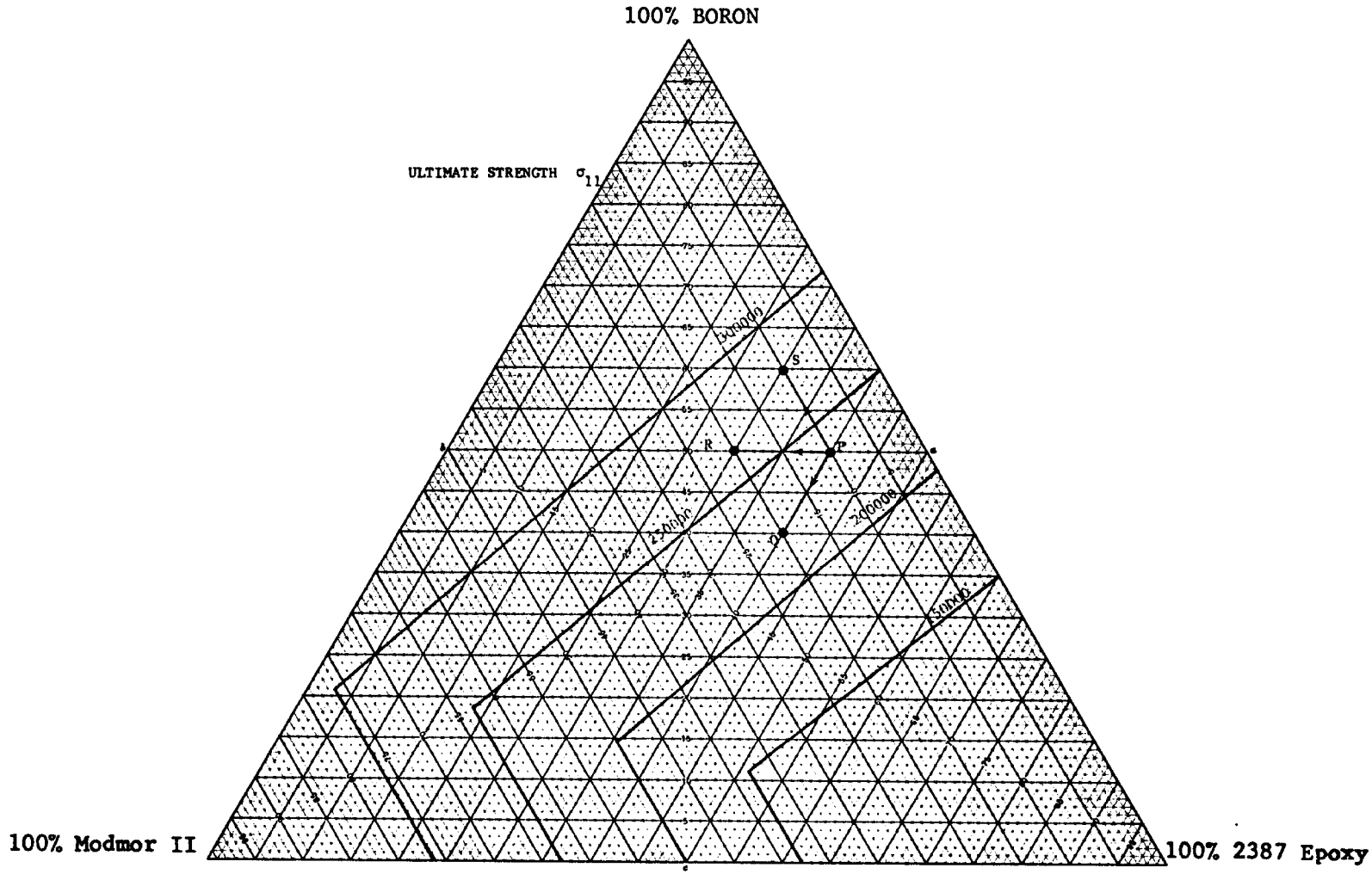

Figure 21. Ultimate Strength σ_{11} of Boron/Modmor II/2387 Epoxy Composite; Ternary Diagram.

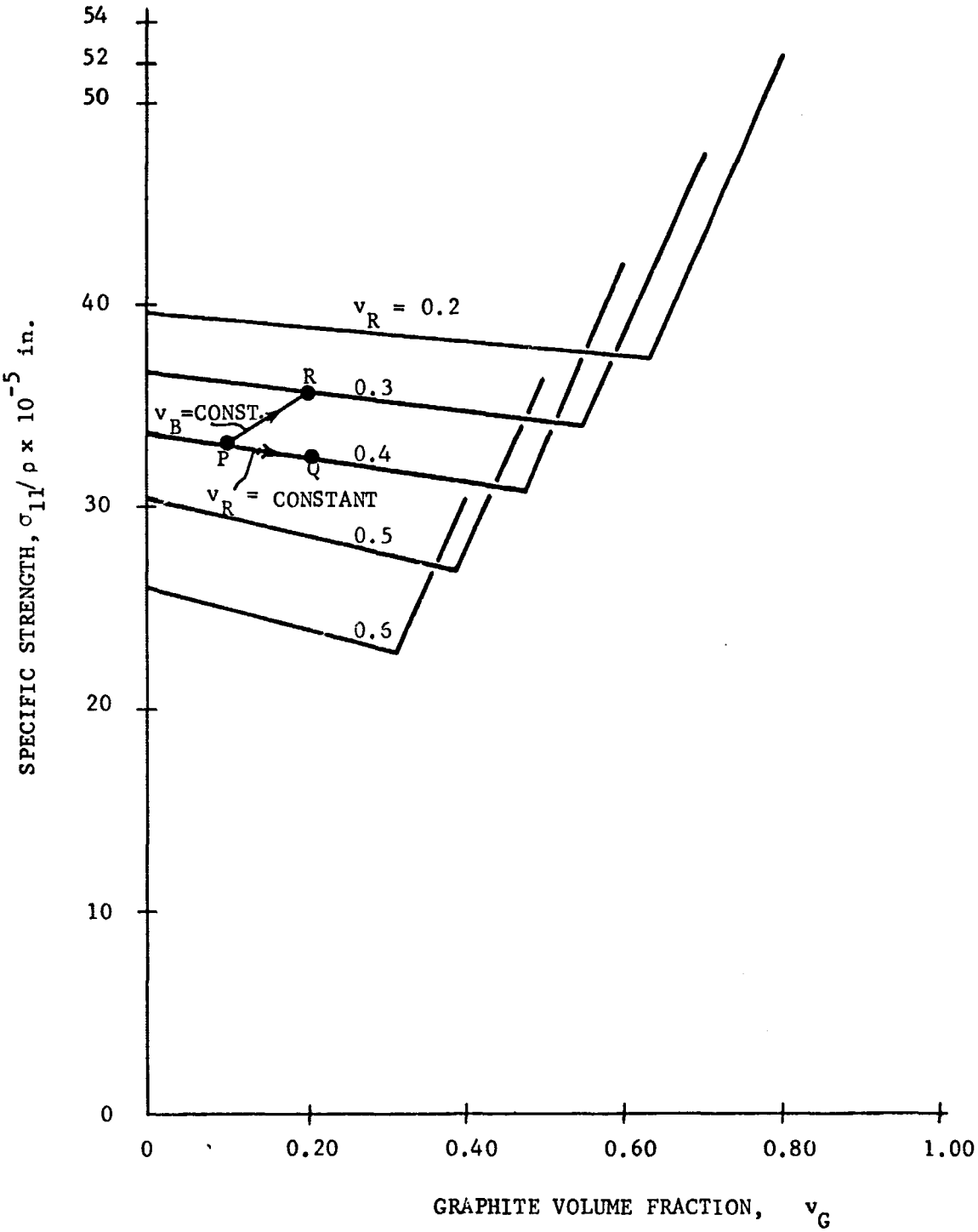

Figure 22. Specific Strength σ_{11}/ρ of Boron/Modmor II 2387 Epoxy Composite.

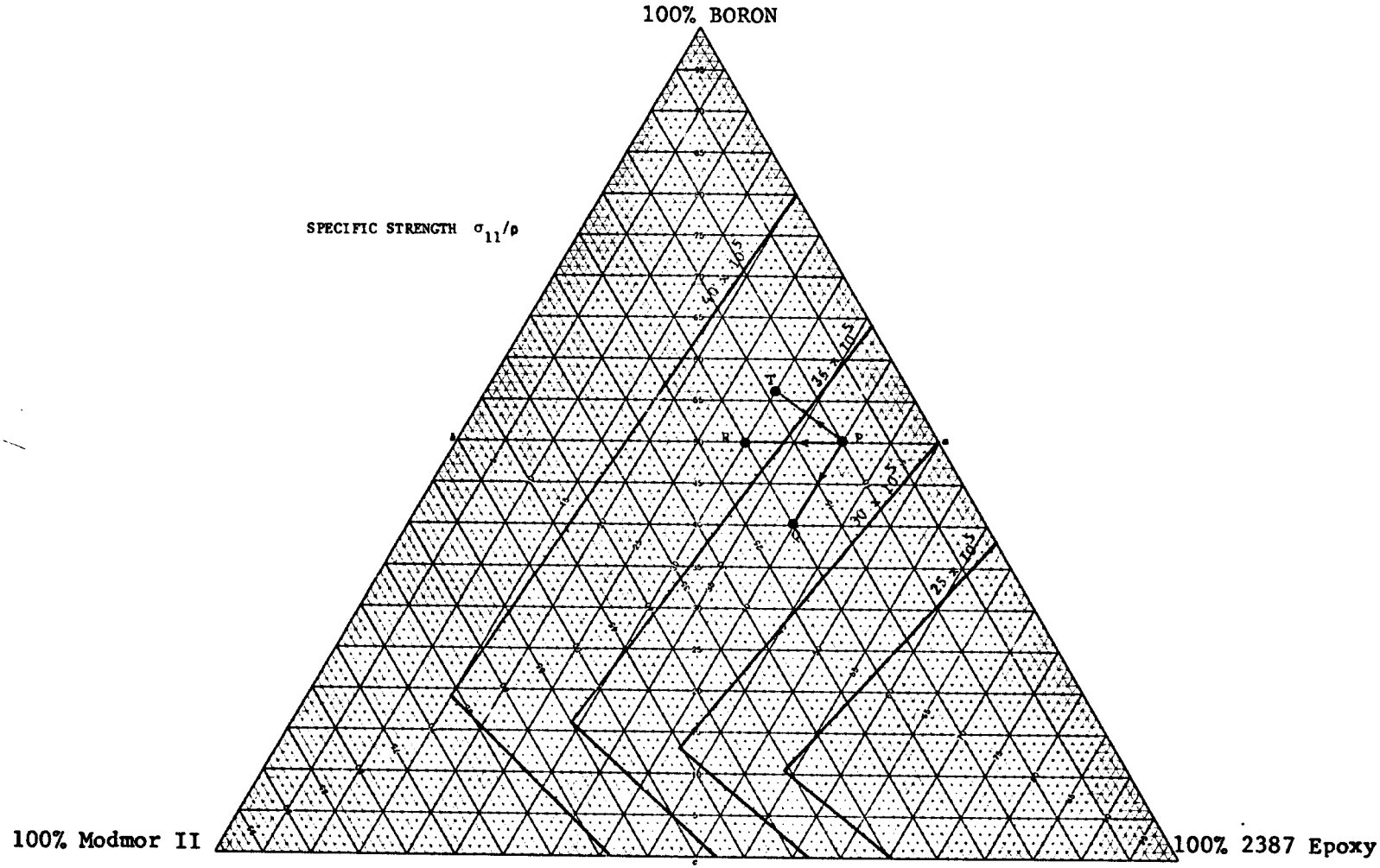

Figure 23. Specific Strength σ_{11}/ρ of Boron/Modmor II/2387 Epoxy Composite; Ternary Diagram.

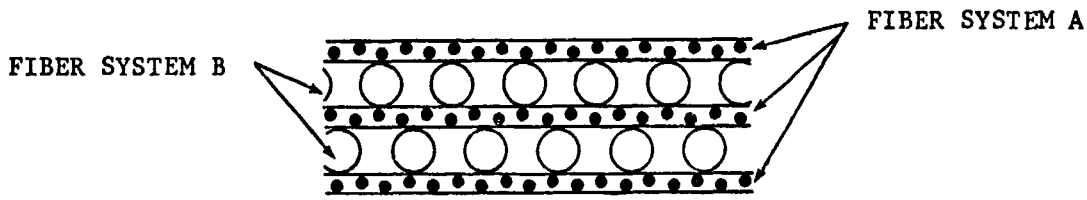

a) INTERLEAVED OR LAMINATED

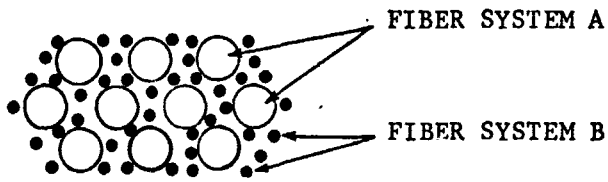

b) MIXED

Figure 24. Hybrid Composite Concepts.

discussion. The interleaved composite B can be analyzed as a structure consisting of alternating dissimilar plies. Since optimum graphite laminates have graphite volume fractions v_G in the range of 60% this laminate has a potential for an increased total fiber volume fraction without (perhaps) loss of overall laminate strength. As Figure 19 illustrates, however, the laminate may fail when the weakest ply fails, with an actual reduction in laminate ultimate strength. The mixed composite C may be visualized as an array of boron fibers in a "matrix" of graphite-stiffened epoxy. This "matrix" has the properties of the corresponding graphite/epoxy composite, and the overall laminate properties are estimated using an increased matrix-to-fiber modulus ratio.

The procedure for determining the moduli for each concept will be illustrated, using a 50% boron/epoxy reference composite. The augmented composite A is formed by increasing the boron volume fraction v_B to, say, 65%. The laminar composite B is formed by interleaving with graphite/epoxy plies to achieve the proportions $v_B = 50\%$, $v_G = 15\%$ and $v_R = 35\%$. The mixed composite C is formed by mixing the boron and graphite fibers in the volume proportion 50:15, then controlling the final resin content to achieve the proportions $v_B = 50\%$, $v_G = 15\%$ and $v_R = 35\%$. Since the longitudinal modulus E_{11} and Poisson's ratio ν_{12} are linear functions of the volume fractions, the rule of mixtures can be applied directly to each type of laminate:

A. Augmented Composite

a) $E_{11} = [0.65\ (60) + 0.35\ (0.5)] \times 10^6 = 39.2 \times 10^6$ psi

b) $\nu_{12} = [0.65\ (0.2) + 0.35\ (0.35)] = 0.253$

B. and C. Hybrid Composites

a) $E_{11} = [0.50\ (60) + 0.15\ (38.9) + 0.35\ (0.5)] \times 10^6$
$= 36.0 \times 10^6$ psi

b) $\nu_{12} = [0.50\ (0.2) + 0.15\ (0.2) + 0.35\ (0.35)] = 0.253$

The transverse modulus E_{22} and in-plane shear modulus G_{12} can be estimated using the Halpin-Tsai equations [11].

A. Augmented Composite

a) $E_{22} = \dfrac{1 + 2(0.65)\eta_1}{1 - 0.65\ \eta_1}\ (0.5 \times 10^6) = 3.09 \times 10^6$ psi

where $$\eta_1 = \frac{\frac{60}{0.5} - 1}{\frac{60}{0.5} + 2} = 0.975$$

b) $$G_{12} = \frac{1 + 0.65\eta_2}{1 - 0.65\eta_2}(0.185 \times 10^6) = 0.845 \times 10^6 \text{ psi}$$

where

$$\eta_2 = \frac{\frac{25}{0.185} - 1}{\frac{25}{0.185} + 1} = 0.985$$

B. Interleaved Composite

The laminate consists of alternating boron/epoxy and graphite/epoxy plies, each with the same resin volume fraction $v_R = 0.35$.

a) $$E_{22B}(\text{boron/epoxy}) = \frac{1 + 2(0.65)\eta_1}{1 - 0.65\,\eta_1}(0.5 \times 10^6)$$

$$= 3.09 \times 10^6 \text{ psi}$$

$$E_{22G}(\text{graphite/epoxy}) = \frac{1 + 2(0.65)\eta_3}{1 - 0.65\eta_3}(0.5 \times 10^6)$$

$$= 1.03 \times 10^6 \text{ psi}$$

where

$$\eta_3 = \frac{\frac{1.5}{0.5} - 1}{\frac{1.5}{0.5} + 2} = 0.40$$

Then by the rule of mixtures:

$$E_{22}(\text{laminate}) = \left[\frac{0.50}{0.65}(3.09) + \frac{0.15}{0.65}(1.03)\right] \times 10^6$$

$$= \underline{2.62 \times 10^6 \text{ psi}}$$

b) $$G_{12B}(\text{boron/epoxy}) = \frac{1 + 0.65\eta_2}{1 - 0.65\eta_3}(0.185 \times 10^6)$$

$$= 0.845 \times 10^6 \text{ psi}$$

$$G_{12G}(\text{graphite/epoxy}) = \frac{1 + 0.65\eta_4}{1 - 0.65\eta_4} (0.185 \times 10^6)$$

$$= 0.725 \times 10^6 \text{ psi}$$

where

$$\eta_4 = \frac{\frac{4}{0.185} - 1}{\frac{4}{0.185} + 1} = 0.912$$

Then, by the rule of mixtures:

$$G_{12}(\text{laminate}) = \left[\frac{0.50}{0.65} (0.845) + \frac{0.15}{0.65}\right](0.725) \times 10^6$$

$$= 0.817 \times 10^6 \text{ psi}$$

C. Mixed Composite

The "matrix" of this composite is a graphite/epoxy mixture, with graphite volume fraction $v_G/(1 - v_B) = 0.30$. The composite itself consists of 50% volume fraction boron fibers in this "matrix".

a) $$E_m(\text{"matrix"}) = \frac{1 + 2(0.30)\eta_3}{1 - 0.30\eta_3} (0.5 \times 10^6)$$

$$= 0.71 \times 10^6 \text{ psi}$$

$$E_{22}(\text{laminate}) = \frac{1 + 2(0.50)\eta_5}{1 - 0.50\eta_5} (0.71 \times 10^6)$$

$$= 2.7 \times 10^6 \text{ psi}$$

where

$$\eta_5 = \frac{\frac{60}{0.71} - 1}{\frac{60}{0.71} + 2} = 0.965$$

b) $G_m(\text{"matrix"}) = \dfrac{1 + 0.30\eta_4}{1 - 0.30\eta_4}(0.185 \times 10^6) = 0.325 \times 10^6$ psi

$$G_{12}(\text{laminate}) = \frac{1 + 0.50\eta_6}{1 - 0.50\eta_6}(0.325 \times 10^6) = 0.805 \times 10^6 \text{ psi}$$

where

$$\eta_6 = \frac{\frac{4}{0.325} - 1}{\frac{4}{0.325} + 1} = 0.85$$

The transverse and shear strengths of the three laminates cannot be computed directly from the equations and curves presented herein, but their relative values can be estimated using stress concentration factors determined with the aid of [15], [16] and [17]. If it is assumed that laminate failure occurs when a critical tensile stress σ or shear stress τ is developed in the matrix, then the estimated laminate strength is inversely proportional to the stress concentration factor. Other, more sophisticated, failure criteria could be applied, but the trends from this simpler assumption are believed indicative of the influences of the three laminate improvement methods.

For the augmented composite A, the stress concentration factors can be determined directly from the curves in [15] and [16]. For the interleaved composite B, each type of ply must be considered separately, and the average stresses must be properly distributed between the plies. For the mixed composite C, the total concentration factor is the product of the "matrix" (graphite/epoxy) and the laminate (boron/"matrix") concentration factors. These procedures will be illustrated in the following paragraphs:

A. <u>Augmented Composite</u>

$$v_B = 0.65, \quad E_B/E_R = 120$$

a) Transverse normal stress concentration factor = 2.15 (from [15]).

$$\sigma = 2.15\,\sigma_{22}$$

$$\therefore \sigma_{22} = \sigma/2.15 \text{ estimated ultimate strength}$$

b) In-plane shear stress concentration factor = 2.83 (from [16]).

$$\tau = 2.83\,\tau_{12}$$

$$\therefore \tau_{12} = \tau/2.83 \text{ estimated ultimate shear strength}$$

B. Interleaved Composite

a) Boron/epoxy ply: $v_B = 0.65$, $E_B/E_R = 120$,

$$E_{22B} = 3.09 \times 10^6 \text{ psi}$$

Graphite/epoxy ply: $v_G = 0.65$, $E_G/E_R = 4$,

$$E_{22G} = 1.03 \times 10^6 \text{ psi}$$

Average stress σ_G in boron/epoxy ply:

$$\frac{\sigma_B}{\sigma_{22}} = \frac{E_{22B}}{E_{22}} = \frac{3.09}{2.62} = 1.18$$

Average stress σ_G in graphite/epoxy ply:

$$\frac{\sigma_G}{\sigma_{22}} = \frac{E_{22G}}{E_{22}} = \frac{1.03}{2.62} = 0.393$$

Transverse normal stress concentration factor in boron/epoxy ply = 2.15 [15].

$$\sigma = 2.15\,\sigma_B = 2.54\,\sigma_{22}$$

Transverse normal stress concentration factor in graphite/epoxy ply = 1.30 [15].

$$\sigma = 1.30\,\sigma_G = 0.511\,\sigma_{22}$$

$\therefore$ σ_{22} = Minimum of $(\sigma/2.54, \sigma/0.511) = \sigma/2.54$ estimated ultimate strength.

b) Boron/epoxy ply: $v_B = 0.65$, $G_B/G_R = 135$,

$$G_{12B} = 0.845 \times 10^6 \text{ psi}$$

Graphite/epoxy ply: $v_G = 0.65$, $G_G/G_R = 21.6$,

$$G_{12G} = 0.725 \times 10^6 \text{ psi}$$

Average stress τ_B in boron/epoxy ply:

$$\frac{\tau_B}{\tau_{12}} = \frac{G_{12B}}{G_R} = \frac{0.845}{0.817} = 1.035$$

Average stress τ_G in graphite/epoxy ply:

$$\frac{\tau_G}{\tau_{12}} = \frac{G_{12G}}{G_{12}} = \frac{0.725}{0.817} = 0.890$$

In-plane shear stress concentration factor in boron/epoxy ply = 2.83 [16].

$$\tau = 2.83\ \tau_{12B} = 2.93\ \tau_{12}$$

In-plane shear stress concentration factor in graphite/epoxy ply = 2.50 [16].

$$\tau = 2.50\ \tau_{12B} = 2.23\ \tau_{12}$$

$$\therefore \tau_{12} = \text{Minimum of } (\tau/2.93,\ \tau/2.23) = \tau/2.93$$

estimated ultimate shear strength.

C. Mixed Composite

a) Graphite/epoxy "matrix": $v_G = \frac{0.15}{0.50} = 0.30$, $E_G/E_R = 4$,

$E_m = 0.71 \times 10^6$ psi

Boron/"matrix" laminate: $v_B = 0.50$, $E_B/E_m = 84.5$,

$E_{22} = 2.7 \times 10^6$ psi

Transverse normal stress concentration factor in the graphite/epoxy matrix = 1.25 [15].

Transverse normal stress concentration factor in the boron/"matrix" laminate = 1.70 [15].

$$\sigma = (1.25)(1.70)\,\sigma_{22} = 2.13\,\sigma_{22}$$

$$\sigma_{22} = \sigma/_{2.13} \text{ estimated ultimate strength}$$

b) Graphite/epoxy "matrix": $v_G = 3.30$, $G_G/G_R = 21.6$,

$$G_m = 0.325 \times 10^6 \text{ psi}$$

Boron/"matrix" laminate: $v_B = 0.50$, $G_B/G_m = 77$,

$$G_R = 0.805 \times 10^6 \text{ psi}$$

In-plane shear stress concentration factor in the graphite/epoxy matrix = 1.47 [16].

In-plane shear stress concentration factor in the boron/"matrix" laminate = 1.50 [16].

$$\tau = (1.47)(1.50)\,\tau_{12} = 2.21\,\tau_{12}$$

$$\tau_{12} = \tau/_{2.21} \text{ estimated ultimate shear strength}$$

The results of these computations are summarized in Table II, where the specific moduli and specific strengths are compared against those of the augmented composite A. It can be seen from this table that the properties of the augmented composite A and the mixed composite C are similar in many respects. The latter has a slightly lower specific transverse modulus E_{22}/ρ, but somewhat higher specific strength σ_{22}/ρ and τ_{12}/ρ. The laminated composite B is comparable to the mixed composite C in all but the specific transverse and shear strengths. The reason for the differences in these strengths rests in the degree of fiber intermixing. In the laminated composite there is no fiber intermixing, while in the mixed composite there is complete fiber intermixing. Since the degree of fiber intermixing in actual hybrid laminates would be expected to fall somewhere between these two extremes, then their specific transverse and shear strengths should, likewise, fall between the values shown in Table II.

The properties of the three enhanced composites are compared against those of the reference composite in Table III. Note that all three of the alternatives lead to higher specific modulus, (as expected) but that none achieve improved specific transverse and shear strengths. Since the specific longitudinal strength $\sigma_{11/\rho}$ is improved by all three approaches, this alone may justify the use of the enhanced composites. The benefits to be derived from the use of hybrid composites must be weighed against

the penalties, and a study similar to the one performed herein should be performed for each proposed combination before a choice can be made. In many design applications such as panels, skins and webbings, it is a conservative practice to ignore the contributions of transverse and shear strengths and moduli of the unidirectional ply. Using this concept, the plies are oriented in the structure so that all load components are safely accommodated by fiber tension or compression, and the contributions of the matrix to these functions are assumed to be of a stabilizing or relieving nature (netting analysis). A more important load-bearing function could be assigned to the matrix only if the transverse and shear properties were somehow significantly improved. This improvement would have to be an absolute, rather than relative, increase of strength and modulus. Although the hybrid concept leads to large relative increases in transverse and shear moduli, the absolute values of these increases are still not sufficient to warrant departure from this design procedure.

The main justification for the hybrid concept appears to lie in its potential for improved longitudinal strength and moduli. These improved properties can be achieved by either of the three enhancement concepts described here, although, as Table II indicates, the choice of concept is a matter of engineering judgment. An obvious use of the mixed composite concept is in application where the boron/epoxy prepreg cannot be used effectively. The radius-of-curvature limitation on boron structures could be alleviated by employing graphite in regions requiring small radii (as in closeouts, for example). The transition between a boron panel, with its excellent compressive properties, and the graphite closeout, with its formability could be accomplished by means of the hybrid composite. This concept will be developed in a later section.

TABLE II

COMPARISON OF ESTIMATED HYBRID COMPOSITE PROPERTIES
RELATIVE TO PROPERTIES OF THE AUGMENTED COMPOSITE

	Augmented Composite A $v_B = 0.65$, $v_G = 0.$	Laminated Composite B $v_B = 0.50$, $v_G = 0.15$	Mixed Composite C $v_B = 0.50$, $v_G = 0.15$
E_{11}/ρ	100%	98%	98%
E_{22}/ρ	100%	91%	93%
σ_{12}/ρ	100%	103%	102%
v_{12}	0.253	0.253	0.253
σ_{11}/ρ	100%	98%	98%
σ_{22}/ρ	100%	90%	107%
τ_{12}/ρ	100%	91%	120%

TABLE III

COMPARISON OF ESTIMATED ENHANCED-COMPOSITE
PROPERTIES RELATIVE TO PROPERTIES OF THE 50% BORON/EPOXY REFERENCE COMPOSITE

	Reference Composite $v_B = 0.50$ $v_G = 0.$	Augmented Composite A $v_B = 0.65$, $v_G = 0.$	Laminated Composite B $v_B = 0.50$, $v_G = 0.15$	Mixed Composite C $v_B = 0.50$, $v_G = 0.15$
E_{11}/ρ	100%	117%	115%	115%
E_{22}/ρ	100%	145%	132%	135%
σ_{12}/ρ	100%	139%	143%	142%
v_{12}	0.275	0.253	0.253	0.253
σ_{11}/ρ	100%	112%	110%	110%
σ_{22}/ρ	100%	73%	66%	78%
τ_{12}/ρ	100%	59%	54%	71%

SECTION III

DEVELOPMENT OF BORON/MODMOR II/2387 EPOXY LAMINATES

PROCESSING STUDY

A process study was performed to develop prepregging, layup and cure techniques for producing the hybrid laminates. In addition to those problems inherent to the production of boron/epoxy and graphite/epoxy laminates, the hybrid concept introduces the problem of fiber mixing. As the previous section indicates, the prospective improvements in specific modulus and strength are small for the Boron/Modmor II/2387 Epoxy laminate; so the fiber mixing must be achieved with very small additional prepreg costs if the concept is to be economically feasible. Approaches using chopped graphite fibers were rejected on grounds that collimation would be expensive to achieve, while randomly oriented graphite fibers would not adequately improve the longitudinal properties. It is recognized that the latter approach would lead to improvements of shear and transverse properties, but these improvements would not be sufficient to warrant changes of design procedures. Moreover, chopped-fiber mats would tend to create a distinctly laminar structure (B) with many crossed fibers and stress concentrations. The continuous graphite fibers, on the other hand, can be incorporated directly into the filament winding processes used to produce boron/epoxy prepregs; and their unidirectionality lends maximum effect to the longitudinal properties of the ply.

Basically, there are three methods for incorporating graphite filaments into a boron/epoxy prepreg:

a) Graphite fibers are drum-wound over boron/epoxy prepreg.

b) Boron fibers are drum-wound over graphite/epoxy prepreg.

c) Boron/epoxy and graphite/epoxy prepregs are sandwiched together.

Although the three methods appear equivalent, it is more desirable to wind the boron over the graphite (method b) than to wind graphite over boron (method a). Method b will lead to better collimation of the graphite fibers, since these fibers are stretched slightly when the prepreg is straightened after removal from the drum. This feature is also important when hybrid tape is being produced: the graphite should be on the concave side whenever the prepreg is formed on a curved surface. Method c has the advantage that each prepreg can be prepared using the handling techniques best adapted to it, and each can be inspected prior to formation of the hybrid.

A second problem related to that of fiber mixing is the necessity for achieving low graphite volume fractions. If a 12% graphite volume fraction is required, for example, Modmor II tows must be spread to a density of only one tow per inch in a ply of closely packed boron/epoxy prepreg. Available yarn forms have proven much too dense to achieve this low density; only continuous and tow forms, such as Modmor or Courtaulds graphite, could be spread to such densities in this study.

A third problem was that of curing the prepreg after it was laid up. Although the mechanical handling properties of the prepreg were governed by the large-diameter boron fibers, it was found that the wetting area of the graphite fibers was so large (even in small proportions) that their presence governed the resin flow and cure characteristics of the laminate. The small amounts of graphite effectively retarded resin flow along the boron fibers, and the resulting cure cycles were similar to those used for graphite/epoxy laminates.

During the course of this study, eleven 6" x 6" laminates were laid up, 6 plies thick, and autoclave cured in accord with the cycles summarized in Table IV. The purpose of this study was to develop methods for insuring fiber mixing and to determine basic cure characteristics of the hybrid prepreg. It is recognized that many cure cycles may be proposed and studied, once these fundamental problems have been settled. The main features of the layup and curing of these laminates will be summarized in the paragraphs to follow.

1. Prepreg resin content and distribution - are governed by the fiber mixing requirement. The resin content must be sufficient to purge the voids during the bleed-out stage, and it must be properly distributed through the prepreg in order to insure infiltration of graphite fibers throughout the ply. During this study, resin distribution was accomplished in the following steps.

   a) Approximately 70% of the total resin required was hot melt coated onto a Mylar sheet.

   b) Graphite was then laid over the resin film in the specified tow density and width. No attempt was made to force the resin through the tows.

   c) The sheet, with graphite and epoxy, was stretched around a one-meter-circumference drum. This process tended to straighten and collimate the graphite fibers.

   d) Boron fibers were wound over the graphite fibers in the prescribed between - centers spacing.* This winding process encouraged resin wetting of

* In the wider spacings, a tendency to separate was noted due to irregularities in graphite layer thickness.

TABLE IV

SUMMARY OF CURE CYCLES IN PREPREG STUDY

PANEL	PROCESS	TEMP. °F	TIME, MINUTES	EXTERNAL PRESSURE, psig	INTERNAL VACUUM, in. Hg.
C-7A	Heat up from RT	275	23	0	29
	Hold at Temp.	275	5	0	29
	Heat up	350	15	60	29
	Cure	350	120	100	29
C-7B C-7C C-9	Heat up from RT	275	23	0	29
	Hold at Temp.	275	5	0	29
	Heat up	350	15	100	0
	Cure	350	120	100	0
C-10	Heat up from RT	275	22	0	29
	Hold at Temp.	275	5	0	29
	Heat up	350	7	100	29
	Cure	350	120	100	29
C-11A	Heat up from RT	275	23	0	29
	Hold at Temp.	275	5	0	29
	Heat up	350	12	80	29
	Cure	350	120	80	29
C-11B C-11C	Heat up from RT	275	16	0	29
	Hold at Temp.	275	5	0	29
	Heat up	350	12	100	29
	Cure	350	120	100	29
C-11D	Heat up from RT	275	15	0	29
	Hold at Temp.	275	5	0	29
	Heat up	350	14	100	29
	Cure	350	120	100	29
C-11E C-11F	Heat up from RT	275	11	0	29
	Hold at RT	275	5	0	29
	Heat up	350	12	100	29
	Cure	350	120	100	29

the graphite fibers and intermixing of the boron and graphite fibers.

e) The partial prepreg was removed from the drum, straightened and squeegeed briefly on a platen heated to 200°F. The straightening of the prepreg slightly stretched and collimated the graphite fibers, and the squeegee operation encouraged resin flow through the graphite and boron layers. This flow also improved the intermixing of these fibers.

f) The remaining 30% of the resin was hot melt coated onto a Mylar sheet, which was then placed over the boron fibers using a squeegee operation.

g) The hybrid ply was then squeegeed thoroughly on the 200°F platen to form the prepreg.

Figure 25 illustrates the distribution of materials in the prepreg. Note that this prepreg has a "boron side" and a "graphite side". These sides must be observed during layup in order to insure proper fiber mix during the cure.

2. Laminate cure cycle - in the autoclave was specified so as to promote adequate fiber mixing in the laminate. This process was accomplished in the following steps.

a) The unidirectional laminate was laid up symmetrically, with the boron and graphite sides of adjacent plies facing together. For maximum flexural strength, the outer plies of the laminate should be with the boron sides facing outward, as illustrated in Figure 26. This procedure created a laminate with a "core" of wet resin, and alternating layers of graphite and boron fibers.

b) After adding breather, bleeder cloth and caul plate, the laminate was bagged and placed in a preheated autoclave press. Vacuum was drawn in the bag to attain initial caul plate pressure and to promote migration of voids out of the panel. The presence of the graphite retarded resin flow along the fibers, thus the bleed-out occurred principally along the direction normal to the laminate. The laminate was heated (press speed) to 275°F, then held at that temperature for 5 minutes. This

"hold" permitted excess resin to bleed out of the laminate, carrying air bubbles with it. The resin flow also promoted the intermix of graphite and boron fibers (In this study, a 20 - 25% bleed was employed to insure void-free, well-mixed laminates).

c. After the hold, an external pressure was applied to promote compaction and, through action on the caul plate, to assist in dimensional control of the laminate. The laminate temperature was then increased at press speed to 350°F and held for two hours. The resin cure was completed during this period.

Figure 27 indicates the resin condition during the cure process, as determined prior to its application to the laminate. The very low viscosity at 250°F promotes bleed out and the percentage of bleed can be controlled both through the hold time and the amount of bleeder cloth. Note that gelation begins in the latter stages of the final heat-up, but after the laminate resin content and degree of fiber intermix have already been established.

Since some details of the cure process are governed by the capabilities of the press, it is recommended that any proposed cure cycle be first conducted on a sample laminate in the actual cure fixtures, with the time-temperature cycle recorded. This cycle should then be duplicated on resin of the same batch in standard gel-time apparatus to ascertain the condition of the resin during the actual cure. It is essential, of course, that the viscosity be low throughout the HOLD segment of the process, and that gellation occur at the end of the final heat up.

The physical properties of the eleven laminates are summarized in Table V. The panels C-11A through C-11F were fabricated after the cure was modified to enhance the bleedout. Note that the void content of each of these six laminates is essentially zero. In these six, the press was heated to 275°F before the laminate was placed. The preheating reduced the initial heat-up time, which in turn reduced the degree of resin polymerization. The result was an enhanced bleedout characteristic. A "slower" resin such as NMD 1004 would permit a slower heat-up rate than those used in this 2387 study. Note, in Table V, that the laminates C-11A, C-11B, C-11C are slightly denser (average specific gravity: 1.98) than laminates C-11D, C-11E, C-11F (average specific gravity: 1.94). This occurred because the boron fiber in the former laminates was wound on 0.0046" centers, while it was wound on 0.0052" centers in the latter three. This alteration was made after noting the micrographs* from C-11A, C-11B and C-11C.

*Micrograph preparation is outlined in Appendix B.

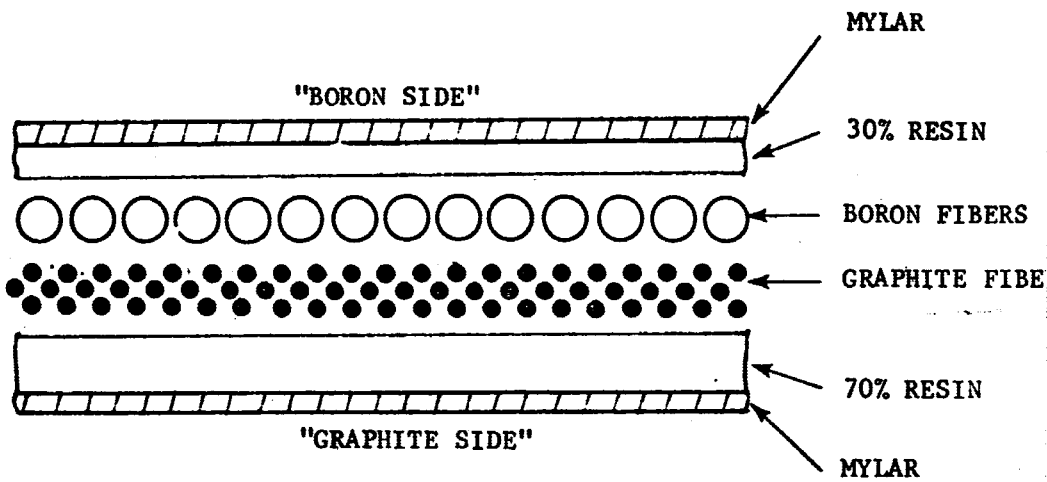

Figure 25. Typical Prepreg Composition.

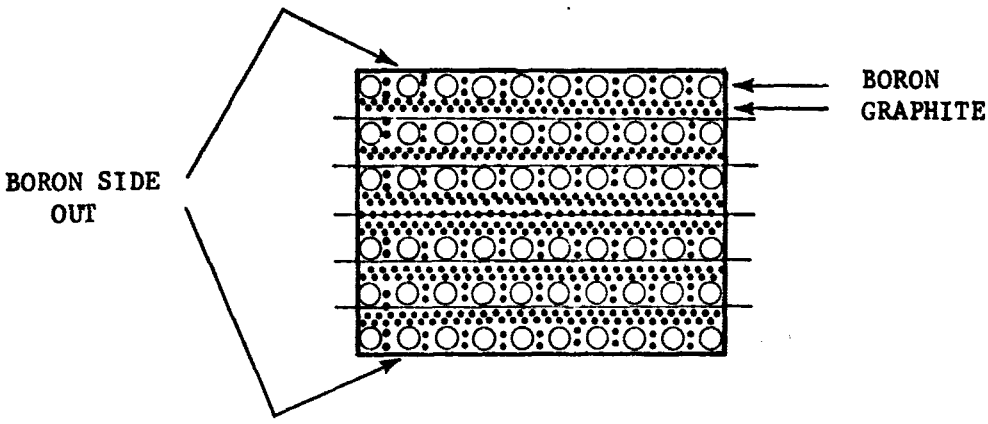

Figure 26. Schematic of Symmetrical Hybrid Layup.

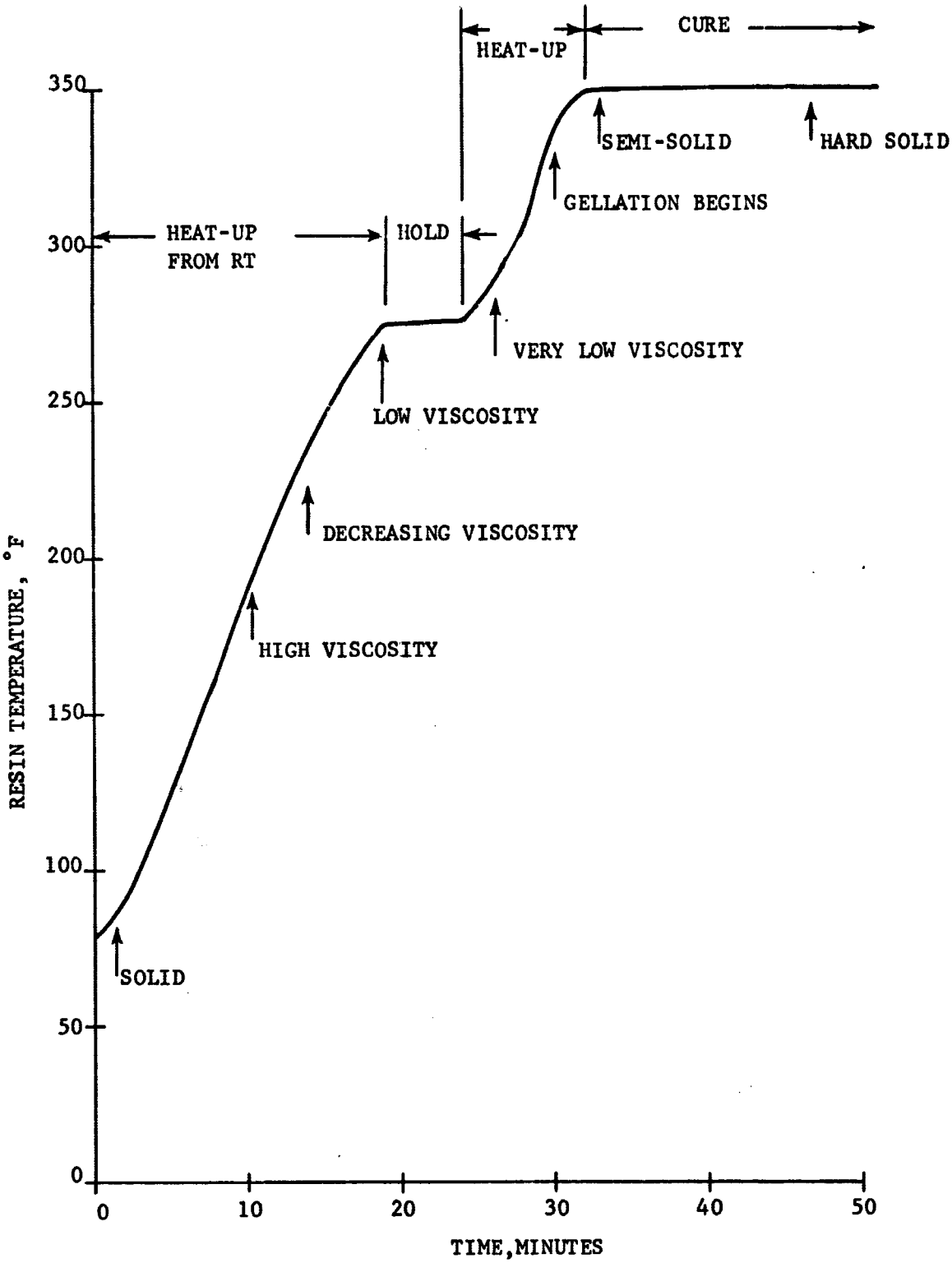

Figure 27. Conditions of 2387 Epoxy Resin (Batch Number 45) During Hybrid Composite Cure Process.

TABLE V.

SUMMARY OF LAMINATE PHYSICAL PROPERTIES OBTAINED DURING THE PROCESS STUDY

PANEL	FIBER RATIO α	RESIN WEIGHT FRACTION, w_R	MEASURED SPECIFIC GRAVITY γ'	VOLUME FRACTIONS			
				v_B	v_G	v_R	v_a
C-7A	0.214	0.200	1.97	0.495	0.155	0.327	0.023
C-7B	0.210	0.303	1.47	0.320	0.103	0.367	0.210
C-7C	0.200	0.247	1.94	0.465	0.139	0.386	0.010
C-9	0.200	0.256	1.95	0.460	0.135	0.405	~0
C-10	0.190	0.305	1.84	0.409	0.113	0.463	0.015
C-11A	0.165	0.229	1.99	0.495	0.120	0.385	~0
C-11B	0.207	0.229	1.98	0.480	0.150	0.370	~0
C-11C	0.197	0.230	1.97	0.485	0.140	0.375	~0
C-11D	0.195	0.252	1.95	0.465	0.135	0.400	~0
C-11E	0.206	0.251	1.94	0.460	0.140	0.400	~0
C-11F	0.206	0.263	1.93	0.450	0.140	0.410	~0

Figure 28 shows a 150X micrograph of specimen C-11C. Note that the boron fibers are placed in a regular rectangular (as opposed to square) array and that they are almost touching within each ply. This adjacency results in excessive stress concentrations, with corresponding reductions in transverse and shear strengths. Moreover, the boron fibers act as a barrier to the movement of the graphite fibers during bleedout, thus complete fiber mixing is not achieved. Figure 29 shows specimen C-11D, for which the wider boron spacing is used. Note that when the boron fiber spacing is increased, the graphite fiber movement is enhanced and the boron fiber array is more nearly square, although the pattern is somewhat more irregular. The use of a slow-curing resin and lamination compaction techniques will lead to improved mixing of the two fiber systems.

PROTOTYPE LAMINATES

In order to test the layup and cure procedures in production-sized setups, two laminates were fabricated using the procedures developed during the process study. One panel (A-115) was a nine-ply, 12" x 12.5" laminate, while the other (B-120) was a twenty-one-ply, 5" x 5" laminate with the same cure specification. The cure cycles for the two panels are summarized in Table VI. Note that the cures turned out to be identical except for the heat-up times, which are longer than those specified (Refer to C-11D, C-11E, C-11F in Table IV). The resulting cured laminates exhibited considerably lower specific gravities and correspondingly higher void contents than anticipated. Table VII summarizes the physical properties of these two laminates. The very high void contents are directly attributable to the increased heat-up time. At first, it was believed that this was inherent to the larger press used in this portion of the study, but it was ascertained that the press had not been preheated for either panel. This accounted for the increased heat-up time. As the micrographs of Figures 30 and 31 reveal, the resin gelled prematurely in both laminates and the entrained air was not successfully carried out of the laminate. The higher void content of panel B-120 is due to the greater laminate thickness. Note in these figures that the graphite fibers had only begun to mix with the boron when the resin gelled.

Despite the high void contents, the decision was made to test the laminates. Laminate B-120 was tested in compression, while laminate A-115 was tested in longitudinal tension, longitudinal flexure, in-plane shear and short-beam shear. All tests were performed in accord with the specifications outlined in Appendix C. Table VIII summarizes the results of these tests. The "measured" values in this Table are based upon the test data, while the "predicted" values are calculated from the actual fiber volume fractions. This comparison base is a good one for the tensile, flexural and compressive properties and a similar normalization concept is used in [20]. Since the shear properties depend more heavily on the resin properties, it is difficult to determine a normalized value of shear strengths. Thus, they were omitted. The resin contents encountered in these two panels exceed the levels studied previously in Reference [20], thus the conclusions drawn in [20] may not be directly applicable to Table VIII.

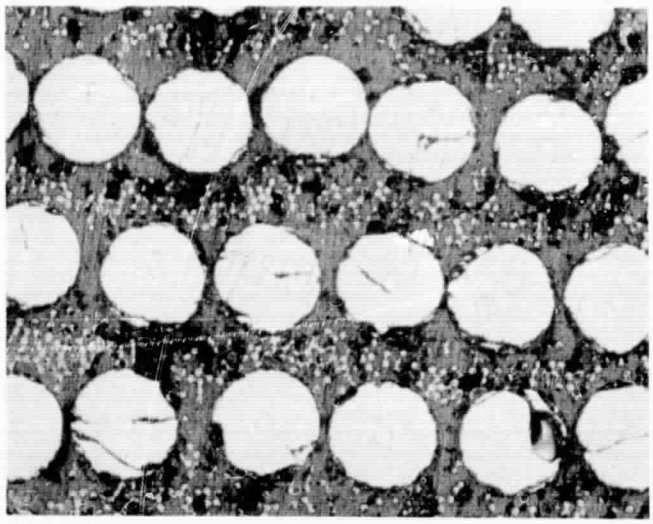

Figure 28. Micrograph (150 X) of Specimen C-11C.

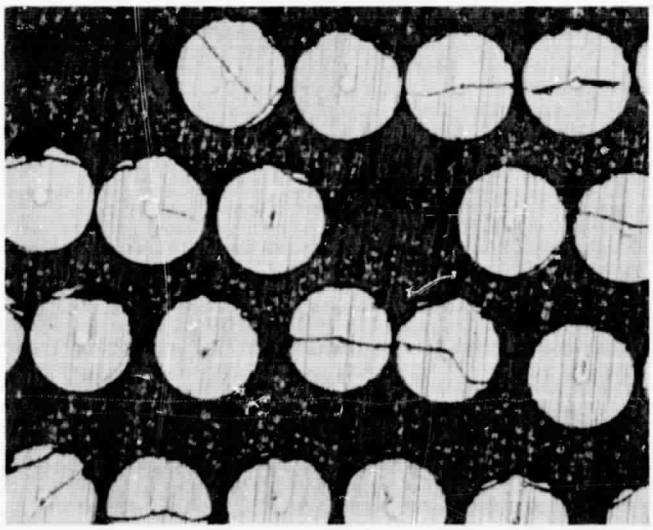

Figure 29. Micrograph (150 X) of Specimen C-11D.

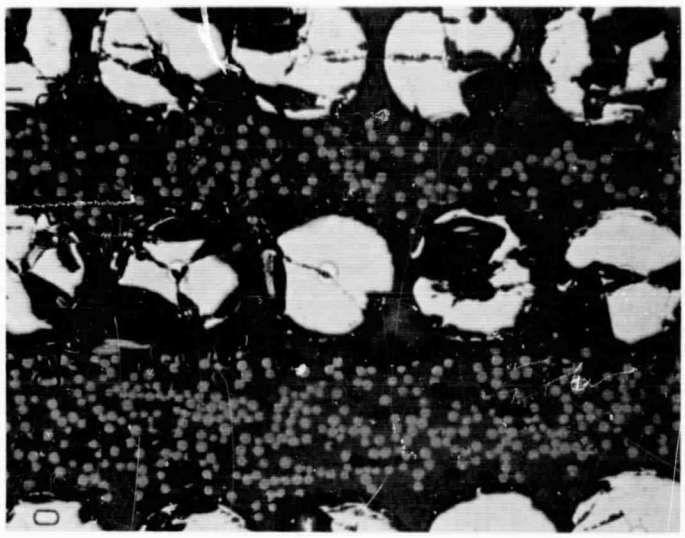

a) 200X

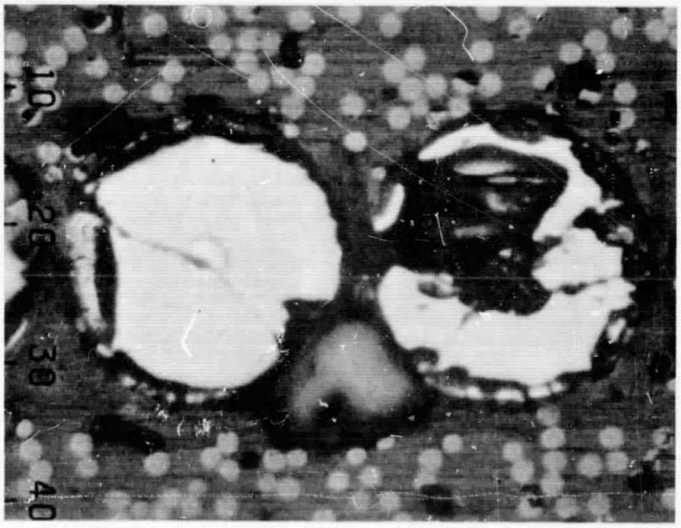

b) 400X

Figure 30. Micrographs of Prototype Panel Specimen A-115.

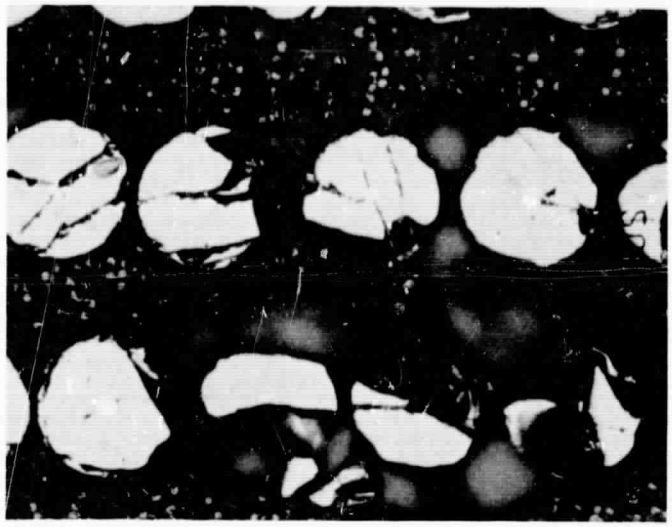

a) 200X

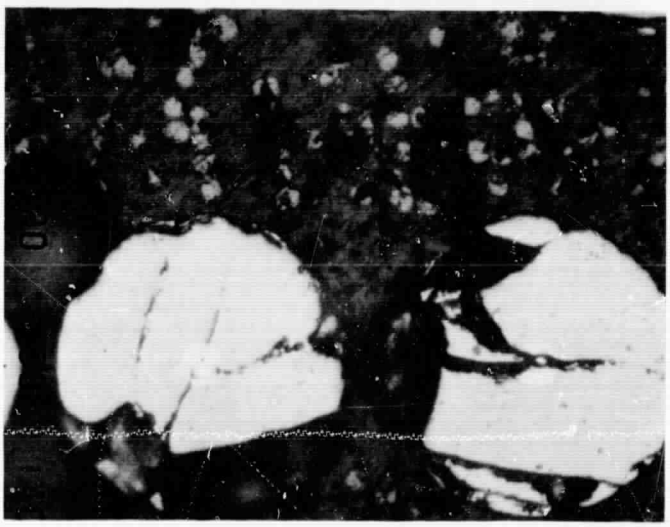

b) 400X

Figure 31. Micrographs of Prototype Panel Specimens B-120.

TABLE VI

SUMMARY OF CURE CYCLES IN PROTOTYPE LAMINATE STUDY

PANEL	PROCESS	TEMP. °F	TIME, MINUTES	EXTERNAL PRESSURE, psig	INTERNAL VACUUM, in. Hg.
A-115	Heat up from RT	275°	45	0	29
	Hold at Temp.	275°	5	0	29
	Heat up	350°	25	100	29
	Cure	350°	120	100	29
B-120	Heat up from RT	275°	24	0	29
	Hold at Temp.	275°	5	0	29
	Heat up	350°	25	100	29
	Cure	350°	120	100	29

TABLE VII

SUMMARY OF LAMINATE PHYSICAL PROPERTIES OBTAINED DURING THE PROTOTYPE LAMINATE STUDY

PANEL	FIBER RATIO α	RESIN WEIGHT FRACTION, w_R	MEASURED SPECIFIC GRAVITY γ'	VOLUME FRACTIONS			
				v_B	v_G	v_R	v_a
A-115	0.087	0.263	1.87	0.492	0.057	0.406	0.045
B-120	0.195	0.263	1.78	0.415	0.125	0.385	0.075

TABLE VIII

SUMMARY OF TEST RESULTS FOR PROTOTYPE LAMINATES

PANEL	PROPERTY	MEASURED psi	PREDICTED psi
A-115 $v_a = 0.045$	LONGITUDINAL TENSILE STRENGTH	**	225,000
	LONGITUDINAL TENSILE MODULUS	28.9×10^6	32×10^6
	LONGITUDINAL FLEXURAL STRENGTH	209,900	225,000
	LONGITUDINAL FLEXURAL MODULUS	25.7×10^6	$30.5 \times 10^{6*}$
	IN-PLANE SHEAR MODULUS	1.08×10^6	0.70×10^6
	INTERLAMINAR SHEAR STRENGTH	9,980	--
	BORON SIDE IN COMPRESSION	10,240	--
	BORON SIDE IN TENSION	9,720	--
B-120 $v_a = 0.075$	LONGITUDINAL COMPRESSIVE STRENGTH	171,500	210,000
	LONGITUDINAL COMPRESSIVE MODULUS	31.9×10^6	32×10^6

**FAILED AT GRIPS, AVERAGE STRESS 95,200 psi.

*CALCULATED FROM EQUATIONS IN [19], WHICH CORRECT FOR SHEAR.

The interlaminar shear strengths recorded in Table VIII appear to be somewhat dependent upon the position of the "boron" side. When the laminate is cured, one outer surface resembles that of a boron laminate, while the other resembles that of a graphite laminate. This occurs because of the inherent asymmetry of the prepreg. The resulting laminate has a neutral plane which does not coincide with the mid-plane. Both averages are within the observed standard deviation, so no further conclusions can be drawn from this data alone. Table IX presents the interlaminar shear strength data in more detail.

TEST LAMINATES

A total of six test laminates were fabricated to evaluate the effect of adding graphite to the boron/epoxy laminate. The modified procedure (with preheated press) was used to produce these panels. Three panels (218A, 227A and 304A) were 12" x 12.5" laminates, nine plies thick, while the remaining three (218B, 227B and 304C) were 5" x 5" laminates, twenty-one plies thick. The cure cycles for the six panels are summarized in Table X. Note in this Table that panels 304A and 304C are subjected to standard boron/epoxy cure cycles. Since these two panels contained no graphite, the resin flow would have been excessive if the hybrid cure procedures had been used. Table XI summarizes the physical properties of the six laminates. As this Table shows, the volume fractions are maintained to ±1% for the three configurations. Micrographs of the three 9-ply laminates are shown in Figure 32 (micrographs for the thicker laminates are similar). Note that the graphite fibers have mixed reasonably well with the boron/fibers in panel 218A; but a layered structure is evident in panel 227A, which has a higher graphite content. The higher graphite fiber content of the latter may retard the resin flow sufficiently that complete fiber mix is not readily achieved using 2387 resin. For this higher fraction, a slower curing resin would enhance the mixing. The large spot near the center of Figure 32b (Panel 218A) is a void. Analysis indicates that this laminate has about 0.5% voids, although no other voids were visible at this magnification (150X).

The compositions of the six laminates are shown in the ternary diagram of Figure 33. For the concept evaluation phase, it would have been more desirable to follow the path A-A' shown in this figure rather than the path A-B which was actually taken. The fast curing characteristics of the 2387 resin prevented this approach — it proved nearly impossible to achieve the resin bleedout required to reduce the resin contents of panels 218 and 227 to those desired (at proportions X and Y, respectively). When the Hold time was extended, the resin gelled prematurely. When the temperature at Hold was reduced, the resin was too viscous to bleed as required. As noted previously, a slower curing resin and a higher compaction pressure would have facilitated the required reduction in resin content. Reduction of prepreg resin content is a less desirable alternative.

TABLE IX

SHORT BEAM SHEAR STRENGTH DATA FOR PROTOTYPE LAMINATE A-115

SPECIMEN	SPAN (in)	WIDTH (in)	THICKNESS (in)	FAILURE LOAD (lb)	SHEAR STRENGTH ksi ± σ	COMMENTS
A-120-1	0.36	0.255	0.059	187	9.35	BORON SIDE UP
-3	0.36	0.253	0.060	190	9.38	
-5	0.36	0.255	0.059	216	10.80	
-7	0.36	0.253	0.060	222	10.95	
-9	0.36	0.252	0.059	194	9.76	
-11	0.36	0.253	0.059	222	11.17	
AVERAGE					10.24 ± 0.76	
A-120-2	0.36	0.254	0.060	178	8.78	BORON SIDE DOWN
-4	0.36	0.253	0.058	179	9.13	
-6	0.36	0.252	0.059	194	9.76	
-8	0.36	0.255	0.058	224	11.35	
-10	0.36	0.253	0.060	187	9.23	
-12	0.36	0.254	0.058	197	10.05	
AVERAGE					9.72 ± 0.84	

TABLE X

SUMMARY OF CURE CYCLES FOR TEST LAMINATES

PANEL	PROCESS	TEMP. °F	TIME, MINUTES	EXTERNAL PRESSURE, psig	INTERNAL VACUUM, in. Hg.
218A	Heat up from RT	275	14	0	29
	Hold at Temp.	275	5	0	29
	Heat up	350	9	100	29
	Cure	350	120	100	29
218B	Heat up from RT	275	19	0	29
	Hold at Temp.	275	5	0	29
	Heat up	350	13	100	29
	Cure	350	120	100	29
227A	Heat up from RT	275	9.5	0	29
	Hold at Temp.	275	5	0	29
	Heat up	350	8	100	29
	Cure	350	120	100	29
227B	Heat up from RT	275	12	0	29
	Hold at Temp.	275	5	0	29
	Heat up	350	8	100	29
	Cure	350	120	100	29
304A	Heat up from RT	275	18	3	0
	Hold at Temp.	275	18	3	0
	Heat up	350	12	3	0
	Cure	350	120	3	0
304C	Heat up from RT	275	18	3	0
	Hold at Temp.	275	18	3	0
	Heat up	350	12	3	0
	Cure	350	120	3	0

TABLE XI

SUMMARY OF LAMINATE PHYSICAL PROPERTIES OBTAINED DURING THE TEST LAMINATE STUDY

PANEL	FIBER RATIO α	RESIN WEIGHT FRACTION, w_R	MEASURED SPECIFIC GRAVITY γ'	VOLUME FRACTIONS			
				v_B	v_G	v_R	v_a
218A	0.206	0.244	1.94	0.458	0.144	0.393	0.005
218B	0.197	0.252	1.94	0.460	0.138	0.402	~0
227A	0.470	0.231	1.88	0.373	0.265	0.362	0
227B	0.429	0.240	1.88	0.380	0.250	0.370	0
304A	0	0.231	2.06	0.604	0	0.386	0.010
304C	0	0.221	2.10	0.620	0	.380	0

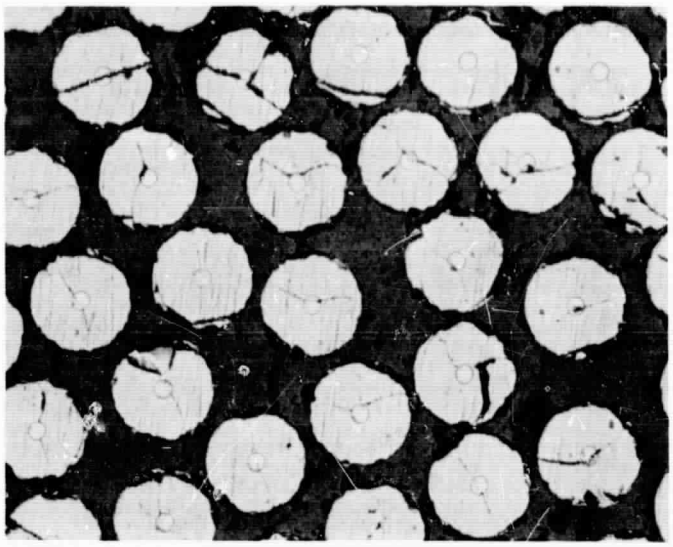

a) Panel 304A (No Graphite)

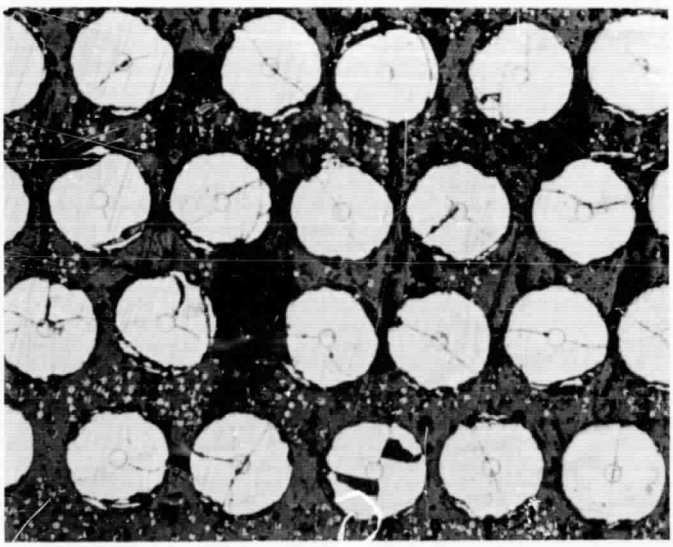

b) Panel 218A (14.4% Volume Graphite)

Figure 32. Micrographs (150 X) of Test Laminates.

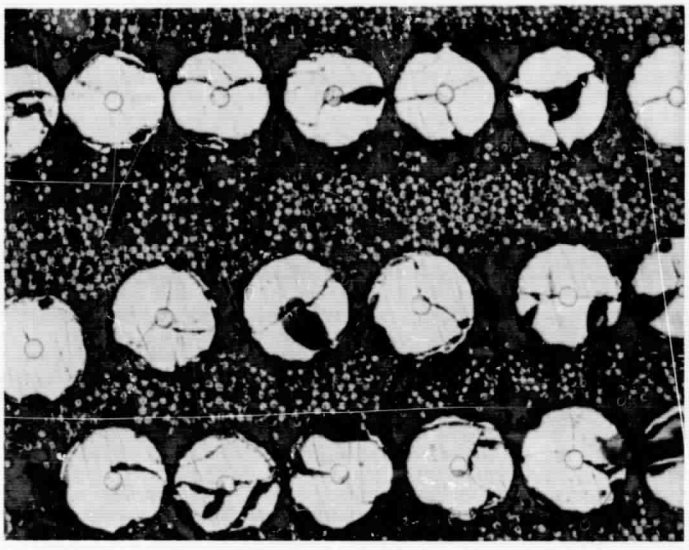

c) Panel 227A (26.5% Volume Graphite)

Figure 32. (Cont'd) Micrographs (150 X) of Test Laminates.

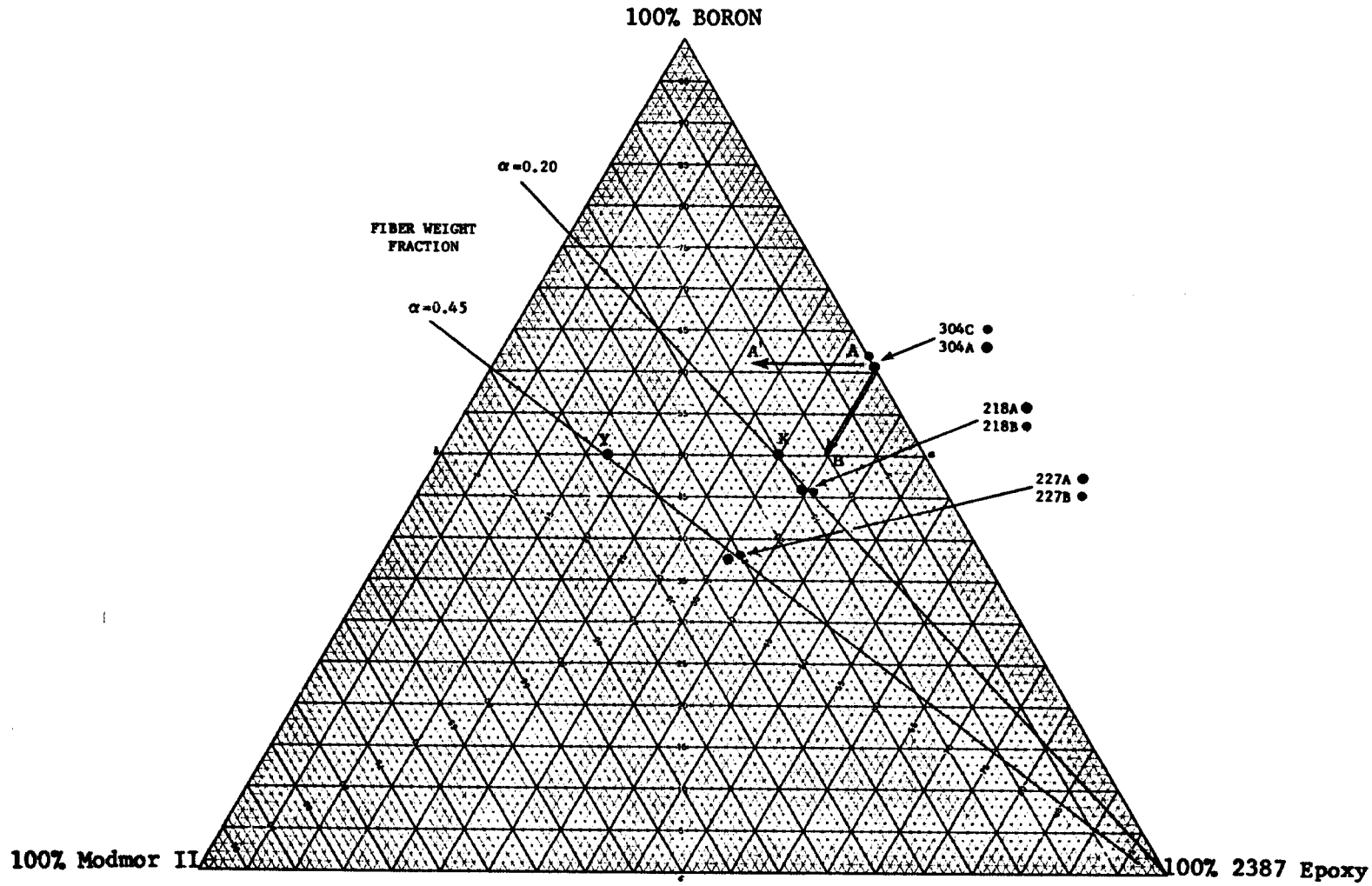

Figure 33. Compositions of Test Laminates, shown on the Ternary Diagram.

The six laminates were tested to obtain preliminary strength and stiffness data. Panels 218B, 227B and 304C were tested in compression, while panels 218A, 227A and 304A were tested in longitudinal tension, longitudinal flexure, transverse tension, in-plane shear and short-beam shear. Tests were performed in accord with the specifications shown in Appendix C. Tables XII and XIII summarize the mechanical properties obtained from these tests, based on averages of at least three replicates. Note that the longitudinal tensile and compressive strengths are not adequately defined by these results, although the other moduli and strength properties appear to be correct indications. The Halpin-Tsai equations provide accurate predictions of the transverse tensile modulus and in-plane shear modulus of panel 304A, and if higher transverse and shear moduli had been assumed for the graphite fibers, these equations would have also provided better predictions for panels 218A and 227A than Table XII indicates. The expected improvements can be deduced from Figures 17 and 18, which plot the effect of graphite fiber anisotropy on these properties. The short beam shear data is incomplete because some specimens failed in flexure. For the mixed composite, the mode of failure depends not only on the strengths of the fibers and resin but also upon the placement of the fibers in the laminate. As the test results for panel 218A reveal, the placement of the high-strength boron fiber on the tensile face permits development of the (presumably) full interlaminar shear strength. On the other hand, when the graphite fibers are on the tensile face, the failure becomes flexural and the full interlaminar shear strength is not developed. In panel 227A, the interlaminar shear strengths varied, depending upon the location of the boron face. Since the failure surface does not coincide with the neutral surface in either case, the differences in observed strengths are probably attributable to the distances between these surfaces. The flexural moduli are predicted from the measured tensile and shear moduli by the relationship [19]

$$E = E' \left\{ 1 + \left[1.096 \left(\frac{t}{L} \right)^2 - 0.323 \left(\frac{t}{L} \right)^3 \right] \frac{E}{G} \right\} \qquad (23)$$

where E' is computed from the classical bending theory and is the "observed" value, t/L is the beam depth-to-span ratio, and E/G is the modulus ratio of the laminate (not of the individual ply).

EVALUATION OF THE CONCEPT

Tables XII and XIII are based upon tests performed on only one laminate of each configuration, and upon only three to five replicates, thus no firm conclusions can be drawn until more laminates and configurations are considered. It appears that the Halpin-Tsai equations will provide reliable predictions of transverse and shear moduli if correct inputs are provided. The tables also show that laminates of reasonable interlaminar shear strength can be easily made using the hybrid prepreg and cure procedures developed in this study. The laminates produced from the hybrid composite are basically sound, as the flexure and short-beam shear tests indicate, and the predicted values are (with some exceptions) reasonably close to

those measured.

The real question which remains to be settled is whether the benefits to be gained from the use of hybrid laminates are worth their additional cost. A better evaluation of these properties, from the weight-savings viewpoint, can be made from studying the specific properties of the laminates. Table XIV summarizes these properties. As this table reveals, the specific transverse and shear properties are improved by the inclusion of graphite, but the effects on longitudinal properties are not well defined. The improvements in shear and transverse tensile properties are in reasonable agreement with theory, but as Table XIV reveals the magnitudes of these improvements are not, in themselves, sufficient to warrant choice of the hybrid boron/graphite/epoxy material over the boron/epoxy material. Unless significant improvements could be shown for longitudinal properties, no fundamental advantages can be seen in using this particular hybrid concept as a replacement for boron/epoxy.

TABLE XII

SUMMARY OF MECHANICAL PROPERTIES OF TEST LAMINATES

PROPERTY	PANEL 304A (0° GRAPHITE)		PANEL 218A (14.4% GRAPHITE)		PANEL 227A (26.5% GRAPHITE)	
	MEASURED	PREDICTED	MEASURED	PREDICTED	MEASURED	PREDICTED
LONGITUDINAL TENSION						
MODULUS, 10^6 psi	30.8	36.0	28.3	34	22.4	33.0
ULTIMATE STRENGTH, ksi	118.4*	172.0++	126.2*	131.0++	84.7*	106.0++
LONGITUDINAL FLEXURE						
MODULUS, 10^6 psi	23.3	29.3+	27.0	27.2+	24.9	21.6+
ULTIMATE STRENGTH, ksi	209.9	172.0	217.2	131.0	186.6	106.0
TRANSVERSE TENSION						
MODULUS, 10^6 psi	2.45	2.75	2.77	2.30	3.35	2.25
ULTIMATE STRENGTH, ksi	2.73	--	6.05	--	5.92	--
TRANSVERSE FLEXURE						
MODULUS, 10^6 psi	1.64	2.41+	2.61	2.70+	4.19	3.34+
ULTIMATE STRENGTH, ksi	5.65	--	8.53	--	11.93	--
IN-PLANE SHEAR						
MODULUS, 10^6 psi	0.743	0.75	1.04	0.82	1.23	0.90
SHORT BEAM SHEAR STRENGTH						
BORON SIDE IN COMPRESSION, ksi	**	--	**	--	15.1	--
BORON SIDE IN TENSION, ksi	--	--	15.5	--	14.5	--

*FAILED AT GRIPS. STRENGTH DATA NOT INDICATIVE.

**FLEXURE FAILURE.

+CALCULATED FROM EQUATIONS IN [9], USING MEASURED E AND G AND MAKING CORRECTIONS FOR SHEAR.

++BORON FIBER STRENGTH WAS 285 ± 5 ksi.

TABLE XIII

SUMMARY OF COMPRESSIVE PROPERTIES OF TEST LAMINATES

PROPERTY	PANEL 304C (0% GRAPHITE)	PANEL 218B (13.8% GRAPHITE)	PANEL 227B (25.0% GRAPHITE)
LONGITUDINAL COMPRESSION			
MODULUS, 10^6 psi	46.9**	22.5	32.8
STRENGTH, ksi*	136.7	191.5	184.9

*FAILURE AT LOADING FACES.

**PREDICTED MODULUS = 41 x 10^6 psi.

TABLE XIV

SUMMARY OF SPECIFIC PROPERTIES OF TEST LAMINATES

PROPERTY	PANEL 304 A,C (0° GRAPHITE)	PANEL 218 A, B (~14% GRAPHITE)	PANEL 227 A, B (~26% GRAPHITE)
LONGITUDINAL TENSION			
SPECIFIC MODULUS, 10^8 in	4.10	4.04	3.30
SPECIFIC STRENGTH, 10^6 in	1.58	1.80	1.25
LONGITUDINAL FLEXURE			
SPECIFIC MODULUS, 10^8 in	3.10	3.85	3.67
SPECIFIC STRENGTH, 10^6 in	2.80	3.10	2.75
TRANSVERSE TENSION			
SPECIFIC MODULUS, 10^8 in	0.33	0.30	0.50
SPECIFIC STRENGTH, 10^6 in	0.036	0.087	0.087
TRANSVERSE FLEXURE			
SPECIFIC MODULUS, 10^8 in	0.22	0.37	0.62
SPECIFIC STRENGTH, 10^6 in	0.075	0.121	0.176
LONGITUDINAL COMPRESSION			
SPECIFIC MODULUS, 10^8 in	6.25	3.21	4.84
SPECIFIC STRENGTH, 10^6 in	1.82	2.73	2.73
IN-PLANE SHEAR			
SPECIFIC MODULUS. 10^8 in	0.10	0.15	0.18

SECTION IV

PRELIMINARY STUDY OF HYBRID COMPOSITE JOINING CONCEPTS

THE TRANSITIONING CONCEPT

The boron/graphite hybrid concept appears to be most useful in certain specialty applications, where the special handling characteristics of the hybrid are desirable. For example, in a boron/epoxy structural element it is usually required to provide a closeout or an interface which permits load transfer into the surrounding structure. The closeout sections generally have complex shapes which the 0.005" diameter boron fiber cannot negotiate without severe over-stress. Graphite fibers, on the other hand, can be easily formed to the complex shapes required in the closeout, but might not be as desirable as boron fibers for the remaining structure. Since the graphite and boron fibers have been found to intermingle very well, it is feasible to fabricate a structural element whose main load-bearing section consists of a boron composite and whose closeout section consists of a graphite composite. The transition section, which would consist of a boron/graphite composite, would provide for transfer of load between the two sections. Because the fibers are intermixed, this transition section would provide a continuous cross-section change between the other two sections, and much of the normally required adhesive bonding would be eliminated. Since the properties of the boron/epoxy and boron/graphite/epoxy materials can be matched through proper design, this transition could be realized without penalty to the structure.

It could be argued at this point that such a structure would not be feasible because at least three different cure cycles would be required: one each in the closeout, transition and load bearing sections of the element. This difficulty can be reduced by adding a small quantity of graphite fiber to the boron prepreg. As this study has indicated, the presence of the graphite fibers retards the resin flow characteristics sufficiently that the graphite/epoxy cure cycle may be employed. The extent of this effect could not be studied within the scope of this program, but it appears that only small volume fractions of graphite would be required to permit a single cure cycle for the entire structure.

JOINT FABRICATION AND TESTING

Two simple joining configurations were considered, in order to obtain a preliminary evaluation of the transitioning concept. Two panels, 6" x 10" length were fabricated using the interleaving schedules A and B illustrated in Figure 34. As this Figure indicates, the simplest interleaving patterns were employed to obtain a transition between a hybrid boron/graphite/epoxy laminate and a graphite/epoxy laminate. It is assumed that the graphite/epoxy laminate is part of some appropriate close-out section,

such as a "bathtub" fitting or a "box-end" fitting, while the boron/graphite/epoxy laminate is part of the loaded section of the element. The hybrid section contains 12 - 14% volume graphite fibers, added to influence the cure characteristics of the hybrid section and to provide for more efficient load transfer between the two laminates. At first it would appear that transition A (Figure 34b) is inherently stronger than transition B (Figure 34c) because its "bonded area" is three times that of the latter. This is not necessarily correct, however, since the forces required to cause shear failure in these bonds, even in transition B, exceed the tensile failure forces by at least 400%. The strength of Transition A would be, at best, 50% of the lowest parent laminate strength, since at sections X and Y only half the available fibers are actually sustaining the load. The strength of Transition B would be, at best, 80% of the lowest laminate strength, since at sections X' and Y' only 80% of the available fibers are carrying load. In contrast with Transition A, however, this percentage increases with the laminate thickness. In both cases, stress concentrations at the steps will reduce the strength below these upper levels. The "effective modulus" of the transition section would be difficult to determine or predict, since the stress field is not uniform throughout the thickness of this region. Strain gages mounted in these regions would record strains of the outer layers only. In Transitions A and B these strains would increase from zero at X and X' to unknown values at Y and Y'. Extensometers mounted in these sections would measure average displacements over the gage length of the outer layers only, and would lead to poor estimates of the effective modulus.

The two laminates, designated 331-A and 325-B, were laid up and cured using the cycles shown in Table XV. Each laminate, complete with transition section, was cured in a single process; it was not necessary to provide separate cures for each section. The physical properties of the laminates are shown in Table XVI. The correspondence of physical properties shown in Table XVI is to be expected, since the two laminates differ only with respect to the transition pattern.

After curing, each laminate was fitted with bonded glass tabs and cut into 3/4" wide tensile test specimens. One specimen from Laminate 331A was sectioned at positions U, V and W, as shown in Figure 34b, and micrographs were prepared to evaluate the extent of fiber mixing. Micrographs (150X) of these sections are shown in Figure 35. These photographs reveal no voids in the laminate, and indicate relatively good fiber mixing in the hybrid section (Figure 35a). The transition section (Figure 35b) exhibits the laminated structure expected using this layup procedure, and the graphite/epoxy section (Figure 35c) shows slight evidence of excessive resin at the interfaces between the prepreg layers. The resulting shear properties would not be expected to reduce the laminate tensile strengths significantly, since the "bond" area in the transition is much larger than that required to prevent shear failure.

Tensile test results are summarized in Table XVII. As this table indicates, the failures occurred at the boundary (Y or Y') between the transition section and the graphite/epoxy section. Examination of both sets of specimens revealed that failure originated in the graphite/epoxy section. The relatively low, nearly equal, strength values (42.4 and 48.0 ksi, respectively) indicate the existence of large stress concentrations at these boundaries, probably due to the distortions occurring at the boron fiber ends.

EVALUATION OF THE CONCEPT

Further studies of these concepts were not within the scope of this contract, so additional specimens were not fabricated. In future studies, it will be necessary to develop means for dispersing the boron fiber ends in the transition section in order to avoid the rows of fiber ends which occurred in these test laminates. In order to ensure continuity of the laminate surfaces it is also advisable to apply a "finishing" layer, probably of graphite epoxy, to the surfaces of the entire laminate. These layers would provide continuous transfer of load across the transition section, as well as "smoothing over" sources of potential laminate fractures.

The smooth transitions which can be achieved with this design concept are shown in Figure 36. If the strength reductions associated with transitions A and B can be tolerated, a bond-free, perforation free, aerodynamically smooth transition section can be easily achieved in this way. By use of improved lamination patterns, the strengths of these transitions can be improved, thus enhancing the feasibility of this concept in practical design applications. Since it is felt that the mixed-composite transition merits further study, its use is incorporated in the recommended demonstration article.

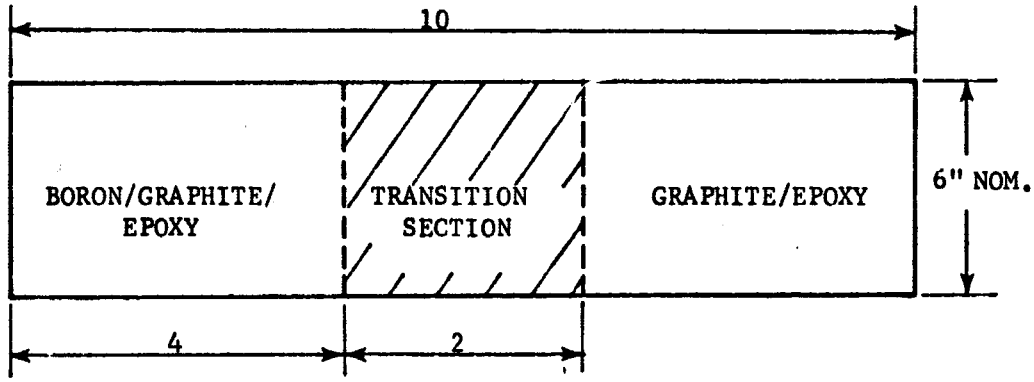

a) General Panel Configuration, Plan View.

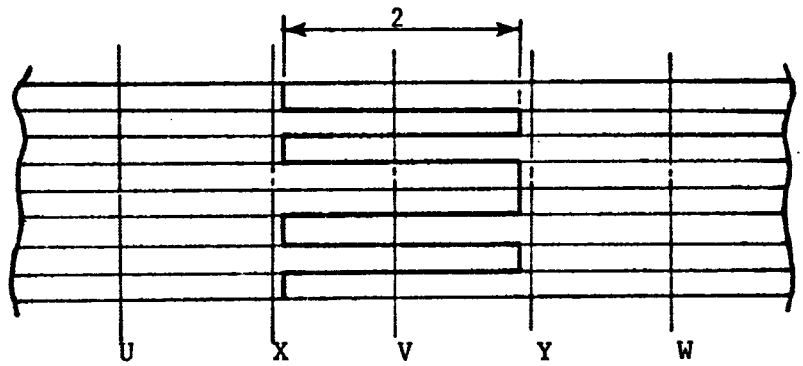

b) Transition Section: Interleaving Schedule A.

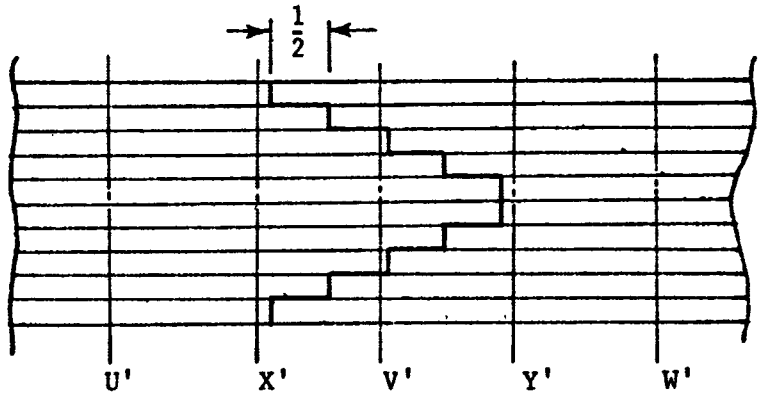

c) Transition Section: Interleaving Schedule B.

Figure 34. Hybrid Transitioning Concepts.

TABLE XV

SUMMARY OF CURE CYCLES FOR HYBRID JOINTS

LAMINATE	PROCESS	TEMP. °F	TIME, MINUTES	EXTERNAL PRESSURE, psig	INTERNAL VACUUM, in. Hg.
331-A (Transition A)	Heat up from RT	275	13	0	29
	Hold at Temp.	275	5	0	29
	Heat up	350	9	100	29
	Cure	350°	120	100	29
325-B (Transition B)	Heat up from RT	275	12	0	29
	Hold at Temp.	275	5	0	29
	Heat up	350	10	100	29
	Cure	350	120	100	29

TABLE XVI

SUMMARY OF TRANSITION LAMINATE PHYSICAL PROPERTIES

LAMINATE	SECTION	FIBER RATIO α	RESIN WEIGHT FRACTION w_R	MEASURED SPECIFIC GRAVITY γ'	MEASURED OVERALL SPECIFIC GRAVITY γ_o
331-A (TRANSITION A)	GRAPHITE/ EPOXY	∞	0.375 (v_R=0.460)	1.50	1.70
	BORON/ GRAPHITE/ EPOXY	0.206	0.244 (v_R=0.395)	1.94	
325-B (TRANSITION B)	GRAPHITE/ EPOXY	∞	0.375 (v_R=0.460)	1.50	1.71
	BORON/ GRAPHITE/ EPOXY	0.206	.244 (v_R=0.395)	1.94	

a) Position U, Boron/Graphite/Epoxy Section

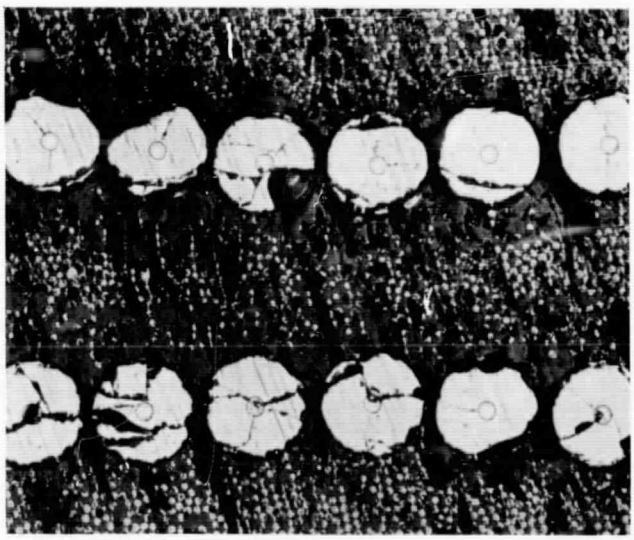

b) Position V, Transition Section

Figure 35. Micrograph (15) X) of Transition Laminate 331A.

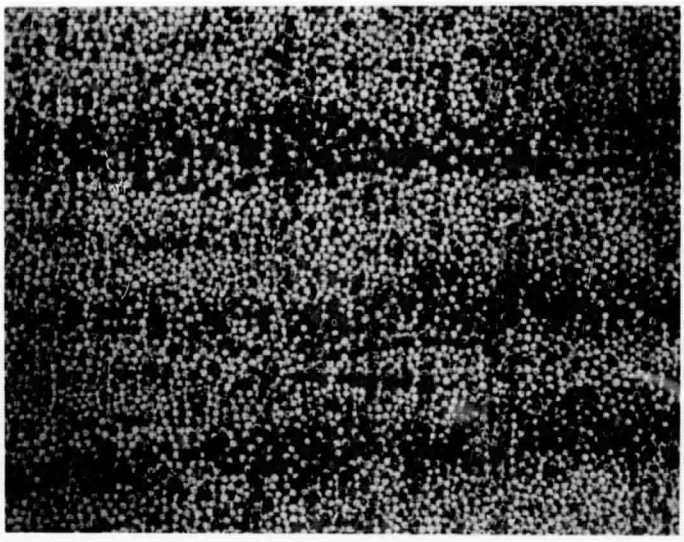

c) Position W, Graphite/Epoxy Section

Figure 35 (Cont'd). Micrograph (150 X) of Transition Laminate 331A.

TABLE XVII

TENSILE STRENGTHS OF TEST LAMINATES

LAMINATE	SPECIMEN	CROSS-SECTIONAL AREA, in^2 IN THE FAILURE ZONE	FAILURE LOAD lb.	ULTIMATE STRENGTH ksi	FAILURE LOCATION
331-A (TRANSITION A)	1	0.04147	1525	36.8	Y
	2	0.03770	1690	44.8	Y
	3	0.04147	1600	38.6	Y
	4	0.04147	2040	49.2	Y
	5	0.04147	1775	42.8	Y
	6	0.04147	*	*	*
	7	0.04147	**	**	**
	ULTIMATE STRENGTH = 42.4 ± 4.4 ksi				
325-B (TRANSITION B)	1	0.04823	2575	53.4	Y'
	2	0.05194	2125	40.9	Y'
	3	0.04823	2560	53.1	Y'
	4	0.05565	2480	44.6	Y'
	5	0.05565	2675	48.1	Y'
	6	0.05194	**	**	**
	ULTIMATE STRENGTH = 48.0 ± 4.8 ksi				

*SECTIONED FOR MICROGRAPHS

**SAVED

a) Laminate 331-A

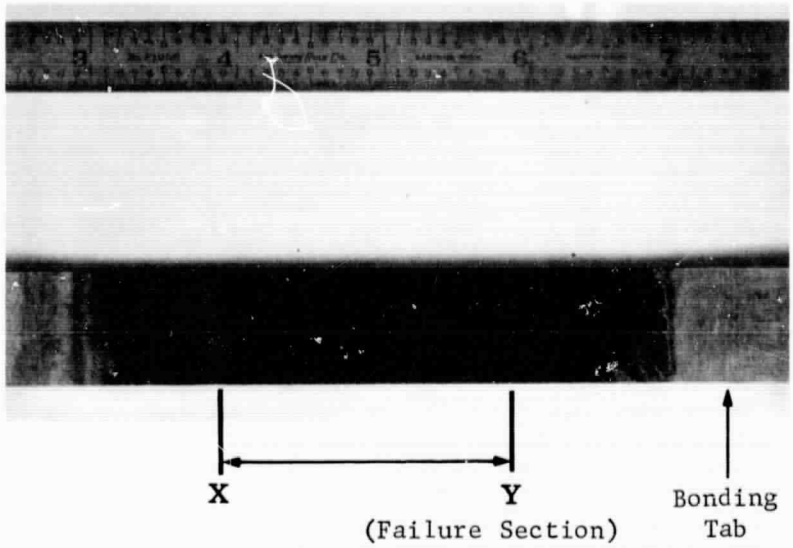

b) Laminate 325-B

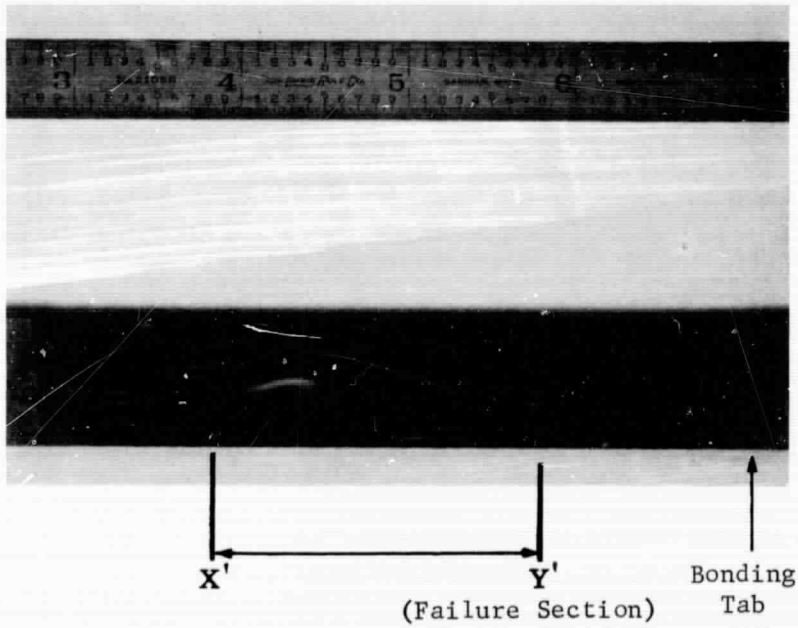

Figure 36. Tensile Specimens Cut From Transition Laminates.

SECTION V

SELECTION OF DEMONSTRATION ARTICLE

SUBCONTRACTOR

A study was performed by North American Rockwell Corporation (NAR), under contract to WRD, with the aim of selecting a technically significant, practical demonstration article which would utilize the capabilities of the hybrid composite material. In order that appropriate weight and performance comparisons could be made, the functions of established metal hardware were considered. Both current and future space hardware were evaluated in the applications survey — current hardware because direct comparisons could be made, and future hardware because they represent the best potential for advanced composites applications. The selection was narrowed down to four components: two from the Apollo Service Module and two from the Space Shuttle System. These items were chosen because they could be reduced to small structural demonstration articles.

APPLICATIONS SELECTION

The cylindrical high-gain antenna boom of the Apollo vehicle deploys from the side of the Service Module (see Figure 37). It is critical in angular deflection, with 140×10^{-6} radians maximum allowable rotation between the ends. The current structure is machined from beryllium, which has a higher specific modulus than the competitive hybrid material but which cannot be formed to the variety of shapes possible with the hybrid material. These shapes, which would increase the diameter of the tube's center section, would result in a greater flexural stiffness for a given cross-sectional area. Studies of boron/epoxy composites show that practical configurations can be achieved which obtain higher specific stiffnesses than the beryllium design, yet maintain the current end fitting design.

A second candidate is the stand-off strut for the Space Shuttle boost vehicle. One proposed fuselage configuration employs load bearing tanks which are separated from the aerodynamic heat shield surface by means of these struts. A quarter-section of a typical station for this design is shown in Figure 38. As this figure indicates, the stand-off struts are primarily long column compression members, an application for which the high modulus boron/epoxy and boron/graphite/epoxy materials are particularly well-suited.

The fuselage shell of the Space Shuttle boost and orbiter vehicles makes up a large percentage of the vehicular structural weight. Weight reductions in this shell will contribute directly to either increasing the payload, or reducing overall system weight, or increasing the safety margins of other components. One method for weight reduction would require unidirectional composite reinforcement of the titanium stiffeners in the sheet-stringer fuselage panels. Comparisons of all-titanium and boron/epoxy-reinforced designs have shown that weight savings of 15 to 28% could be realized, depending upon the load level and thickness proportions of the sheet and stringer.

An Apollo Service Module radial beam truss structure is shown in Figure 39. Its main function is to provide support for the Apollo Command Module. Since it is part of the moon orbiting system, this element must be considered part of the payload. Table XVIII summarizes the maximum pad loads for the six radial beams used in this structure. Data for the critical systems load and environmental conditions, applicable design parameters and performance of the current metal radial beam structure are contained in Reference [21].

The inboard leg of Number 5 radial beam truss was recommended as the most appropriate demonstration article. This choice was based upon the following considerations:

a. Unidirectional material can be employed, thus utilizing the best capability of fiber composites.

b. The beam cap loads are of sufficient magnitude to make the cap-to-web weight ratio significant.

c. The beam is of sufficient size that weight reductions will have meaningful influence on the overall structural weight.

d. A documented analysis (Reference [21]) is available for the current aluminum design.

In addition, the performance of future space vehicles would benefit from the improved beam element. For example, the Space Shuttle System is expected to use a number of beam elements, some of which are located in the thrust structure of the booster vehicle. A weight reduction in this structure would be extremely beneficial because of the already tail-heavy condition of the booster (due to the weight of the engines).

The full-scale demonstration article is 32.28 inches long and is currently machined from 7075-T6 aluminum plate. Two approaches have been recommended by NAR for utilization of the hybrid material: the first would replace a portion of the beam with unidirectional composite material, while the second would replace the entire element with an all-composite beam. Since the strength and stiffness achieved by the boron/graphite/epoxy material are not significantly greater than those achieved by the augmented boron/epoxy material, it is felt that any of the four structures could be practically realized using the boron/epoxy or graphite/epoxy materials alone. For current application, the hybrid material would not provide improvements sufficient to warrant the added expense.

The potential of the hybrid material appears to lie in its ability to produce transition sections. The structure finally selected was based upon the recommended demonstration article, but emphasizes the advantages of the hybrid material over either the graphite/epoxy, boron/epoxy or aluminum materials. This structure is discussed in the next Section.

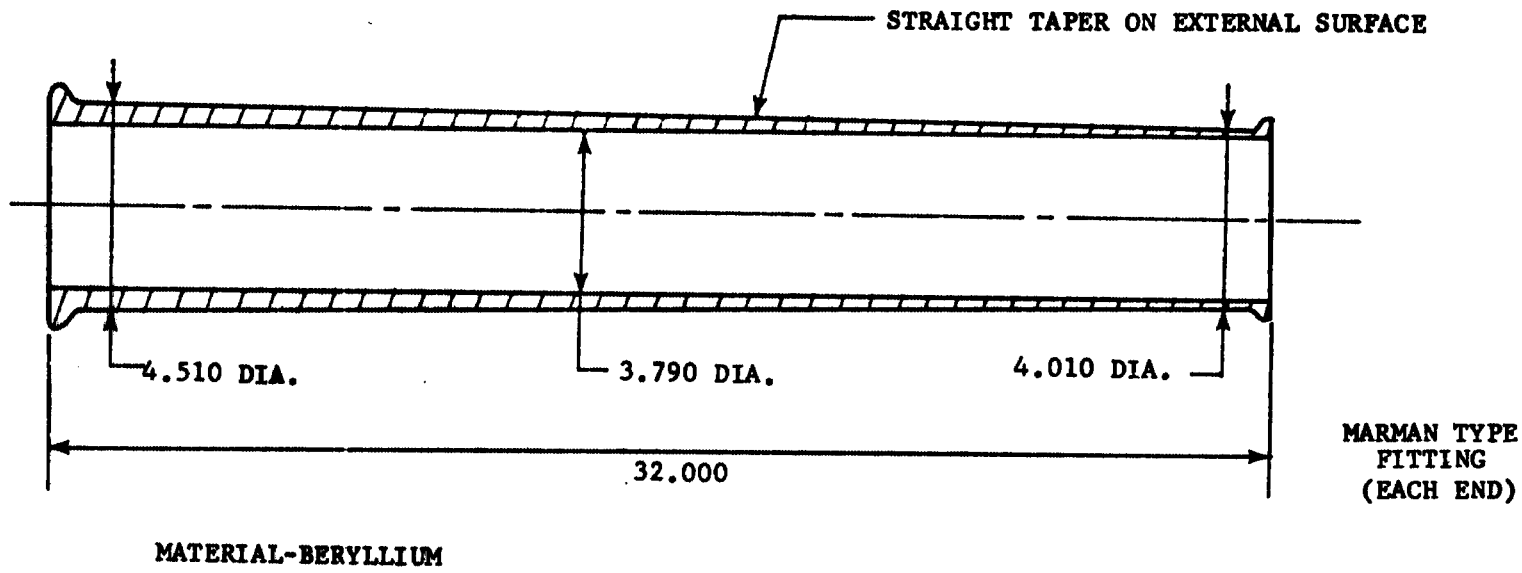

Figure 37. High-Gain Antenna Boom.

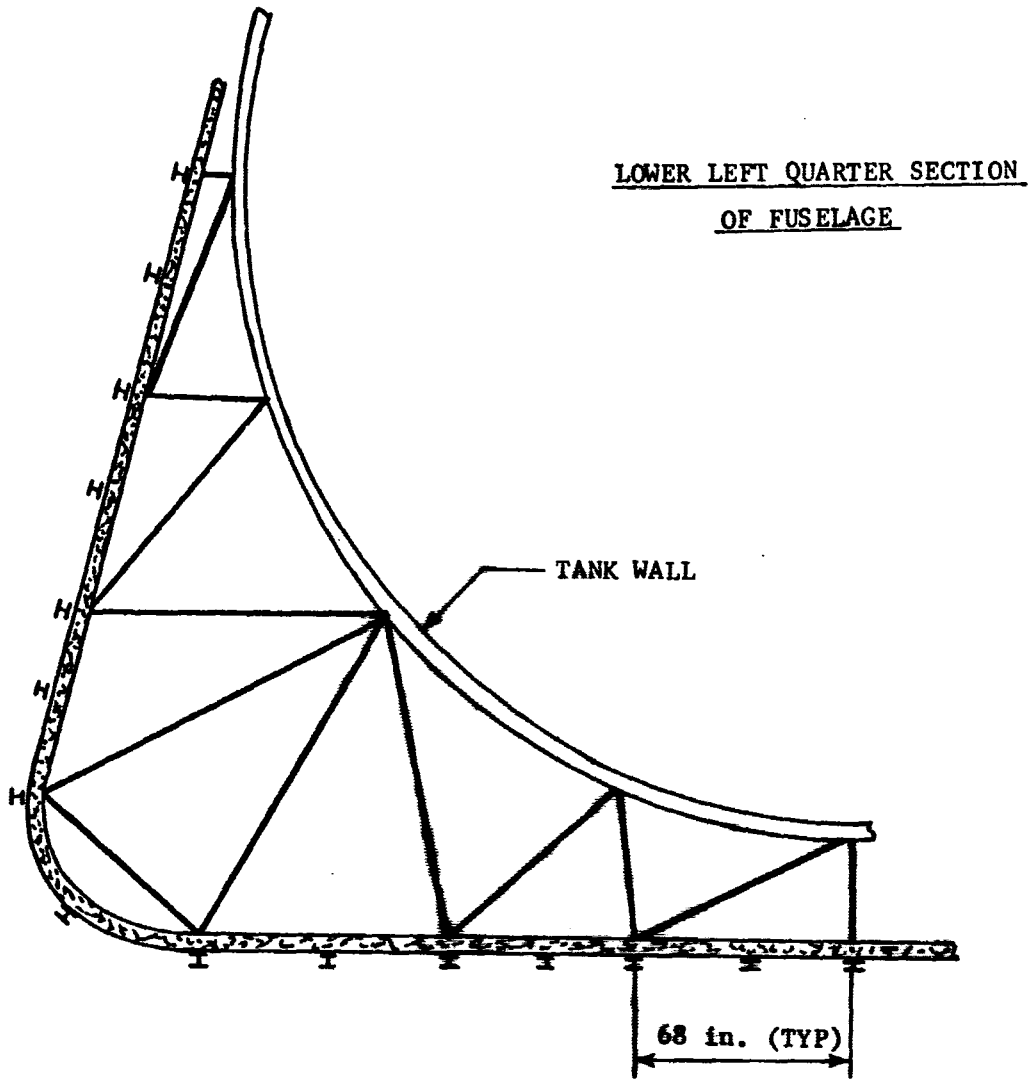

Figure 38. Space Shuttle Fuselage Structure.

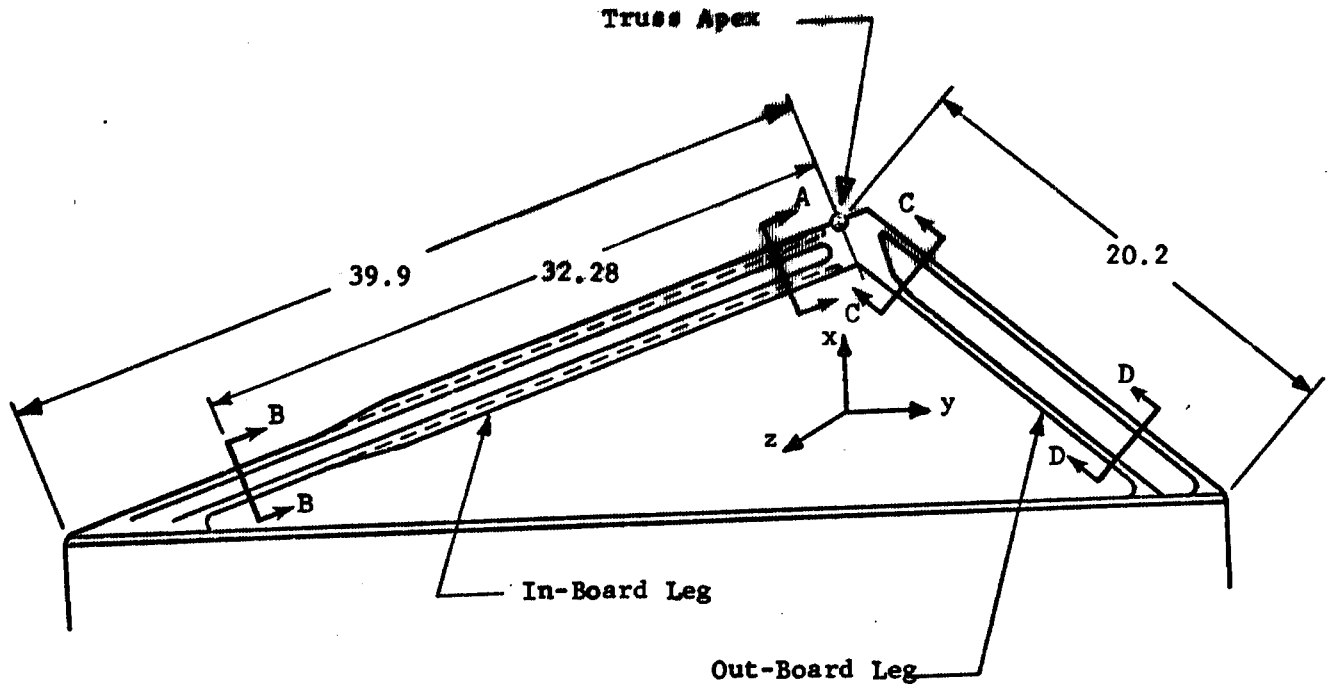

Figure 39. Apollo Service Module Radial Beam Truss.

TABLE XVIII

MAXIMUM PAD LOADS FOR SERVICE MODULE RADIAL BEAM TRUSS (EXCERPTED FROM [21])

RADIAL BEAM NUMBER	CONDITION NUMBER (SEE [21])	PAD LOADS AT TRUSS APEX*			
		NORMAL Px, lb.	SHEAR		MOMENT
			Py, lb.	Pz, lb.	Mym, lb-in.
1	20353	-31645	4	19	66
	20253	-21549	7	19	68
	21253	-21143	-6	-23	-102
2	20255	-40549	20	3625	-88156
	21355	-40243	-1343	-917	-40100
	21255	-40120	-132	-8914	-40788
3	21356	-22735	-12	--	-57
	21256	-22710	0	-12	-57
4	20251	-36212	345.6	2772.4	-76506
	21457	-38850	1450	-8166	-39778
	21257	-38638	315	-7855	-40736
5	20458	-24734	-3	20	71
	20258	-24708	-6	21	73
	21258	-23140	4	-27	-123
6	20252	-33958	261.4	4020.6	-71761
	21352	-37641	-822	-8064	-37198
	21252	-37513	-24	-7966	-37394

*TAKEN DIRECTLY FROM [21]. THE NUMBER OF SIGNIFICANT FIGURES SEEMS EXCESSIVE.

SECTION VI

PROPOSED DESIGN AND FABRICATION OF A MIXED COMPOSITE BEAM

INTRODUCTION

Studies conducted under this Contract indicate that the hybrid boron/graphite concept will be of most value in the design of material transition sections. In compressive sections with gentle curvatures, boron is an appropriate reinforcement because of the compressive strength and stability of its laminates. On the other hand, graphite is an appropriate reinforcement in closeout sections because of its machinability and ability to conform to very small radii. The recommended beam element is an excellent example of a structure whic.. requires both features. The central span of this beam must be stiff to withstand buckling, while the end sections must be capable of interfacing with other parts of the structure. To accomplish these requirements, the central section could contain a relatively high volume fraction of boron fibers, while the closeout section would consist of high strength (or, if necessary, high-modulus) graphite fibers. A transition section, in which the boron volume fraction decreases to zero, could be easily achieved because of the ability of graphite to nest between the boron fibers. It is felt that a high-performance beam structure, incorporating the best features of both fiber systems, could be produced on the basis of what is now known about boron/epoxy, graphite/epoxy and mixed boron/graphite/epoxy composite systems.

DESIGN OF THE COMPOSITE BEAM

When a beam acts under combined bending, compression and shear, each subelement performs a specific task which can best be accomplished using a specific composite material. Consider the I-beam cross-section, for example. The caps of the beam act under tension or compression and, for maximum stiffness, a high modulus fiber oriented along the beam longitudinal axis provides the best performance. When the loading does not reverse itself, it is advantageous to use boron fibers in the compressive cap and/or graphite fibers in the tensile cap. The webs of the beam act primarily in shear (assuming the caps sustain most of the tensile/compressive loads). For maximum stiffness, laminates with fiber orientation $\pm 45^{\circ}$ to the longitudinal axis should be employed. When web buckling is critical, boron fibers along the compressive axes ($\pm 45^{\circ}$) provide the best stability. The stiffness of the central span of the beam is most critical to the overall buckling stability of the beam, thus it should have as high an EI product as practical. The end sections must make transitions into other elements of the structure, and must possess a high degree of machinability and formability to accomplish this transition without undue stress concentration. Although boron fibers are well-suited for reinforcing the central span, it is evident that they do not possess the flexibility required to form the end closures. Thus, a practical boron/epoxy beam,

complete with end closures, is not feasible. Graphite fibers, on the other hand, possess the flexibility to form very small radii in the end closures but the compressive properties of graphite laminates are inferior to those of the boron laminates. The best features of each fiber system can be incorporated into a practical beam using fabrication methods already in existence.

When beams are designed using metals, the modulus of the beam material is constant along its entire length. The only way to achieve the optimum cross-sectional area and EI product everywhere along the beam span is to machine a cross section which varies continuously along the length. This is achieved by first rough-machining, then chem-milling the beam to the final shape. The alternative, a built-up beam, is too heavy for use in the upper stages of space vehicles. On the other hand, when the beam is constructed of composite materials, it is possible to tailor not only the cross-sectional shape but also the modulus of the material, in order to meet the requirements. Although the layup procedure is more complicated, it is possible to maintain less exotic cross-sections with composite materials, thus the increased material costs can be more than offset by the considerably reduced fabrication costs.

A case in point is that of the radial beam truss. This component provides the support for the service moduli, stabilizes the aft bulkhead against the effect of tank inertia loads and transfers engine thrust loads into the outer shell. Each radial beam is an integral unit fabricated from a 2½" 7075-T6 aluminum alloy plate. This plate is first rough machined, then chem-milled to the blueprint dimensions to eliminate the overlaps and fasteners involved in the usual bult-up construction. In radial beam number 5, the cross-section of the inboard leg must transition between the shape AA (Figure 40a) and BB (Figure 40b), while the cross-section of the outboard leg must transition between the shape CC (Figure 41a) and DD (Figure 41b). Details of this beam, and the accompanying analysis, are included in Reference [21].

It is recommended to build a beam incorporating boron, graphite and epoxy materials which will meet the same performance requirements imposed on one of the metallic beams. Since the modulus as well as the cross-section can be tailored, less radical cross-sections can be formed, although the proposed molding technique is adaptable to fairly complex cross-sections. Nominal size and shape of the proposed composite beam is shown in Figure 42. A 20" long x 2 1/4" wide and 2" deep I-beam will be built with integral web and cap, and with a continuous transition into the close-out end section. Through proper design and placement of fibers, this cross-section can provide the strength and stiffness of the aluminum counterpart.

After the design shape of this beam has been finalized for the boron/graphite/epoxy material, one beam will be fabricated. The cross-section will be laid up in four sub-elements as indicated in Figure 43. Upon curing, these sub-elements will form a single-element

cross-section with all the continuity advantages of the metallic counterpart. In the hybrid composite beam, the center span of both the cap and web/cap sub-elements will consist of boron/epoxy or boron/graphite/epoxy material, which gradually transitions to graphite/epoxy at the closeout sections. Curing will take place in a mold, designed to maintain important beam dimensions as well as the closeout configuration.

Since the design and fabrication functions are very interdependent, close coordination must be maintained between these functions in order to properly execute this task.

EVALUATION OF THE ELEMENT

It is appropriate to design and/or fabricate a counterpart beam of graphite/epoxy or aluminum to the same design loads, in order to provide a basis for evaluating the hybrid beam. Tests should include combined bending and compression, in order to better simulate the loads on the radial beam element.

FABRICATION OF THE BEAM

It was planned to fabricate a hybrid beam based on a space application mutually agreed upon between the WRD Project Engineer, the NASA Project Engineer and our subcontractor North American Rockwell (NAR). The beam to be fabricated was selected as a radial beam truss in the service module of the Apollo system. Details of the design and loads for the beam truss were provided as a part of the subcontract to NAR. Their final report is contained in Appendix D. Due to increased scope deemed to be necessary by the NASA Project Engineer and WRD in the area of transition joints and analysis, the fabrication of this beam could not be accomplished within the cost and schedule allotted for the program.

In addition, it was felt by the NASA Project Engineer and WRD (after the study of the boron/graphite hybrid material) that sufficient advantage would not be gained through the use of the hybrid approach to warrant fabrication of a sub-component. The advantages and disadvantages of the hybrid material approach is discussed in more detail in the summary and conclusions.

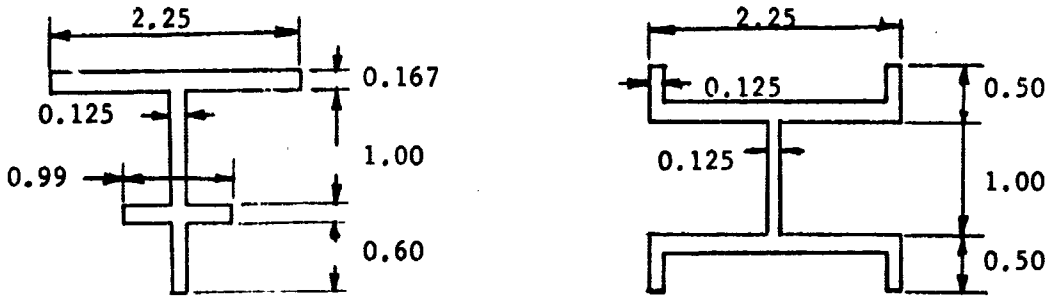

a) SECTION AA

b) SECTION BB

Figure 40. End Cross-Sections of Inboard Leg of Radial Truss Number 5.

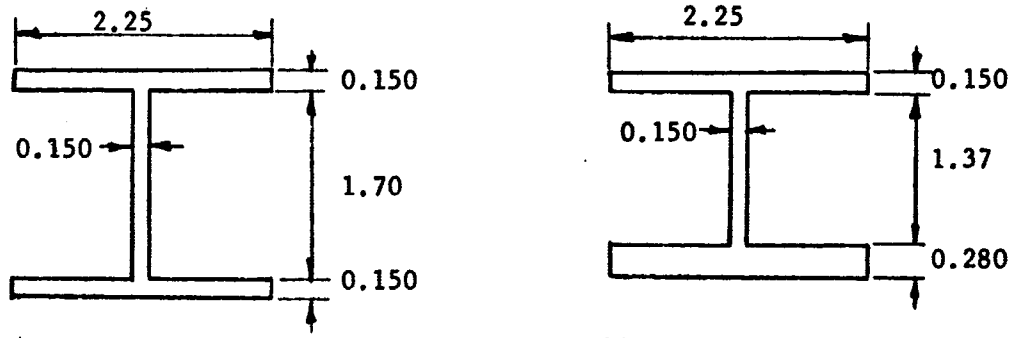

a) SECTION CC

b) SECTION DD

Figure 41. End Cross-Sections of Outboard Leg of Radial Truss Number 5.

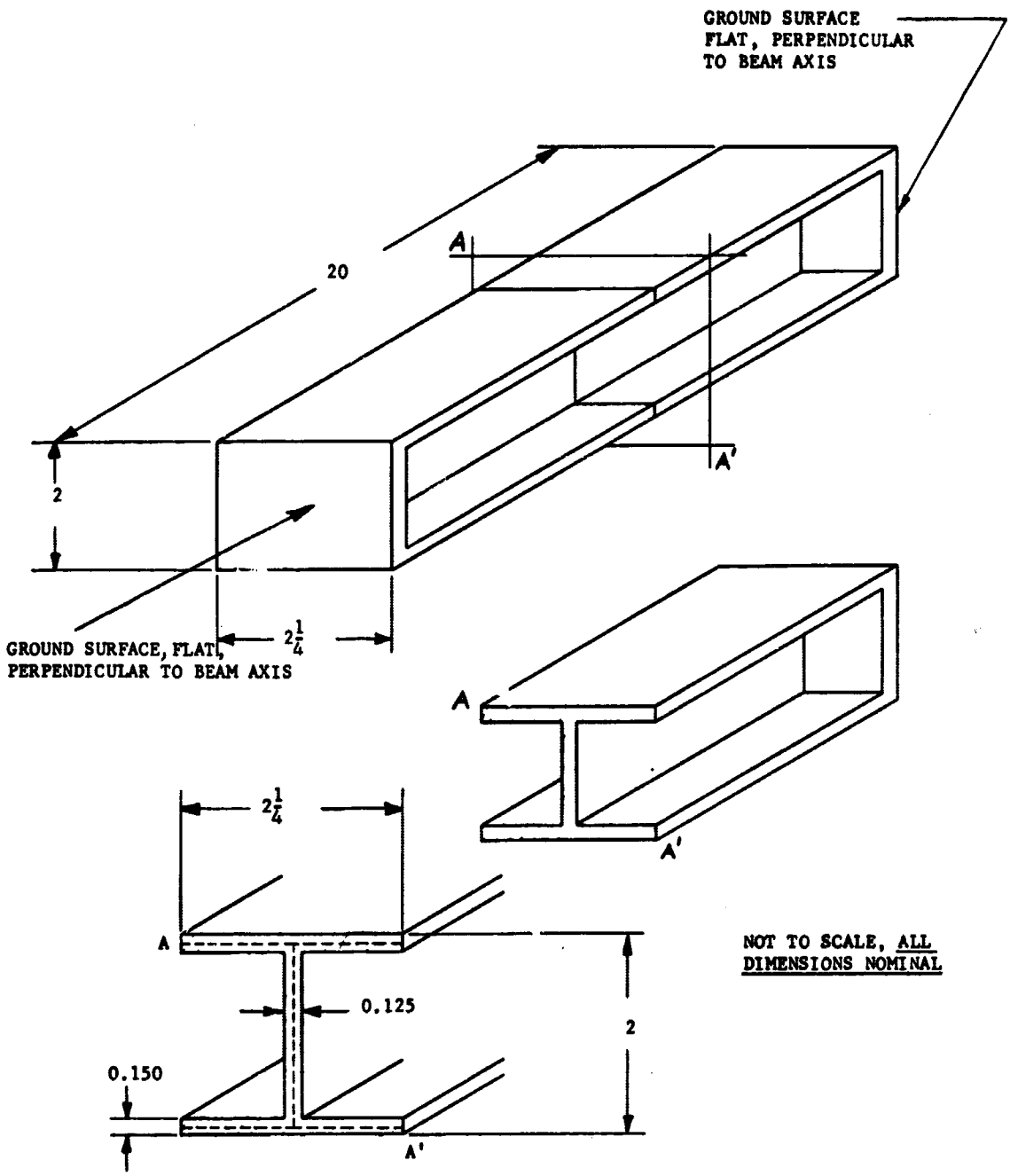

Figure 42. Proposed Composite Beam.

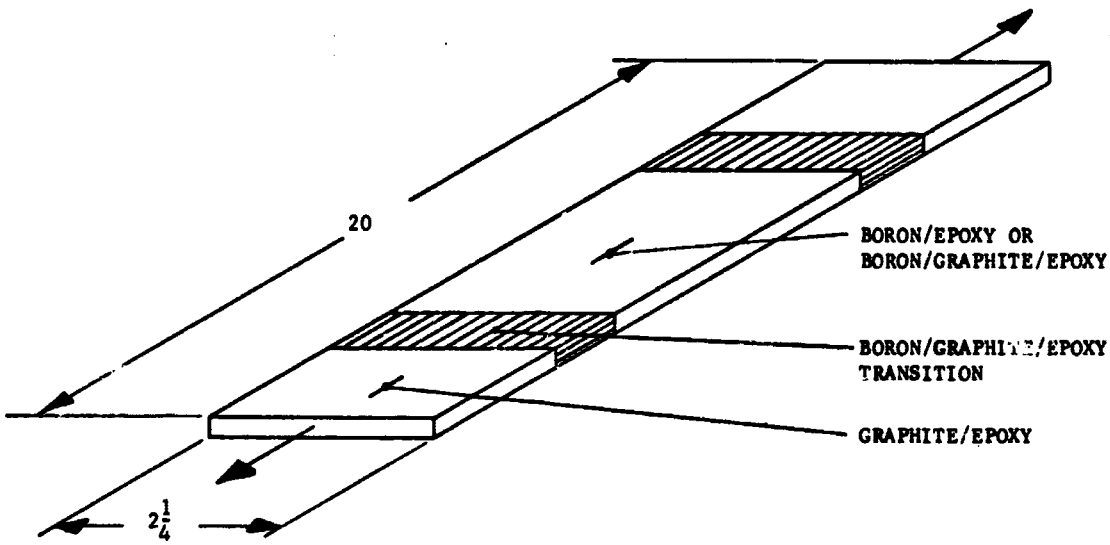

CAP - PRIMARILY UNIDIRECTIONAL 0°

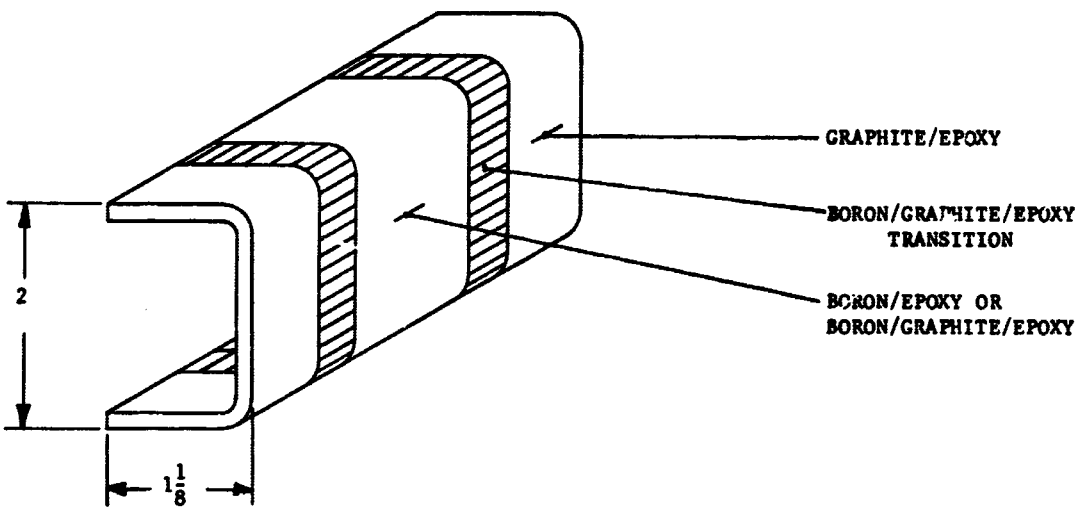

WEB/CAP 0° AND ±45°

Figure 43. Elements of Mixed Composite Beam.

SECTION VII

SUMMARY AND CONCLUSIONS

The objective of the work presented in this report is to develop, evaluate and demonstrate the feasibility of the high-modulus, mixed-fiber, plastic composite concept. It is particularly intended to determine the conditions under which the mixed-fiber concept, when incorporated into a single structure, will yield a more efficient structure than one consisting of a single-fiber concept.

The emphasis of this study has been placed on the mixed composite, with intermingled fiber systems, rather than the laminated composite, with alternating layers of different prepregs. In this connection, a mixed boron/graphite/epoxy prepreg has been developed and evaluated for strength and modulus properties.

Two joining concepts have been developed, on the basis of this prepreg study, which have desirable properties for forming smooth, bond-free, perforation free transitions between graphite/epoxy and boron/epoxy sections. Whittaker Research and Development Division (WRD) has teamed with the Space Division of North American Rockwell Corporation (NAR) to select a representative demonstration hardware concept. A structural component, the Number 5 radial beam truss of the Apollo Command Module, was selected for further evaluation. A modified component, incorporating the transitioning capabilities of the mixed fiber concept, was recommended as the demonstration article.

Based upon the results of this program, the following conclusions and recommendations are made:

1. The boron/graphite/epoxy hybrid composite is a feasible engineering material, in that it possesses excellent mechanical properties and can be easily produced within small tolerances on the constituent volume fractions.

2. Collimated graphite fibers are superior to glass, asbestos or even uncollimated graphite fibers as a reinforcement of boron/epoxy laminates. Graphite is lighter, stiffer and stronger than the latter fibers, and the collimation produces greater improvement of the prepreg's longitudinal properties. When properly mixed and cured, the hybrid laminate also exhibits excellent "interlaminar" shear and transverse tensile strengths.

3. Despite the improved transverse tensile modulus E_{22} and in-plane shear modulus G_{12} of the boron/graphite/epoxy hybrid, these improvements are not of sufficient magnitude to warrant changes in current conservative design procedures. The main benefit to be gained from this composite lies in its improved longitudinal strength and modulus. However, since similar improvements can be obtained by increasing the boron volume fraction, alone, even this benefit is not sufficient to warrant one-for-one replacement of existing boron/epoxy systems.

4. The most feasible applications of the boron/graphite/epoxy composite lie not in replacement of existing composites, but, rather, in areas where the existing materials have shortcomings. One such concept, developed herein, is that of transitioning between boron/epoxy structural elements and graphite/epoxy closeout sections. When properly employed, this concept achieves the following benefits:

   a) A perforation - free, bond-free, aerodynamically smooth transition is obtained between the joining sections;

   b) The best properties of the two fiber systems can be utilized in the same structural element without incurring excessive weight penalties in the joining process; and

   c) A small quantity of graphite, when added to the boron/epoxy section, permits a single-step cure of the entire structural element.

5. The ternary diagram is shown to be an effective graphical tool for evaluating proposed process changes. The Halpin-Tsai equations, when mapped onto the ternary diagram, provide satisfactory estimates of the transverse tensile modulus E_{22} and in-plane shear modulus G_{12} of hybrid composites with low graphite volume fractions.

6. The cure of the hybrid composite has the following features:

   a) Its cure cycle is closely related to that of the graphite/epoxy composite, due to the effects of the graphite fibers on the resin flow;

   b) A somewhat high resin content must be incorporated into the prepreg in order to promote fiber intermixing during the cure. Consequently, relatively large

amounts of bleedout must be accommodated during the cure; and

c) Fiber mixing is enhanced by means of a "HOLD" sequence (5 minutes at 275°F for NMD 2387 epoxy) prior to the final cure sequence. For a "slow" resin such as NMD 1004, a longer HOLD time could be used, with better resulting fiber intermix.

7. As discussed above, the use of the hybrid concept is very desirable in the transition area between the boron and the graphite reinforced composite areas. The advantage of boron, of course, lies in its high compressive strength combined with its high modulus. The combination of high strength and modulus in the same type graphite fiber is yet to be achieved. In addition, due to its small diameter fiber in yarn form, graphite is much more difficult to laminate in a straight collimated unidirectional composite. This results in reduced translation efficiency compared to boron/epoxy composites.

8. Further investigation is recommended in the following areas:

   a) Transitioning concepts should be studied in more depth, and transition designs with higher tensile and flexural strength should be sought;

   b) Hybrid composites employing slower curing resin systems should be considered; and

   c) Automated techniques for incorporating graphite fibers into boron/epoxy prepreg should be developed.

9. The hybrid beam outlined in Section VI is recommended as a suitable article for demonstrating the effectiveness of the hybrid concept. This item is chosen because it has high potential weight reduction, because a documented analysis is available for comparison purposes, and because it is a significant element in current and future space programs.

REFERENCES

1. Duft, B., Wolcott, C., "Short Fiber Orientation and Fabrication Techniques, Whittaker Internal R&D Report 225-002, 1965.

2. _____, "Evaluation of Short Boron Fiber and Continuous Glass Fiber Composites," Whittaker R&D Proposal 100-2518A, submitted to U.S. Army Aviation Laboratories, 30 March 1966.

3. Smith, M. B., "Evaluation of High-Temperature Resins in Asbestos Fiber Reinforced Laminates," AFML-TR-67-389, Contract No. AF33(615)5071, Whittaker R&D Report MJO 397, March 1968.

4. Boyle, G., "Further Research on Resin-Impregnated, Collimated Boron Filaments and Improved High-Modulus, High Strength Filaments and Composites," AFML-TR-68-371, Contract No. F33615-67-C-1607, Whittaker R&D Report MJO 358, November 1968.

5. Beeler, D., "Classification and Investigation of Manufacturing Concepts for Advanced Composite Components," Whittaker Internal R&D Report 9000-304001, October 1969.

6. Chase, V., "Specialty Components Capability Development," Whittaker Internal R&D Report 9000-305001, October 1969.

7. Evensen, H., Berg, K., "Feasibility of S-Glass/Modmor II/2387 Epoxy Mixed Composites," Whittaker Internal Engineering Report 70-E2, 5 March 1970.

8. Elkin, R. A., "Interlaminar Shear of Filament-Wound Reinforced Plastics," US Naval Ordnance Laboratory Report N60921-7094 USNOL, 30 July 1964.

9. Toth, L. W., Boller, T. J., Gamble, N. L., "Development Program for Non-Continuous Advanced Filament-Reinforced Composites," AFML-TR-67-17, Contract No. AF33(615)3318, Goodyear Aerospace Corp. Report No. GER-13058, January 1967.

10. Clark, G. A., Clayton, K. I., "Fabrication Techniques for Advanced Composite Attachments and Joints," AFML-TR-69-151, Contract No. F33615-67-C-1802, North American Rockwell (Columbus Division) Report No. NR 69H-368, May 1969.

11. Ashton, J. E., Halpin, J. C., Petit, P. H., Primer on Composite Materials: Analysis, Technomic, Stamford, Conn., 1969, p 107-113.

12. Doner, D. R., Novak, R. C., "Structural Behavior of Laminated Graphite Composites," SPI 24th Annual Technical Conference, Reinforced Plastics/Composites Division, 1969.

REFERENCES (Continued)

13. Halpin, J. C., Tsai, S. W., "Environmental Factors in Composite Materials Design," AFML-TR-67-423, 1967.

14. Whitney, J. M., "Elastic Moduli of Unidirectional Composites with Anisotropic Filaments," J. Composite Materials, Vol. 1, No. 2, p. 188, April, 1967.

15. Adams, D., Doner, D., "Transverse Normal Loading of a Unidirectional Composite," J. Composite Materials, Vol. 1, No. 2, p. 152, April, 1967.

16. Adams, D., Doner, D., "Longitudinal Shear Loading of a Unidirectional Composite," J. Composite Materials, Vol. 1, No. 1, p. 4, January, 1967.

17. Bloom, J. M., Wilson, H. B., "Axial Loading of a Unidirectional Composite," J. Composite Materials, Vol. 1, No. 3, p. 268, July, 1967.

18. Dauksys, R. J., Ray, J. D., "Properties of Graphite Fiber Nonmetallic Matrix Composites," J. Composite Materials, Vol. 3, October, 1969, pp. 684-698.

19. Timoshenko, S., Strength of Materials, Part I: Elementary Theory and Problems, 3rd Ed., D. Van Nostrand Co., New York, (1956), p. 174.

20. Schultz, A. W., "The Effect of Voids on the Mechanical Properties of High Modulus Graphite Fiber/Epoxy-Reinforced Composites," AVATD-0153-69-RR, 26 August 1969.

21. _____, Structural Analysis-Apollo Block II Spacecraft, Volume V Service Module, Book 2 of 5, Report SD67-1103-1, NASA Contract NAS9-150, December, 1968.

APPENDIX A

RESIN CONTENT DETERMINATION IN BORON/EPOXY LAMINATES BY HOT SULFURIC ACID DIGESTION

1. Scope - This method describes a procedure for the determination of the resin content of laminated or molded specimens of boron reinforcements with epoxy resins by sulfuric acid digestion.

2. Equipment and Chemicals

   A. Equipment

      a. Erlenmeyer flask - 300 ml or equivalent with ground joint (T24/40)

      b. Desiccator

      c. Fritted glass filtering crucible, 30 ml, porosity C

      d. Oven, capable of maintaining 400° ± 5°F

      e. phydrion paper

      f. Vacuum source (aspirator)

   B. Chemicals

      a. H_2SO_4 Conc.

      b. Distilled water

3. Sample Size - The sample should be large enough to provide three 1- to 2-gram specimens.

4. Procedure

   1. Weight out a 1-2' gram sample to 0.0001 gm (W_a). Place in a clean, dry flask, and add 100 ml of sulfuric acid (conc.). Place samples in acid and heat in oven at 400°F. Leave overnight to decompose resin.

   2. Filter the mixture (while still hot) using a 30-ml fritted glass filtering crucible of coarse porosity which has previously been dried and tared to 0.0001 gm. (W_2).

3. Wash filtrate with fresh hot H_2SO_4 (about 30 ml).

   Follow with approximately 400 ml of distilled water or until the filtrate is neutral to litmus paper. Break the vacuum and place the crucible in an oven at 350° ±5°F for a minimum of 30 minutes or until a constant weight is attained.

4. Cool to room temperature in a desiccator and weigh the crucible to 0.0001 gm (W_3).

5. <u>Calculations and Reporting</u>

   A. Calculate the resin content as follows:

$$\% \text{ Resin Content} = 100 \frac{W_3 - W_2}{W_a} \times 100$$

   Where W_a = sample weight in grams

   W_2 = weight of crucible in grams

   W_3 = weight of crucible plus carbon or graphite in grams

   B. The range of triplicate determinations should not exceed 1.5%.

APPENDIX B

PREPARATION OF METALLOGRAPHIC SPECIMENS

This appendix outlines the general procedure used by WRD to prepare the specimens for photomicrographs. Since the hardness of boron is much greater than either the graphite or epoxy constituents, great care must be taken to avoid excessive material removal and polishing during preparation of the sample. Not only does the graphite/epoxy "matrix" tend to erode away from the boron filament, but the amount of undesirable graphite/epoxy residue increases. This residue appears to be finely divided graphite and epoxy which adheres in patches to the matrix. Due to the slight undercutting of the matrix, this residue is untouched by further polishing and can be removed only by re-processing the sample. The procedure outlined herein is intended to minimize the amount of this residue.

1. Saw the desired section from the laminate, using a 120 grit diamond saw at about 7200 sfpm. The face to be studied should be at least one inch in length for convenience.

2. Thoroughly clean the entire laminate section with MEK or alcohol, and apply double-backed tape to the surface to be investigated.

3. Place the specimen, tape side down, on a clean glass sheet. Adjust until the laminate is perpendicular to the glass surface.

4. Center 1 1/4" diameter by ½" wide ring over the laminate section. The inside of this ring should be coated with a mold release, such as Polylease 77 Polyethylene lease agent. Fill with a clear specimen potting compound, such as Quickmount acrylic, and cure in place on the glass.

5. Material removal is accomplished on the lapidary wheel using the following procedure:

   a. Remove potting compound until flush with the specimen surface, using 240 grit Carbimet SiC wet grinding paper. Run at low speed for 15 minutes, using light to moderate (over 1 lb) contact force. This operation will require three 8" diameter discs, and must be continued until the cutting action is seen on the specimen surface.

b. Grind surface for 5 minutes each, using low pressure (~1lb) on wet grinding paper with grits 320, 400 and 600 respectively. Grind <u>across</u> the laminate only. Other directions will lead to excessive erosion of the matrix

6. Polishing is accomplished by the following procedure:

   a. Polish dry, at low speed and very light pressure (~8oz), using 945 grit Manning emery polishing paper.

   b. Buff using AB Alpha Polishing Alumina No. 2 (Hex lattice structure, 0.3 microns) diluted 10 parts by volume with distilled water. Use Beuhler polishing cloth, and apply at high speed, low pressure for 2-3 minutes only.

7. Inspect the sample under the microscope for residue. It will appear as black patches in the matrix, partially or completely obscuring the graphite fiber ends. Figure B-I shows the appearance of this residue.

8. If residue appears, process further on the vibrating polisher, using AB Alpha Polishing Alumina No. 3 (cubic lattice structure, 0.05 microns) diluted 10 parts by volume with distilled water. Treat for 4 hours, applying 8 oz. loading weight.

9. If, upon further inspection, the residue is still present in large quantities, it will be necessary to grind the face of the sample and repeat steps 5-7. A residue - free sample is shown in Figure B-2.

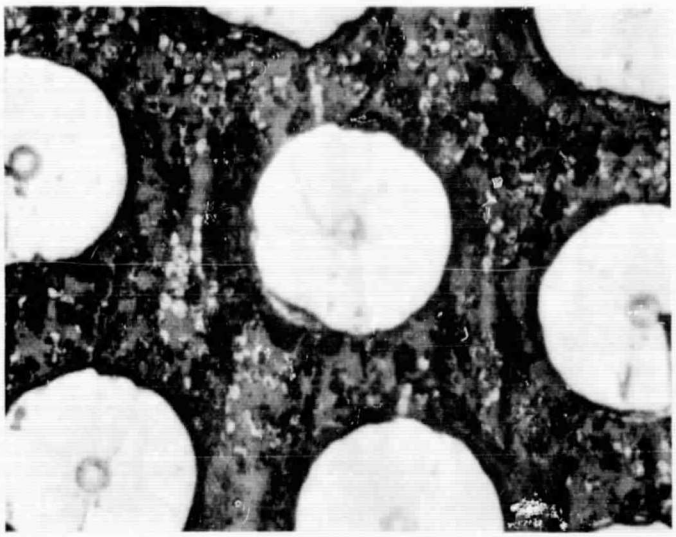

a) 300X

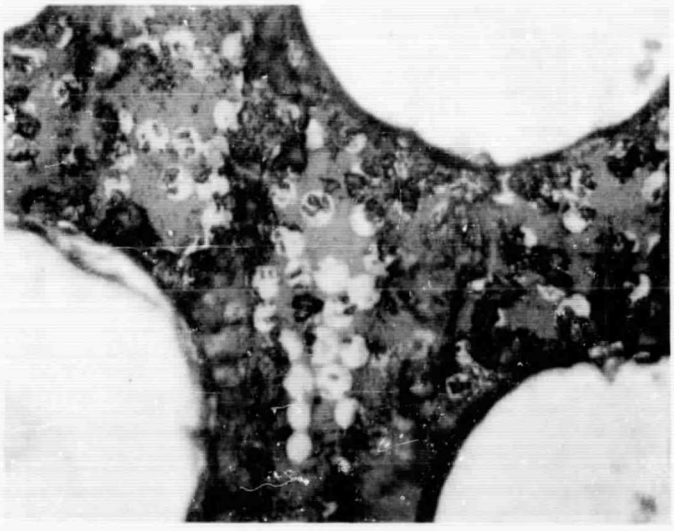

b) 600X

Figure B-1. Residue in Improperly Prepared Boron/Modmor II/2387 Epoxy Metallographic Sample.

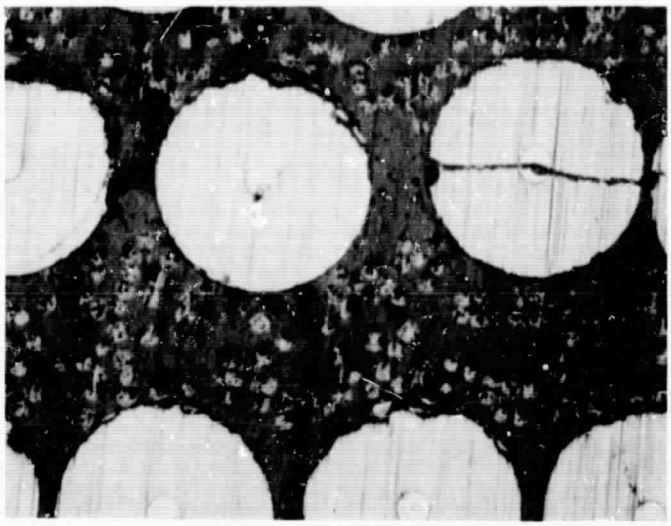

a) 300X

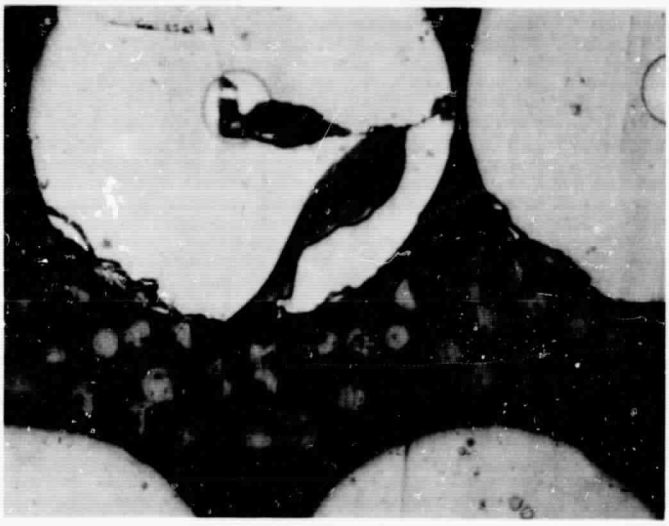

b) 600X

B-2. Residue-Free Boron/Modmor II/2387 Epoxy Metallographic Sample.

APPENDIX C

TEST SPECIFICATIONS

I. Engineering Test Method IT-58-3

LONGITUDINAL AND TRANSVERSE TENSILE STRENGTH AND MODULUS OF UNIDIRECTIONAL HIGH STRENGTH COMPOSITES

A. Application - This test method shall be used for unidirectional, 90° transverse, 0° - 90° crossply, and specified angleply orientations with loading parallel or perpendicular, as required, to the outer plies.

B. Test Specimen Configuration - The unidirectional, 90° transverse, 0° - 90°, and specified angleply orientations employed for tensile tests shall be straight-sided coupons with adhesive-bonded fiberglass tabs, except as noted in C.2. Each specimen shall be of a uniform cross section over the entire length and shall not have a taper greater than 0.003 inch in any direction. The tensile specimen configurations for the various orientations are described in Figures C-1 and C-2.

C. Grip Tabs

1. Construction - Construct the grip tabs from unidirectional Scotchply 1002"S", 181E fiberglass-epoxy prepreg laminates, or equivalent, depending on the laminate orientation. The grade of fiberglass, number of plies, orientation, and tab configuration shall be specified on an applicable specimen configuration drawing. Attach the fiberglass tabs to the specimen by adhesive bonding with a suitable adhesive such as Epon 901/B1, FM-123, Epon 9604, FM-150, or Metlbond 329. The type of adhesive selected shall be capable of withstanding the test temperature. For test temperatures to 180 F (82 C), use Epon 9604, FM-123, or equivalent adhesive. For elevated temperature tests, 180 to 350 F (82 to 177 C), use Metlbond 329, FM-130, or equivalent adhesive.

2. Transverse Specimens - For transverse (90°) specimens, fiberglass tabs are not required when specimens are to be tested for transverse properties over a test temperature range of -67 to 350 F (-55 to 177 C).

D. Test Specimen Machining - Machine test specimens from the laminate or test part with the longitudinal axis machined parallel to the direction of the outer laminate plies. Prior to machining, clearly indicate on the specimen the laminate orientation. After rough

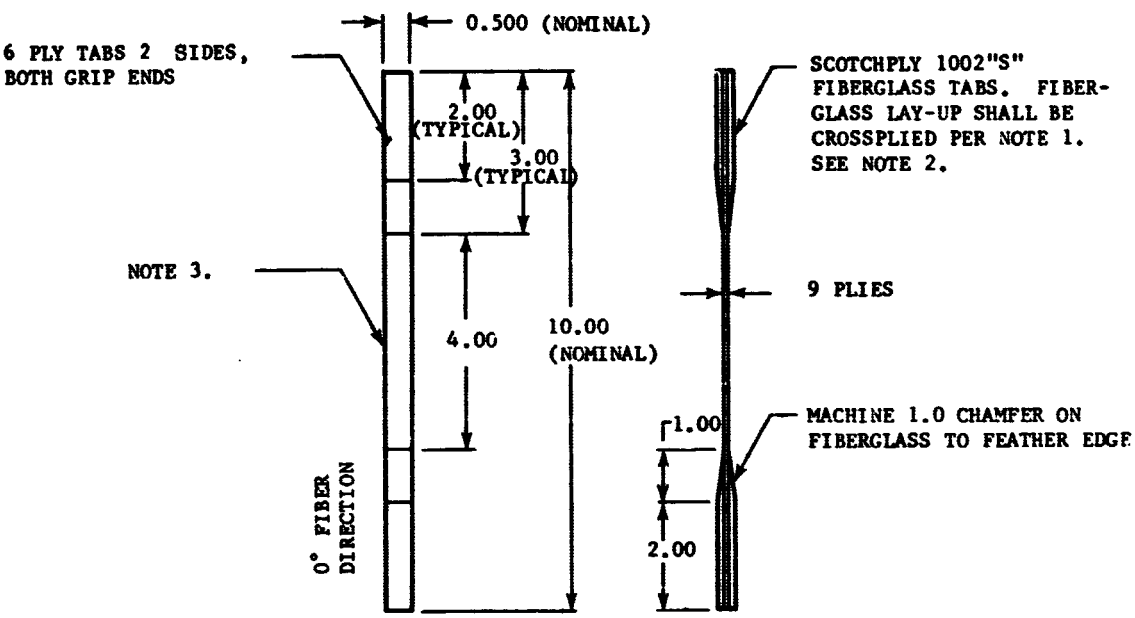

.XX DIMS SHALL BE ±0.030

.XXX DIMS SHALL BE ±0.010

NOTES:
1. SCOTCHPLY 1002"S" TAB ORIENTATION SHALL BE 0° - 90° - 0° - 0° - 90° - 0°.
2. USE 0.085 POUNDS PER SQ FT FM-123-2 ADHESIVE, OR EQUIVALENT.
3. SPECIMEN EDGES SHALL BE PARALLEL TO ±0.002. POLISH EDGES AFTER MACHINING.
4. INSPECT LAMINATES AND TEST SPECIMENS FOR DEFECTS.

Figure C-1. Longitudinal Tensile Test Specimen.

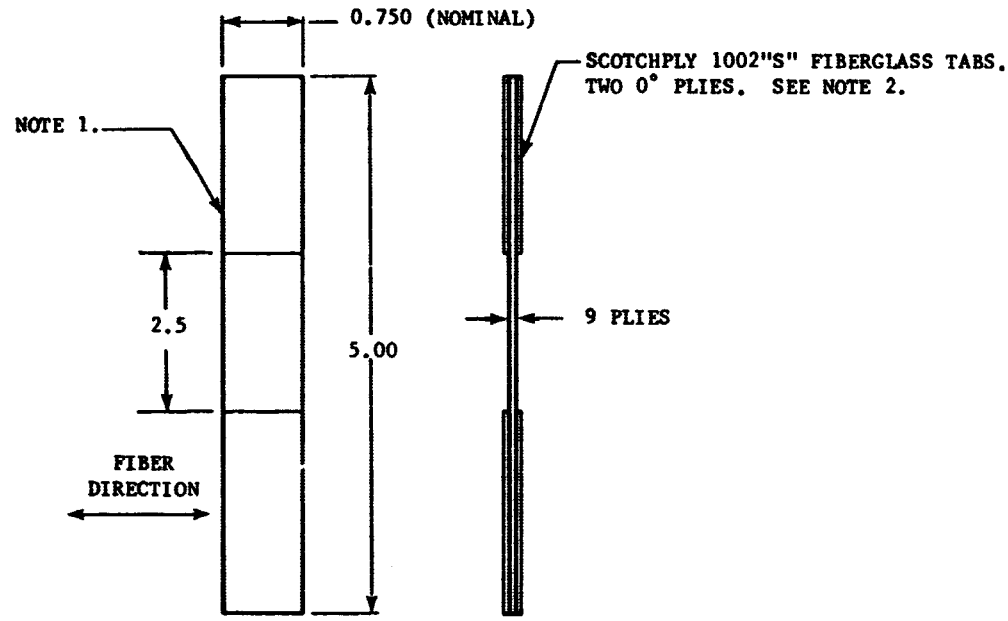

.XX DIMS SHALL BE ± 0.030
.XXX DIMS SHALL BE ± 0.010

NOTES:
1. SPECIMEN EDGES SHALL BE PARALLEL TO ± 0.002. POLISH EDGES AFTER MACHINING.
2. USE 0.085 POUNDS PER SQ. FT. FM-123-2 ADHESIVE, OR EQUIVALENT.
3. INSPECT LAMINATES AND TEST SPECIMENS FOR DEFECTS.

Figure C-2. Transverse Tensile Test Specimen.

trimming, bond the fiberglass tabs to the coupon panels. Grind the laminates to the configuration drawing requirements after the tab bonding operation.

1. Specimen Inspection - Visually inspect, or inspect at 10x magnification, each test specimen prior to test. Further examine any observable flaws or irregularities using appropriate NDT procedures such as dye penetrant or ultrasonics. Record flaws or irregularities as part of the test data.

2. Measurement - Measure the width and thickness of the test specimen to the nearest 0.001 inch at several points along the specimen to obtain the cross-sectional area. If a different test specimen length is used, measure and report the length.

E. Testing Equipment

1. Strain Measuring Devices - For -67 F (-55 C), room temperature, and 180 to 350 F (82 to 177 C) specimen tests, monitor the strains during loading by strain gages. For the -67 to 350 F (-55 to 177 C) test temperatures, use the following strain gages.

   a. Axial Type, Single Element - Micro Measurements EA 06-250BG-120, or equivalent

   b. Two Element 90° Tee - Micro Measurements EA 06-125TF-120 or WA-XX-120WT-120

2. Optional Strain Measuring Devices - Where strain gages cannot be used or are not suitable for testing specimens at -67 F (-55 C), room temperature, and 180 F (82 C), an optional technique for measuring strain shall be an extensometer method. A Class B-1 extensometer, or better, is recommended for tensile coupon tests. The extensometer shall transmit the recorded deformation to a load-deformation recorder.

3. Gripping - Use self-aligning grips which completely enclose the specimen end tabs to grip each end of the coupon. The grips shall have fine serrations for gripping the fiberglass tabs and the untabbed transverse specimens.

4. Thermocouple and Potentiometer - For elevated temperature, 180 to 350 F (82 to 177 C), and low temperature, -67 F (-55 C), attach an iron-constantan thermocouple to the specimen near the center of the top surface. Secure the thermocouple in intimate contact with the specimen. Connect the thermocouple to a potentiometer or suitable recorder.

5. Heat Source - For elevated temperature tests, heat the longitudinal and transverse tensile specimens and fixtures in a furnace chamber or with 2 banks of quartz heating lamps; the furnace chamber is preferred. Control the voltage of the quartz lamps with a powerstat. Allow the specimen to stabilize at temperature for a minimum of 10 minutes prior to loading. Monitor temperature with a thermocouple attached to the specimen.

6. Cooling Source - For low temperature test, place the longitudinal and transverse tensile specimens and fixture in a chamber and cool with liquid nitrogen to -67 F (-55 C). Allow the specimen to stablize at temperature for a minimum of 10 minutes prior to loading. Monitor temperature with a thermocouple attached to the specimen.

7. Load Indicator - Use a calibrated load indicator in testing. Report the accuracy of the calibrated load indicator as a percentage of the full-scale load. Employ the smallest load range compatible with the expected load of the composite test specimen.

F. Specimen Testing - Secure the tensile test specimen in the upper grip of the tensile test machine. The bottom grip is not secured at this time. Attach the strain gage leads from the test specimen to a suitable strain indicator. With no load on the test specimen, zero each gage. Tighten the bottom grip, taking care that the test specimen is aligned axially to the load direction. Check test specimen alignment with the use of a level or the grip stops.

1. Load Increment Selection - Recheck strain gages on the strain indicator and record preload and indicated strain, if applicable. Determine the estimated load at which specimen failure will occur. Select a minimum of 10 load increments that will yield strain readings over the entire range.

2. Speed of Testing - The speed of testing is based on the cross-head speed or grip separation of the testing machine. The testing speed shall be 0.050 inch ± 0.005 per minute.

3. Unidirectional and Angleply Test Specimens - Conduct tests at room temperature and in elevated and low temperature environments in accordance with E.4, E.5, and E.6.

4. Transverse Test Specimens - Bond two layers scotchply on the test specimen grip ends for approximately 1 1/4 inches of length. Conduct tests in accordance with F.1, F.2, and F.3.

G. Calculations

1. Tensile Strength - Calculate the tensile strength from the loads divided by the cross-sectional areas as described in G.1. Express the results in pounds per square inch (psi) and record to 3 significant figures. Use the following equation.

$$F_t = \frac{P}{A}$$

Where: F_t = Ultimate tensile stress, psi

P = Maximum tensile load carried by the specimen, pound

A = Specimen cross-sectional area, square inch

2. Modulus of Elasticity, Tensile

a. Obtain the modulus of elasticity by extending the initial straight-line portion of the load-deflection curve and graphically determining the ratio of stress to corresponding strain. Express the results in pounds per square inch (psi) and record to 3 significant figures.

b. Calculate the tensile modulus of elasticity according to the following equation.

$$E = \frac{F_t}{\epsilon}$$

Where: E = Modulus of elasticity in tension, psi

F_t = Tensile stress, psi

ϵ = Corresponding strain in inches per inch

II. Engineering Test Method No. 301

DETERMINATION OF COMPRESSIVE PROPERTIES OF PLASTIC LAMINATE MATERIALS AT ROOM TEMPERATURE AND ELEVATED TEMPERATURES UP TO 1000°F

A. Scope

This procedure covers the determination of edgewise compressive strength and the compressive modulus of plastic laminate materials at standard laboratory temperature and elevated temperatures up to 1000°F.

B. Related Documents

ATC Report No. ARTC-11, Method No. I

C. Test Specimens

1. The test specimens shall conform to the dimensions shown in Figure C-3.

2. Specimens shall be free from visible imperfections, flaws, scratches, etc.

D. Specimen Preparation

1. Using a circular saw equipped with a diamond blade and a water-base coolant, a 1.00-in. x 3.06-in. blank (see Fig.C-3

2. Specimen blanks shall be ground on each end (approximately 0.03 in.) to the finished length of 3.00 in. A surface grinder equipped with a suitable magnetic chuck, fixture and grinding wheel shall be used. The grinding wheel of the surface grinder shall be in accordance with the nature of the specimens being prepared. A water-base coolant shall be used.

3. The ends of the specimens shall be flat and parallel to each other within 0.0005 in. and perpendicular to the long axis.

4. The ground specimens shall be washed in cool tapwater and dried using soft paper towels or an air jet.

5. The ground specimens shall be visually inspected for flaws, defects, scratches, and other imperfections that would render the specimens unsuitable for testing. Unsuitable specimens shall be so identified and returned to the requester.

6. The ends of the specimen shall not be sanded. Marks left by grinding on the edges of the specimen shall be carefully removed with No. 600 wet-or-dry abrasive paper, used dry. Finishing sanding strokes shall be made in a direction parallel to the long axis of the test specimen.

E. Specimen Conditioning

1. Specimens which have been heat aged shall receive no further conditioning. Specimens which have not been heat aged shall be conditioned prior to testing by one of the two following procedures:

   a. Normal Method - The test specimens shall be conditioned by exposure to standard laboratory atmosphere for a minimum of 48 hours prior to testing.

   b. Alternate Method - When time delay is undesirable, test specimens shall be conditioned by placing in an oven at 140°±5°F for 1 hour. Specimens shall be cooled to room temperature prior to testing.

F. Apparatus

1. Testing Machine - A testing machine having a controllable crosshead speed, properly calibrated load indicator, and a suitable stress-strain recorder shall be used.

2. Holding Blocks - Holding blocks (Figure C-4) shall be used to prevent splitting or crushing of the specimen at the ends.

3. Fixture - A fixture as shown in Figure C-5 shall be used. The fixture shall incorporate leaves or fingers which stabilize the specimen laterally to eliminate buckling effects but will not restrain the specimen axially.

4. Loading Fixtures - The load shall be applied to the specimen utilizing a suitable ball and socket or similar self-aligning device. (See Figure C-5)

5. Extensometer - A properly calibrated extensometer shall be attached to the test specimen (see Figure C-6) using a calibration block that shall establish a gage length of 2.00 in. ±0.020 in.

6. Thermocouples and Potentiometer - An iron-constantan thermocouple shall be used for determining the temperature of the test fixture, and to establish preheating time requirements. A second iron-constantan thermocouple shall be used for determining the temperature of the test specimen. Both thermocouples shall be used in conjunction with a properly calibrated potentiometer.

7. Heat Source - Two banks of quartz heating lamps, one on each side of the specimen, shall be used (see Figure C-7). The voltage to the quartz lamps shall be controllable by a powerstat.

G. Procedure for Testing at Room Temperature

1. A test data sheet shall be prepared, using pertinent information from the Test Request and test specifications.

2. The width and thickness of the specimen (see Figure C-3) shall be measured to the nearest 0.001 in. at several points along the length of the specimen. All specimens not conforming to the dimensions shown in Figure C-3 shall be discarded. The minimum cross-sectional dimensions of acceptable specimens shall be recorded on the test data sheet.

3. The specimen shall be located in the holding blocks, one at each end of the specimen. The centerline of the specimen shall be aligned with the centerline scribed on the upper (recessed) block. The edges of the specimen shall be flush with the edges of the blocks. Slide the specimen unit into the fixture between the two rows of holding leaves, the recessed block at the upper position and the flat block resting on the base of the fixture (Figure C-5).

4. The extensometer, if used, shall be attached to the specimen as near the center as possible, as shown in Figure C-6, using a calibration block that establishes a gage length of 2.00 in. ±0.02 in. The extensometer shall then be connected to the stress-strain recorder system.

5. The stress-strain recorder chart shall be stamped with the rubber stamp provided (see Figure C-8) and the required information filled in.

6. Before testing, the load range which is likely to provide the most accurate and easiest to interpret stress-strain curve shall be selected.

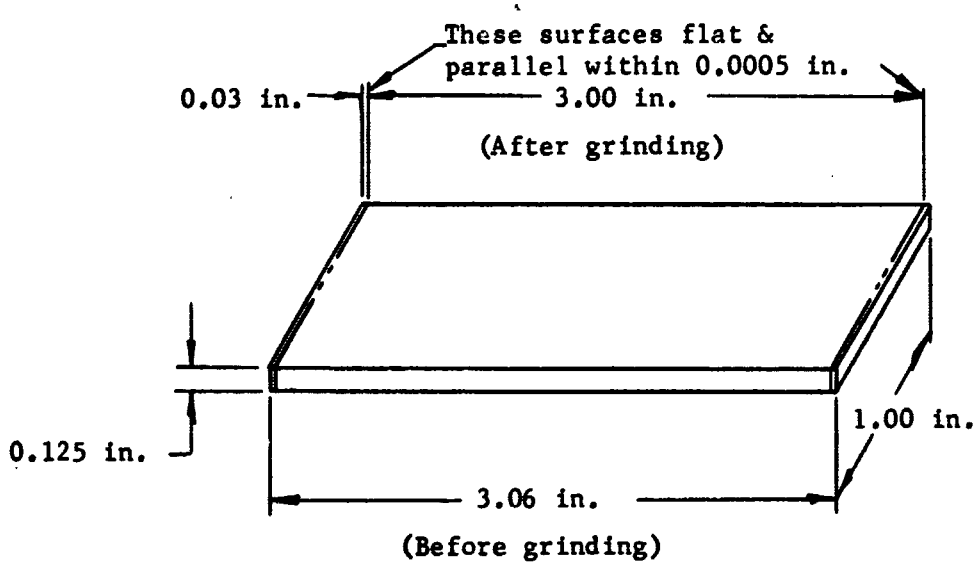

Tolerances, ±0.010 in.

Figure C-3. Compressive Test Specimen.

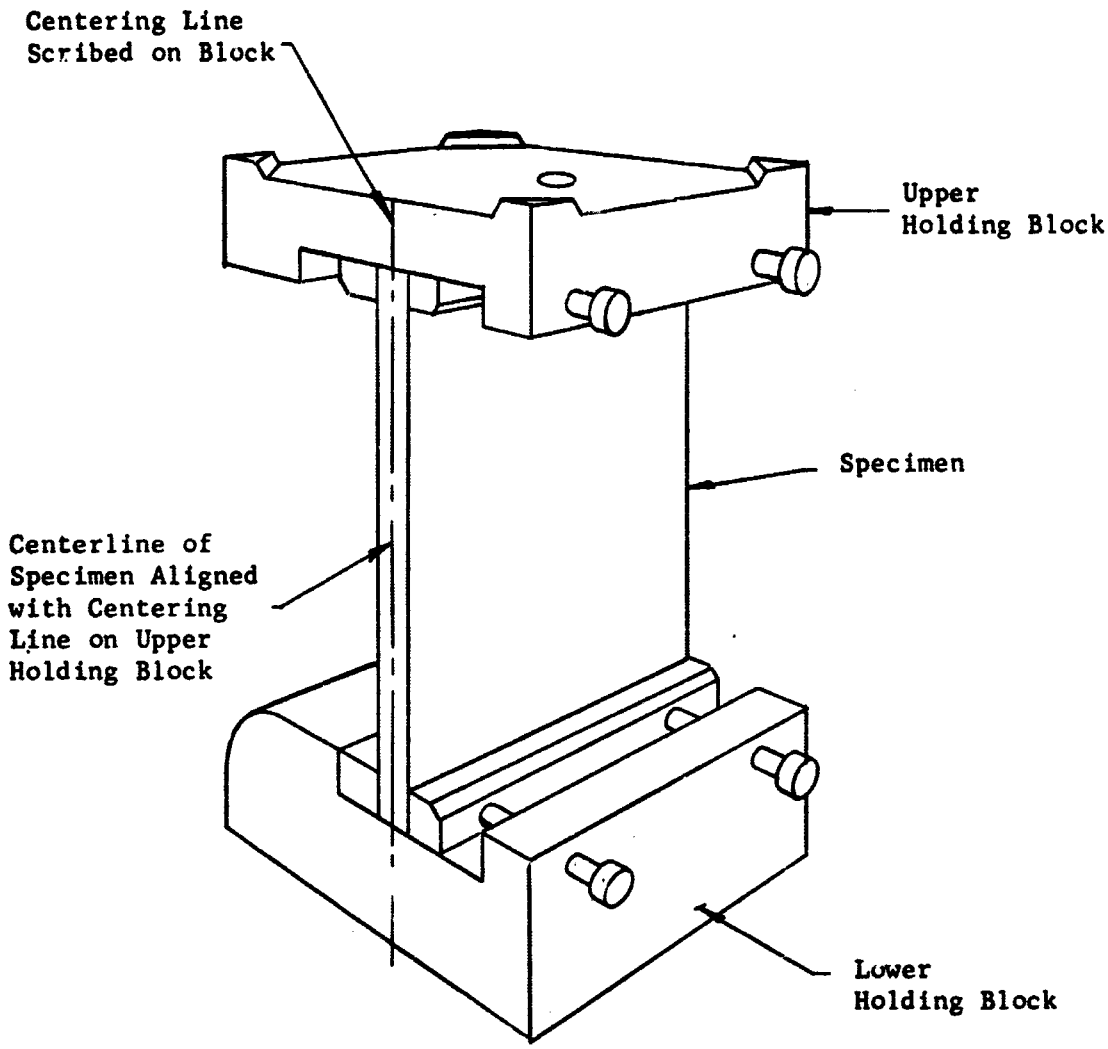

Figure C-4. Compressive Specimen Aligned in Holding Blocks.

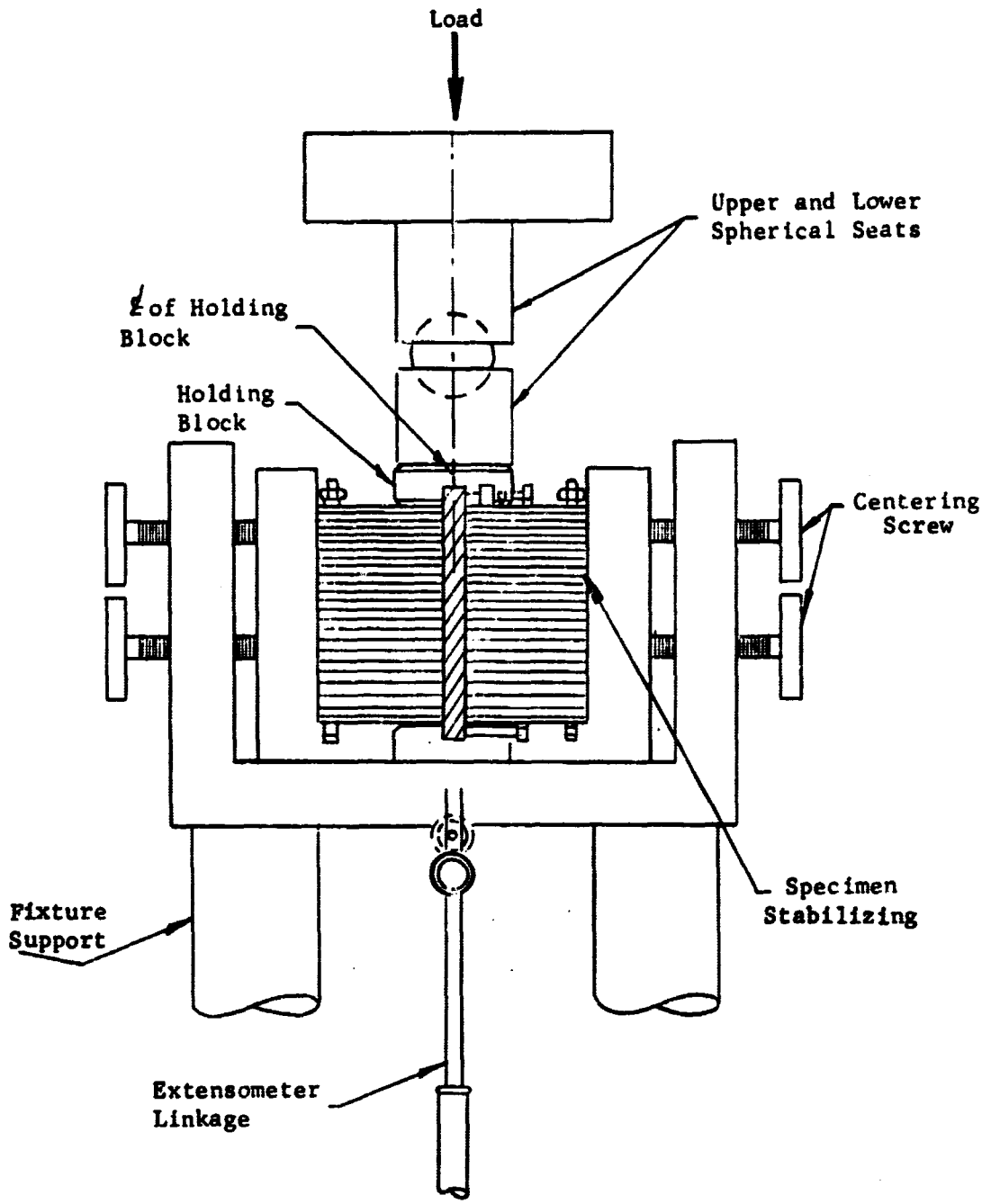

Figure C-5. Compression Test Fixture.

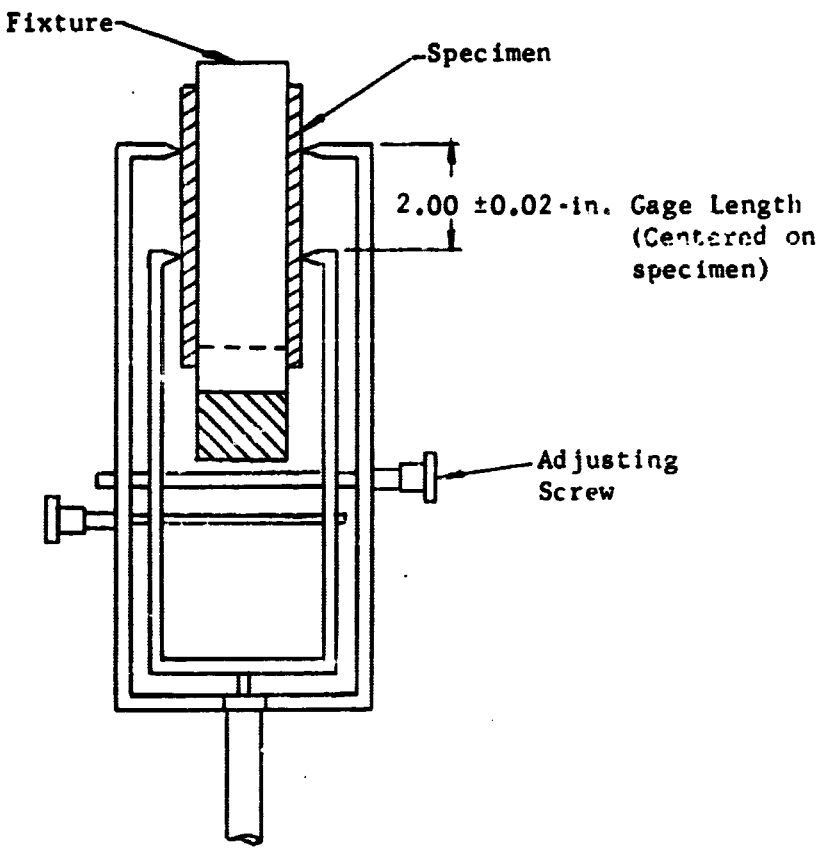

Figure C-6. Extensometer for Compressive Tests.

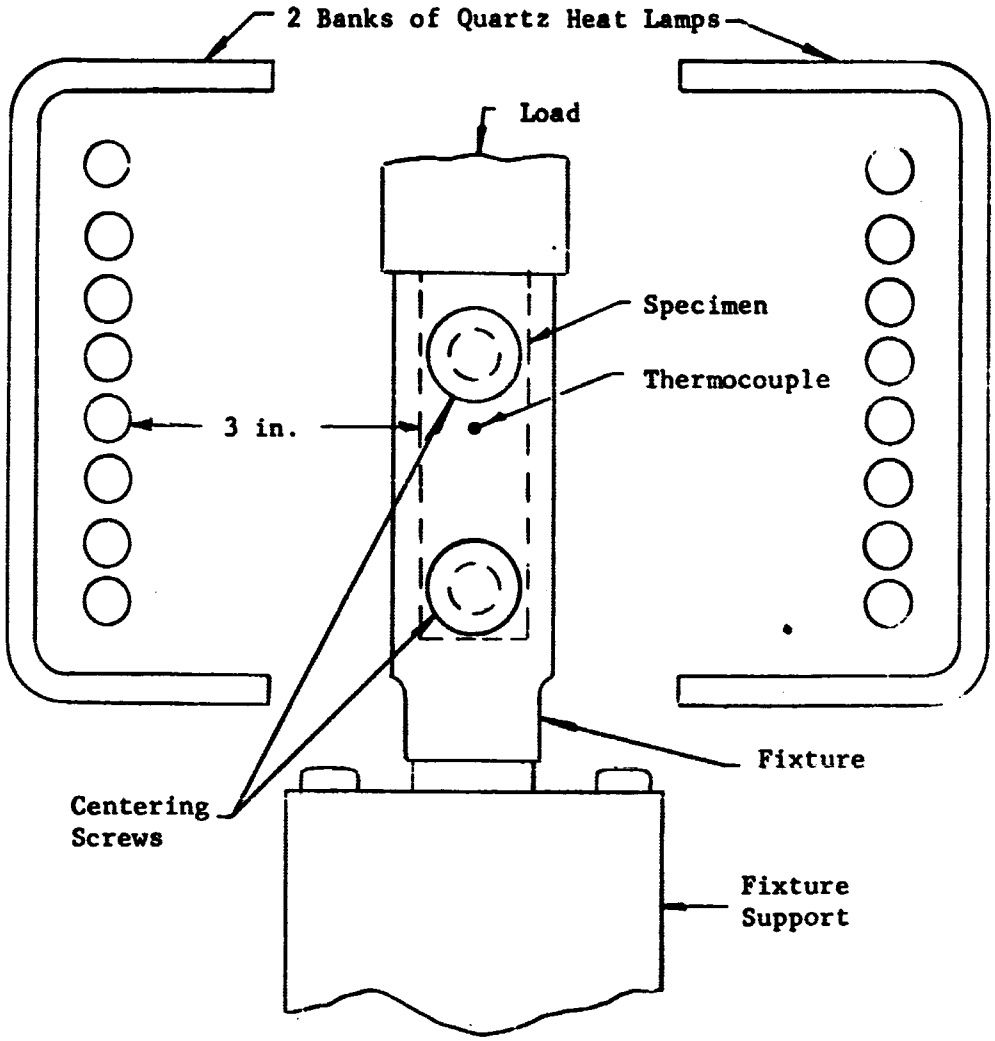

Figure C-7. Location of Quartz Heat Lamps for Elevated Temperature Testing.

Test_____Temp_____

Material_____Specimen No._____

Cross Head Speed_____In/Min. Extens._____

Chart Speed_____In/Min. Extens._____

Load (Full Scale)_____

Conducted By_____Date_____

Witnessed By_____Date_____

Figure C-8. Sample Stamp

7. The test machine shall be set to provide a crosshead speed of 0.050 ±0.005 in./minute.

8. After a stress-strain curve has been obtained the load range may be increased if necessary to record the specimen rupture load.

9. The maximum load carried by the specimen during the test shall be recorded. Notation of improper failure or other comments shall be made as required.

H. Procedure for Testing at Elevated Temperatures

1. A test data sheet shall be prepared, using pertinent information from the Test Request and test specifications.

2. The width and thickness of the specimen (see Figure C-3) shall be measured to the nearest 0.001 in. at several points along the length of the specimen. All specimens not conforming to the dimensions shown in Figure C-3 shall be discarded. The minimum cross-sectional dimensions of acceptable specimens shall be recorded on the test data sheet.

3. The specimen shall be located in the holding blocks, one at each end of the specimen. A shim shall be placed on each side of the specimen so that the pressure of the adjusting screw is on the shim. The centerline of the specimen shall be aligned with the centerline scribed on the recessed block. The edges of the specimen shall be flush with the edges of the blocks. Slide the specimen unit into the fixture between the two rows of holding leaves, the recessed block at the upper position and the flat block resting on the base of the fixture (Figure C-5).

4. The extensometer, if used, shall be attached to the specimen as shown in Figure C-6 using a calibration block that establishes a gage length of 2.00 in. ±0.02 in. The extensometer shall then be connected to the stress-strain recorder system.

5. The stress-strain recorder chart shall be stamped with the rubber stamp provided (see Figure C-7) and the required information filled in.

6. Before testing, the load range which is likely to provide the most accurate and easiest to interpret stress-strain curve shall be selected.

7. The test machine shall be set to provide a crosshead speed of 0.050 ±0.005 in./minute.

8. Two banks of quartz heating lamps shall be installed in the test machine (see Figure C-6). The specimen shall be gradually heated to within 2% of the test temperature as indicated by the thermocouple and potentiometer. Care shall be exercised to prevent overheating. The specimen shall be held at the test temperature for 1 minute prior to testing.

9. After a stress-strain curve has been obtained, the load range may be increased if necessary to record the specimen rupture load.

I. Calculations

1. Compressive Strength - The compressive strength shall be calculated by dividing the maximum load in pounds by the original cross-sectional area of the specimen in square inches. The results shall be expressed in pounds per square inch (psi) and recorded to three significant figures. The following equation shall be used:

$$S_c = \frac{P}{A}$$

Where S_c = ultimate compressive stress, psi

P = maximum compressive load carried by the specimen, lb

A = cross-sectional area of the specimen, square inch

2. Modulus of Elasticity, Compression - The modulus of elasticity shall be obtained by extending the initial linear portion of

the stress-strain curve, determining the slope of the line by dividing the stress by the corresponding strain, and multiplying the slope by the extensometer calibration factor. The result shall be expressed in pounds per square inch (psi) and recorded to three significant figures.

a. A straight line shall be drawn parallel to the initial straight line portion of the stress-strain curve on the chart.

b. A point on the load axis shall be selected through which a perpendicular line is drawn to intersect the extension of the stress-strain line, making a triangle.

c. The sides of the triangle shall be measured to the nearest 0.01 inch.

d. The length of the side of the triangle representing stress shall be divided by the length of the side of the triangle representing strain to obtain the slope, or stress-strain ratio.

e. The modulus shall be obtained by multiplying the slope by the extensometer calibration factor constant. The result shall be expressed in pounds per square inch (psi) and recorded to three significant figures.

f. The modulus shall be calculated in accordance with the following equation:

$$E = \frac{f}{e} \times K$$

Where E = modulus of elasticity in compression

$\frac{f}{e}$ = slope, or stress-strain ratio

K = calibration factor of the extensometer

J. Report

1. The report shall include the following:

a. Complete identification of the material tested, including type, source, etc.

b. Complete identification of the specimen including dimensions, etc.

c. Method of preparing the test specimen

d. Method of testing the specimen

e. Conditioning procedure used

f. Number of specimens tested

g. Speed of testing

h. Temperature of test

i. Ultimate compressive strength, average value

j. Modulus of elasticity in compression, average value

k. Date of test

NOTES:

(1) The test data shall be reviewed and approved by the test engineer in charge of the program before releasing it; however, "preliminary" information may be furnished to the requester with the approval of the test engineer.

(2) The test data shall not be considered final until issued in an approved test report form.

(3) The original test data sheets with the corresponding charts attached shall be kept on file in the Engineering Test Section.

III. Engineering Test Method No. 405

DETERMINATION OF APPARENT SHEAR MODULUS OF PLASTIC MATERIALS AT ROOM TEMPERATURE AND ELEVATED TEMPERATURES

A. Scope

This procedure describes a nondestructive test method for determining the apparent shear modulus or modulus of rigidity of materials in the form of rigid square plates in a plane parallel to the plate surface. The procedure is applicable to orthotropic as well as isotropic materials at room and elevated temperatures. The test procedure itself is nondestructive in nature, although exposure to elevated temperatures may be detrimental to certain materials.

B. Related Documents

ASTM D805
Philco Research Laboratories Engineering Note 2-10-64
Narmco Engineering Report No. 64-E23

C. Test Specimens

Test specimens shall be in the form of flat, square plates of uniform thickness, as shown in Figure C-9. The Type I specimen is intended for room temperature tests and the Type II specimen for elevated temperature tests. The Type I and II specimens shall be the preferred sizes. However, other sizes may be tested provided:

1. The specimen is square, flat, and of uniform thickness.

2. The sides of the specimen are not less than 25 times the thickness nor greater than 100 times the thickness of the panel.

3. The dimensions of a specimen intended for elevated temperature testing do exceed those specified for Type II.

4. The minimum test specimen size is 4.00 in. square and 0.040 in. thick.

D. Specimen Preparation

1. Using a circular saw equipped with a diamond blade and a water-base coolant, the test specimens shall be cut from the sample panel.

2. The cut specimens shall be washed in cool tapwater and carefully dried with soft paper towels or an air jet.

3. The cut specimens shall be visually inspected for cracks, flaws, delamination or other imperfections which would render them unsuitable for testing. Unsuitable specimens shall be so identified and returned to the requester.

E. Specimen Conditioning

1. Specimens which have been heat-aged shall receive no further conditioning. Specimens which have not been heat-aged shall be conditioned prior to testing by one of the following methods:

   a. Normal Method - The test specimens shall be conditioned by exposure to standard laboratory atmosphere for a minimum of 48 hours prior to testing.

   b. Alternate Method - When time delay is undesirable, test specimens shall be conditioned by being placed in an oven at 140°±5°F for 1 hour. Specimens shall be cooled to room temperature prior to testing.

F. Apparatus

1. Testing Machine - A testing machine with a controllable crosshead speed, properly calibrated load indicator, and a suitable stress-strain recorder shall be used.

2. Fixture - A special test fixture as shown in Figure C-10 shall be used.

3. Instrumentation - A properly calibrated extensometer of the linear variable differential transformer (LVDT) type shall be used. The extensometer must be capable of accurate, linear measurement for a minimum of 0.30 in.

4. Thermocouple and Potentiometer - For elevated temperature tests, a properly calibrated thermocouple and potentiometer shall be used to determine specimen temperature.

5. Oven - An air circulating oven suitable for use with the test machine and fixture shall be used for elevated temperature tests.

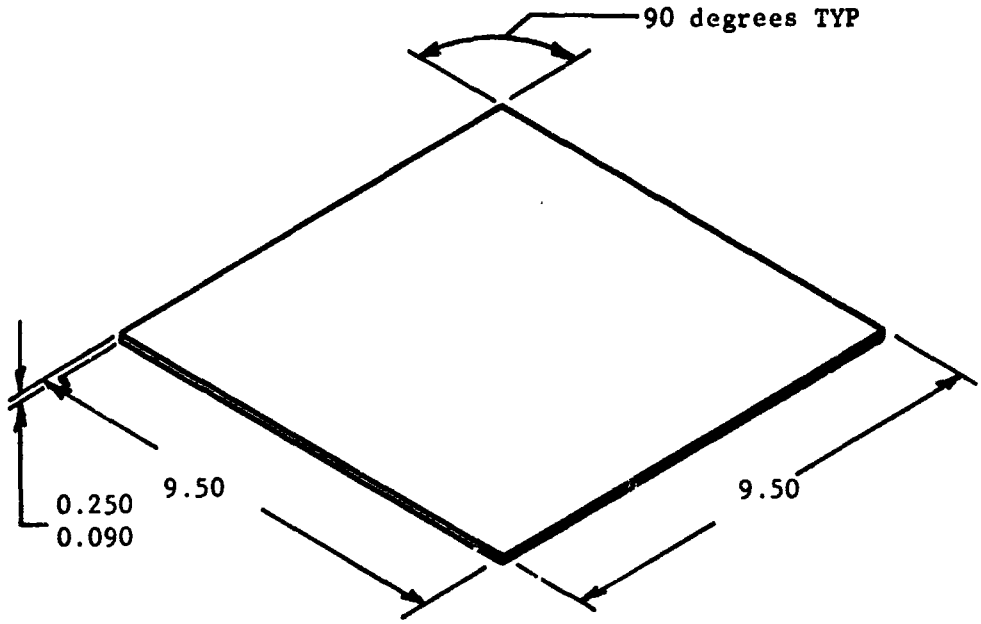

TYPE I

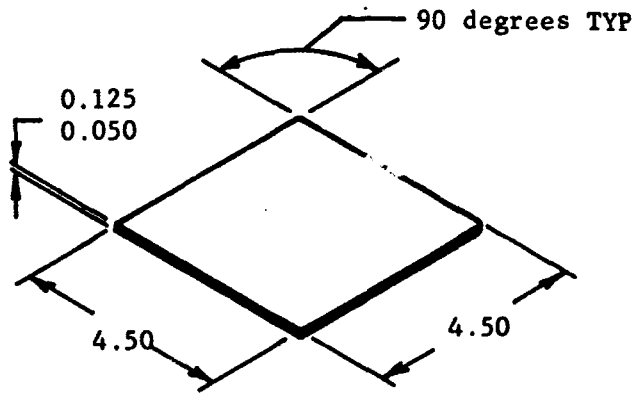

TYPE II

Tolerances: Linear ±0.03 in.
Angular ±0.10 degrees

Figure C-9. Shear Test Specimen Configuration.

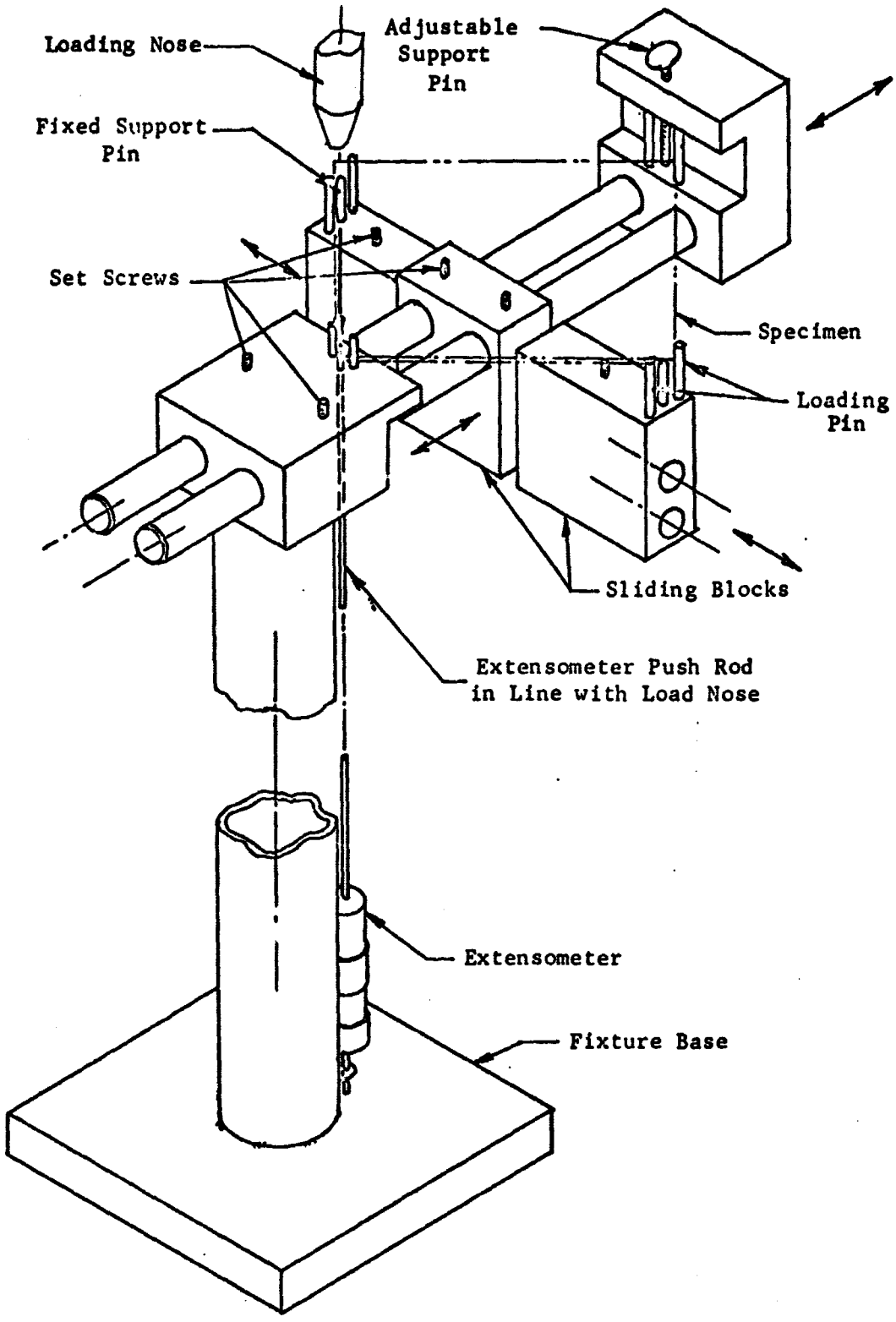

Figure C-10. Shear Test Fixture.

G. Procedure - Room Temperature Tests

1. A test data sheet shall be prepared, using pertinent information from the Test Request and test specification.

2. The specimen length shall be measured along two adjacent sides to the nearest 0.01 in. and the thickness shall be measured at several points to the nearest 0.001 in. A steel square shall be used to check the test specimen corners for squareness. All specimens not conforming to the dimensions and tolerances shown in Figure C-9 shall be discarded. The dimensions of acceptable specimens shall be recorded on the test data sheet.

3. The fixture shall be placed in the test machine and centered. The loading nose shall be directly in line with the extensometer push rod (see Figure C-10).

4. The test specimen shall be placed in the fixture and the supports adjusted, if necessary, so that the specimen is free to slide 0.02 to 0.03 in. in any horizontal direction. Caution: If the specimen is restrained by the fixture, the test results will be invalid.

5. The extensometer shall be connected to the stress-strain recorder and set at zero.

6. A load range which will provide the most easily interpreted load-deflection recording shall be selected.

7. The recorder chart shall be stamped with the rubber stamp provided (see Figure C-11), and the required information filled in.

Test _____ Temp _____

Material _____ Specimen No. _____

Cross-Head Speed _____ In/Min Extens. _____

Chart Speed _____ In/Min Calib. Graph _____

Load (Full Scale) _____

Conducted by _____ Date _____

Witnessed by _____ Date _____

Figure C-11. Test Identification Stamp

8. The test machine shall be set to provide a crosshead speed of 0.10 in./minute.

9. The specimen shall be loaded until an easily interpreted load-deflection line is obtained. The specimen shall not be loaded to the extent that the deflected corner contacts the test fixture.

H. Procedure - Elevated Temperature Tests

1. A test data sheet shall be prepared, using pertinent information from the Test Request and test specification.

2. The specimen length shall be measured along two adjacent sides to the nearest 0.01 in. and the thickness shall be measured at several points to the nearest 0.001 in. A steel square shall be used to check the test specimen corners for squareness. All specimens not conforming to the dimensions and tolerances shown in Figure C-9 shall be discarded. The dimensions of acceptable specimens shall be recorded on the test data sheet.

3. The oven shall be installed in the test machine.

4. The fixture shall be placed in the test machine and centered. The loading nose shall be directly in line with the extensometer push rod (see Figure C-10).

5. The test specimen shall be placed in the fixture and the supports adjusted, if necessary, so that the specimen is free to slide 0.02 to 0.03 in. in any horizontal direction. Caution: If the specimen is restrained by the fixture, the test results will be invalid.

6. The thermocouple shall be attached to the upper surface of the test specimen near the center. The thermocouple shall be affixed with glass fabric adhesive-backed tape, and arranged so that the wires will not interfere with movement of the specimen during test, and then connected to the potentiometer.

7. The extensometer shall be connected to the stress-strain recorder and set at zero.

8. A load range which will provide the most easily interpreted load-deflection recording shall be selected.

9. The recorder chart shall be stamped with the rubber stamp provided (see Figure C-11), and the required information filled in.

10. The test machine shall be set to provide a crosshead speed of 0.10 in./minute.

11. The specimen shall be heated to the test temperature as indicated by the thermocouple and potentiometer, and held at the test temperature for 1 minute before testing.

12. The specimen shall be loaded until an easily interpreted load-deflection line is obtained. The specimen shall not be loaded to the extent that the deflected corner contacts the test fixture.

I. Calculations

1. Apparent shear modulus, or modulus of rigidity, shall be obtained by drawing a straight line on the chart superimposed over the load-deflection line and graphically determining the ratio of load to corresponding deflection. (See Figure C-12).

   a. In accordance with Figure C-12, a straight line shall be drawn superimposed on the load-deflection line.

   b. Point A on the drawn line shall be arbitrarily selected, and a line parallel to the load axis shall be constructed through this point.

   c. Point B shall be arbitrarily selected, and a line parallel to the deflection axis shall be drawn through this point, forming triangle ABC.

   d. Load shall be determined by translating the length of line AC into pounds, using the proper test machine load range.

   e. Corresponding deflection shall be determined by translating the length of line BC into using the proper extensometer calibration factor.

   f. Apparent shear modulus shall be calculated by multiplying 3 times the applied load times the distance squared between the fixture support points along the side of the specimen. The product shall be divided by the thickness of the specimen cubed, times the measured deflection corresponding to the applied load.

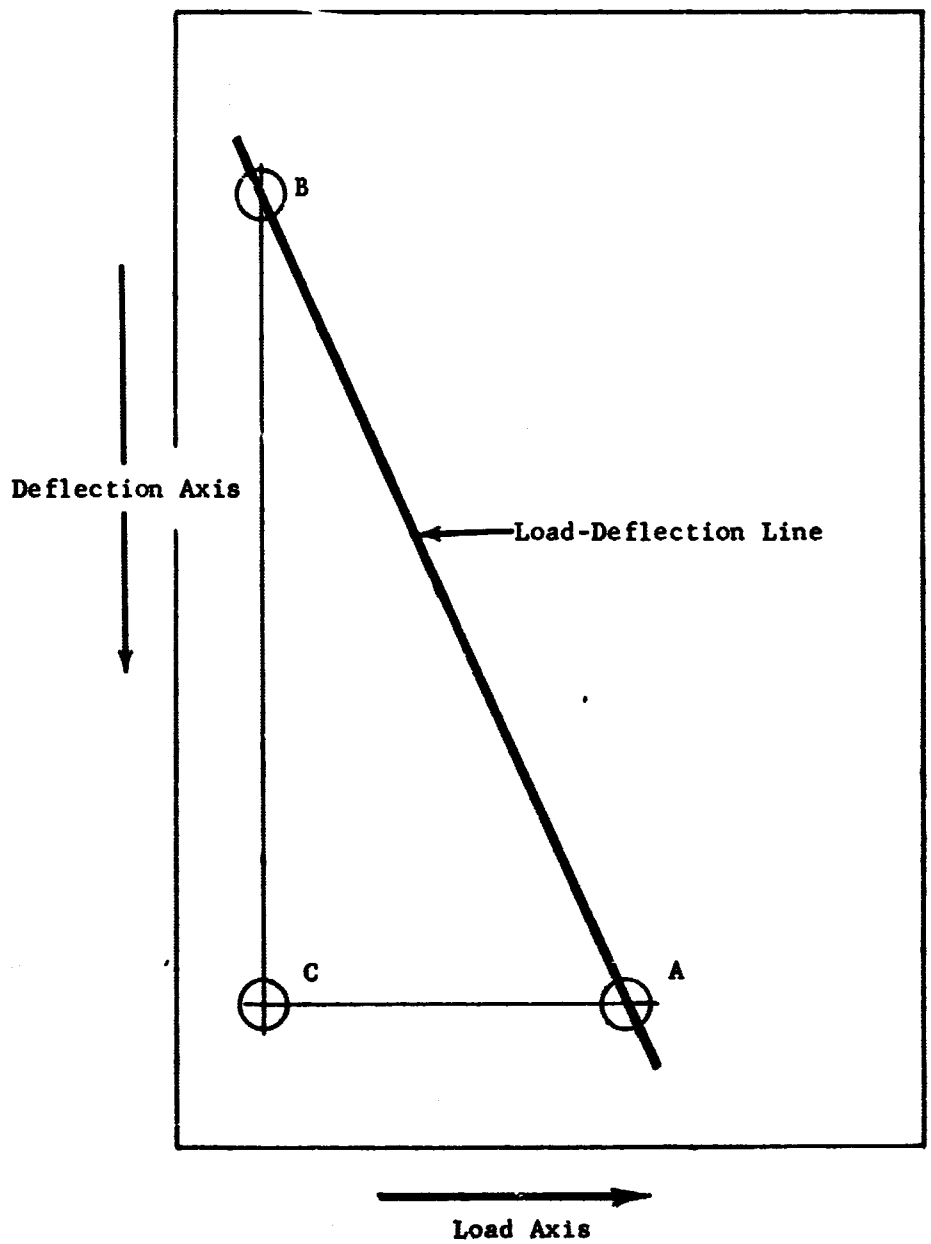

Figure C-12. Typical Shear Panel Load-Deflection Chart.

g. Apparent shear modulus shall be calculated using the following equation, and the result shall be expressed in pounds per square inch (psi) recorded to three significant figures:

$$G = \frac{3\ PL^2}{t^3\ D}$$

where G = apparent elastic modulus is shear parallel to the test specimen, psi

P = load, lb

D = corresponding deflection, in.

L = distance between supporting points along side of specimen, in.

t = specimen thickness, in.

J. Report

1. The report shall include the following:

a. Complete identification of the material tested, including type and source.

b. Complete identification of the specimen including dimensions

c. Method of testing the specimen

d. Conditioning procedure used

e. Number of specimens tested

f. Speed of testing

g. Apparent shear modulus, average value

h. Test temperature

i. Date of test

Notes:

(1) The test data shall be reviewed and approved by the test engineer in charge of the program before release; however, preliminary information may be furnished to the requester with the approval of the test engineer.

(2) The test data shall not be considered final until issued in an approved test report form.

(3) The original test data sheets with the corresponding charts attached shall be kept on file in the Engineering Test Section.

IV. Engineering Test Method IT-58-6

SHORT BEAM SHEAR STRENGTH

A. Application - This test method shall be used for determining interlaminar shear strength of unidirectional laminates with the fibers running parallel to the length of the specimen.

B. Test Specimen Configuration - Figure C-13 shows the test specimen configuration employed for the short beam tests.

C. Test Specimen Machining - Machine the test specimens from the unidirectional composite laminate with the plies parallel to the longitudinal axis. After rough machining, grind the test specimen to the final dimensions, as shown in Figure C-13. The specimen thickness is nominally 0.060 to 0.090 inch.

1. Specimen Inspection - Visually inspect each test specimen prior to test. Further examine any observable flaws or irregularities. Record flaws or irregularities as part of the test data.

2. Measurement - Measure the width and thickness of the specimen to the nearest 0.001 inch at several points along the specimen to obtain the cross-sectional area. Return all specimens not conforming to the dimensions shown in Figure C-13 to the requester. Record the minimum cross-sectional dimensions of acceptable specimens on the test data sheet.

D. Testing Equipment

1. Thermocouple and Potentiometer - For elevated temperature, 180 to 350 F (82 to 177 C), and low temperature, -67 F (-55 C), attach an iron-constantan thermocouple to the specimen near the center of the top surface. Secure the thermocouple to the specimen with 2 layers of glass fabric tape. Take care that the thermocouple is in intimate contact with the specimen. Connect the thermocouple to a potentiometer or suitable recorder.

2. Heat Source - For elevated temperature tests, heat the shear specimens and fixture in a furnace chamber or with 2 banks of quartz heating lamps; the furnace chamber is preferred. Control the voltage of the quartz lamps with a powerstat. Allow the specimen to stabilize at temperature for a minimum of 10 minutes prior to loading. Monitor temperature with a thermocouple attached to the specimen.

3. Cooling Source - For low temperature test, place the shear specimens and fixture in a chamber and cool with liquid nitrogen to -67 F (-55 C). Allow the specimen to stabilize at temperature for a minimum of 10 minutes prior to loading. Monitor temperature with a thermocouple attached to the specimen.

4. Load Indicator - Use a calibrated load indicator in testing. Report the accuracy of the calibrated load indicator as a percentage of the full-scale load. Employ the smallest load range compatible with the expected load of the composite test specimen.

E. Specimen Testing

1. Span-to-Depth Adjustment - Center a 3-point load fixture assembly, shown in Figure C-14, in the test machine. Adjust the specimen supports to a span-to-depth according to the following relationship.

$$\frac{S}{T} = 4 \text{ to } 6$$

Where: S = span, inch

T = specimen thickness, inch

The span would be 0.240 to 0.360 inch for a 0.06-inch thick specimen or 0.400 to 0.600 inch for a 0.100-inch thick specimen. Determine the selection of a span-to-depth ratio by trail tests on a known graphite fiber-reinforced composite laminate to ascertain at which span there will be an interlaminar shear failure. Once determined, use that span-to-depth ratio for that resin-graphite fiber system.

2. Specimen Loading - Adjust the 0.125-inch diameter supports so that the correct span is obtained for the short beam specimen, leaving 0.1 inch, minimum, specimen overhang. The distance from the 0.250-inch diameter loading nose to a support shall be adjusted to equal 1/2 the span. Record the span on the test data sheet.

3. Specimen Centering - Carefully center the test specimen axially and laterally on the supports with the long axis of the specimen perpendicular to the supports. Utilize locating stops or pegs to facilitate alignment of the specimen with respect to the supports.

4. Speed of Testing - The testing speed, based on the crosshead speed of the testing machine, shall be 0.050 inch ± 0.005 per minute.

5. Temperature - Conduct tests at room temperature and in elevated and low temperature environments in accordance with D.1, D.2 and D.3.

6. Loading - Load the test specimen until either a drop in load is observed or the specimen fails. Report any improper failures on the test data sheet.

7. Failure Mode - After failure, remove the specimen from the test fixture and examine the failure visually or at 10x magnification to determine mode of failure. Report failure mode on the test data sheet.

F. Data Reporting

1. Previous Inspection - Report the test specimen inspection results, as outlined in C.1, with the test data.

2. Test Data - Report the interlaminar shear stress in pounds per square inch (psi). Interlaminar shear stress shall not be reported nor considered valid if failure occurred by crushing or compression failure by a combined crushing-tensile type failure. Report any unusual observations noted during the test as part of the test data.

G. Calculations - Calculate the interlaminar shear stress at failure according to the following equation.

$$\tau_i = \frac{3P}{4A}$$

Where: τ_i = Interlaminar shear stress, psi

P = Total load at failure, pounds

A = Cross-sectional area, square inch

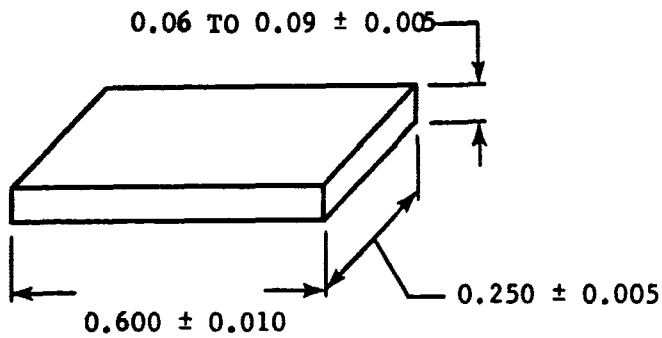

Figure C-13. Short Beam Shear Test Specimen.

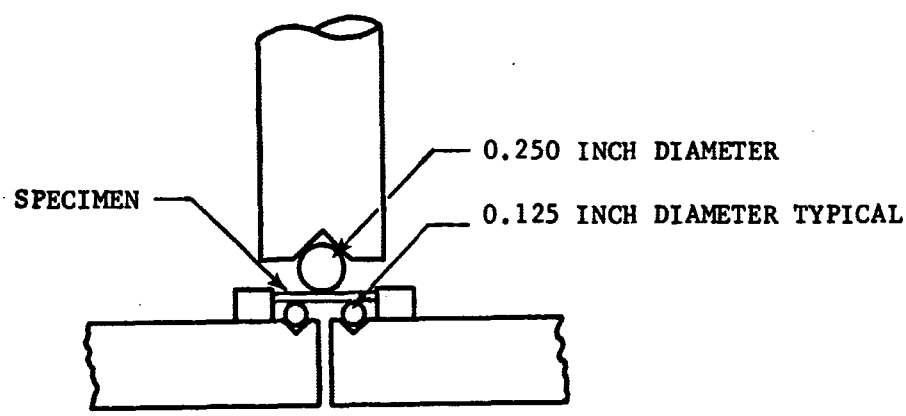

Figure C-14. Short Beam Shear Testing Fixture.

APPENDIX D

SPACE APPLICATIONS

FOR

BORON/GRAPHITE/EPOXY COMPOSITES

CONTRACT W0700 MA

MAY 1970

Prepared by:

F. J. Darms

North American Rockwell Corporation

SPACE APPLICATIONS FOR BORON/GRAPHITE/EPOXY COMPOSITE

I. INTRODUCTION AND SUMMARY

The development of high specific modulus and high specific strength fibers for the reinforcement of plastic matrix materials has resulted in the application of these materials to advanced fighter production aircraft primary structures. Studies of a large number of other aerospace applications have also been conducted. In a majority of these studies, established metal hardware design requirements have been used as a guide for the design, fabrication and structural test of composite demonstration articles in order that accurate performance and weight comparisons could be made.

The purpose of this report is to detail the results of a North American Rockwell Corporation study of space structure applications for a recently developed advanced composite material. This material, which was produced by Whittaker Corporation under NASA Contract 8-24510, consists of a combination of boron and graphite fibers in a matrix of epoxy resin. The material maintains the boron fiber content of standard boron/epoxy materials (nominally 50 percent by volume) with the addition of graphite fibers (approximately 15 percent by volume) as a fill between the larger diameter boron fibers. The resulting composite has a minimal resin content and has the mechanical properties and density consistent with the higher fiber content. Based on the analysis used to establish the controlled spacing of standard boron/epoxy composites, it is North American Rockwell Corporation's (NR) judgment that the tensile strength of cross-plied laminates from this material will be lower than the tensile strengths of straight boron epoxy. For this reason, the material would best be utilized in unidirectional applications.

Both current and future space hardware were considered in the applications review - current hardware because direct performance and weight comparisons can be made, and future hardware because they represent the real area of advanced composite application potential. Final selection of a demonstration article was limited to four components - two for the Apollo Service Module and two for the Space Shuttle System. Selection was restricted to components that would be reduced to a small structural demonstration article.

The 32.28-inch long inboard leg of the Number 5 radial beam truss for the Apollo Service Module was selected for the demonstration article (see Figure D-1). This component is used to provide support for the Command Module and is currently machined from 7075-T6 aluminum plate. Two approaches are recommended for material utilization - one that replaces a portion of the metal in the caps of the beam with unidirectional composite material and a second that employs an all-composite beam. The first approach is preferrred because it uses the major advantages of the higher fiber content composite without the anticipated cross-plied material disadvantages. This approach also permits the use of metal hardware attachment concepts.

The selection of the demonstration article was based on the following:

1. The use of unidirectional material

2. The presence of beam cap loads of a magnitude sufficient to make the cap-to-web weight ratio significant

3. The size of the beam

4. A documented analysis for the current metal design

In addition, the demonstration of the performance of a beam element would be useful for future space vehicles. For example, the Space Shuttle System is expected to use a number of beam elements. Some of these beams are located in the thrust structure of the boost vehicle. A weight reduction in the tail of this vehicle would be extremely beneficial because of the tail - heavy condition resulting in part from the weight of the engines.

II. APPLICATIONS SELECTION

A. Apollo Radial Beams Truss

An Apollo Service Module radial beam truss structure is shown in Figure D-1. The main function of this structure is to provide support to the Apollo Command Module. Maximum pad loads are presented in the table on Figure 1. The design approach, beam loads, plastic analysis and cross-section geometry of the inboard legs of the truss are provided in Paragraph III.

B. Apollo Hi-Gain Antenna Boom

The cylindrical hi-gain antenna boom of the Apollo deploys from the side of the Service Module (Figure D-2). It is angular deflection critical (140×10^{-6} radians angular displacement of one end with respect to the other) and is currently machined from a beryllium cylinder. The specific modulus of the boron/graphite/epoxy material is competititive with, but not as high as, the specific modulus of the beryllium - 5×10^8 lb-inch compared to 6×10^8 lb-inch. If judged by this factor alone, the current material would be more efficient than the composite. However, the composite material can be shaped to configurations that would be unfeasible for beryllium parts. These shapes, which would increase the diameter of the center section of the tube, would permit the development of a greater flexural stiffness for a given cross-sectional area. Studies of boron/epoxy materials have shown that practical configurations exist that would permit the composite to be of greater specific stiffness than the beryllium - while maintaining the current end fitting design.

C. Stand-off Strut

One candidate Space Shuttle boost vehicle fuselage configuration uses load-carrying tanks with the aerodynamic surface heat shield attached by means of stand-off struts. A quarter-section of a typical station for this design approach is shown in Figure D-3. As shown in the figure, the struts were primarily long-column compression numbers. Since design studies of graphite and boron composites have established the performance potential of these

materials for long-column applications, it is believed that the modulus of the boron/graphite/epoxy will result in a higher performance.

D. Compression Panels

The fuselage shell of the Space Shuttle boost and orbiter vehicles will make up a large percent of the structural weight. Weight reductions of this shell can be used to maintain or increase payload, reduce system size or permit increases in the weight or structural margins of safety of other components. One approach to the achievement of a weight reduction would be to use the unidirectional composite material to reinforce the metal stiffener of a titanium sheet-stiffener fuselage panel. Comparison of all-titanium and boron/epoxy (50 percent by volume) reinforced designs have shown that weight savings from 15 percent to 28 percent can be expected, depending on the load level and the relative thickness of the sheet and the stiffeners.

III. DESIGN DATA

Data for the critical systems load conditions, environmental conditions and applicable design parameters, and the performance of the current metal Apollo Service Module No. 5 radial beam truss are contained in Structural Analysis - Apollo Block II Spacecraft, Volume V Service Module, Book 2 of 5, (SD67-1103-1) dated December 1968 under NASA Contract NAS9-150. The short span of the application study did not permit time to obtain NASA release of the applicable portions of this document.

PREPARED BY: R.L.W.	NORTH AMERICAN AVIATION, INC.	
CHECKED BY: [illegible]	SERVICE MODULE	
DATE: 5-7-68	RADIAL BEAM TRUSS	

RADIAL BEAM TRUSS

DWG. NO.
V37-321001
V37-22[illegible]
V37-[illegible]01

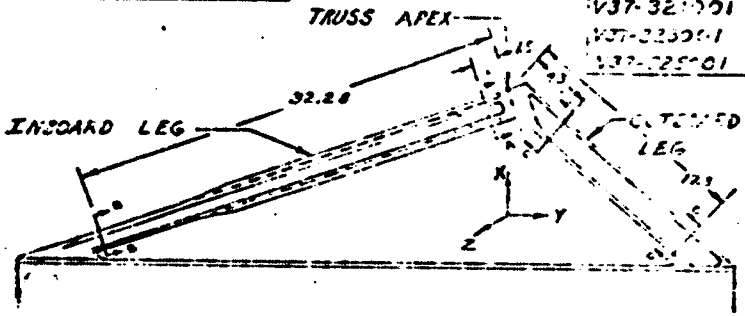

LOCATION OF SECTION PROPERTY CUTS

TYP TRUSS FOR RADIAL BEAMS

TYPICAL FOR BEAMS NOS 1, 3, & 5

TEMPERATURE ≈ R.T.

PREPARED BY: RLW	NORTH AMERICAN AVIATION, INC. SPACE and INFORMATION SYSTEMS DIVISION	PAGE NO. V.3.2.1.4
CHECKED BY: MS	SERVICE MODULE	REPORT NO. SD 67-1103
DATE: 11-21-68	RADIAL BEAM TRUSS	MODEL NO. APOLLO

MAXIMUM PAD LOADS AND TENSION TIE CONDITIONS

LIMIT LOADS

REF SD 67-1105
SECTION V.5.0.0
(THESE LOADS, ONLY, HAVE SEPARATE COORDINATE SYSTEM OF SD 67-1105)

RADIAL BEAM NO.	CONDITION TYPE	CONDITION NO.	PAD LOADS AT TRUSS APEX NORMAL P_x, #	SHEAR P_y, #	SHEAR P_z, #	MOMENT M_m			TENSION TIE LOAD, #
1		20353	-21534	4	19	66			
		20253	-21549	7	19	63			
		21253	-21143	-6	-23	-102			
2		20255	-40549	20	3625	-22156			
		21355	-40293	-1243	-917	-43160			
		21255	-40120	-132	-8714	-40778			
3		21356	-22735	-12		-57			
		21256	-22710	0	-12	-57			
4		20251	-36212	3436	2772.4	-76566			
		21457	-38850	1450	-2166	-39778			
		21257	-35633	315	-7855	-40736			
5		20158	-24739	-3	20	71			
		20258	-24703	-6	21	73			
		21258	-23140	4	-27	-123			
6		20252	-32958	261.4	4320.6	-71761			
		21352	-37641	-532	-8064	-37192			
		21252	-37513	-24	-7966	-37399			
2		20355							41711
		20255							4[illegible]
4		20153							41353
		20253							41297
6		20356							40393
		20256							40034

FORM M107-B-2 REV 8-61 VELLUM

BOOM — HIGH GAIN ANTENNA

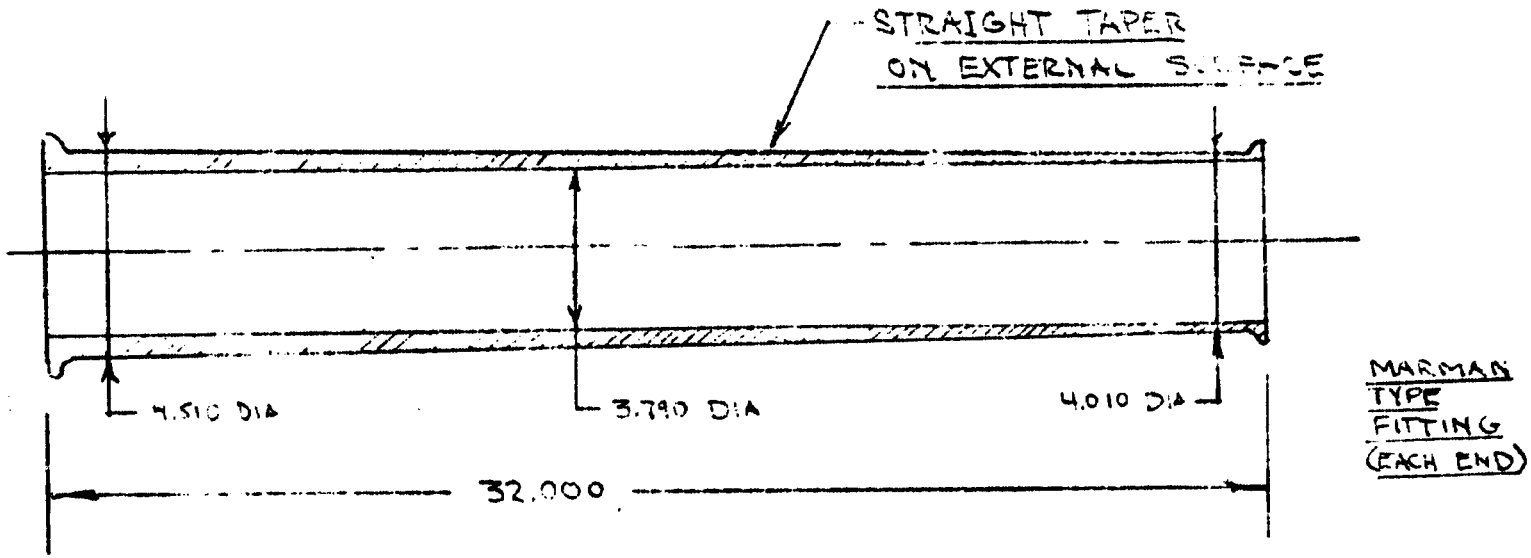

MATERIAL : BERYLLIUM

Figure D-2. Boom - High Gain Antenna

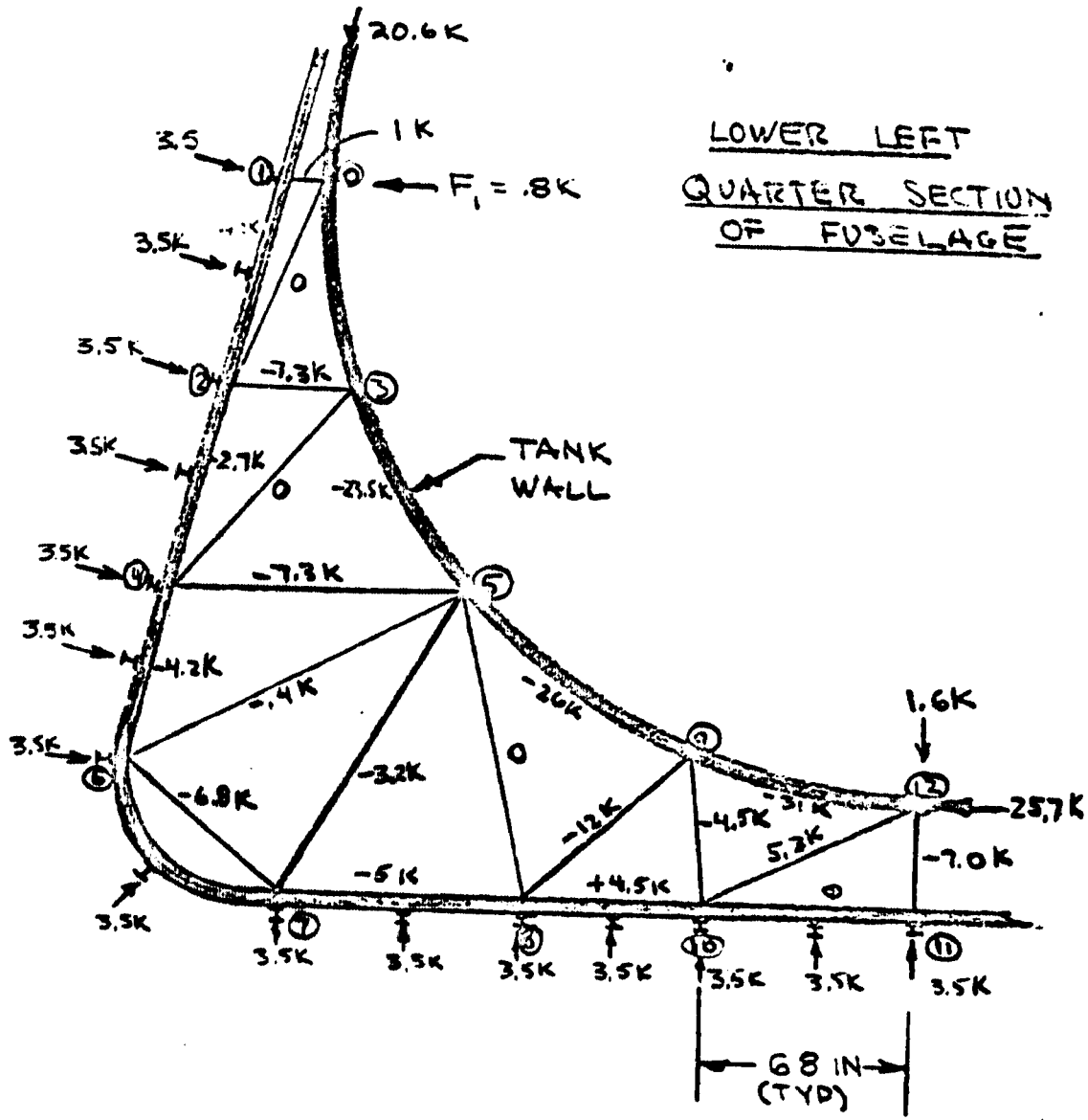

LOWER LEFT QUARTER SECTION OF FUSELAGE

END

DATE

FILMED

FEB 19 1971